NASA CONTRACTOR
REPORT

NASA CR-129041

(NASA-CR-129041) CHARACTERIZATION OF METALS MELTING DISCS SKYLAB EXPERIMENT M551 (Battelle Columbus Labs., Ohio.) 120 p HC $5.25 CSCL 13H

N75-10118

G3/12 Unclas 51126

CHARACTERIZATION OF METALS MELTING DISCS SKYLAB EXPERIMENT M551

By Robert E. Monroe
Battelle Columbus Laboratories
Columbus, Ohio 43201

January 1974

Prepared for

NASA-GEORGE C. MARSHALL SPACE FLIGHT CENTER
Marshall Space Flight Center, Alabama 35812

TABLE OF CONTENTS

	Page
SUMMARY	1
INTRODUCTION	2
SECTION A. EVALUATION OF GROUND CHARACTERIZATION SAMPLES - M551	3
MATERIALS	3
Procedures	4
RESULTS	7
Aluminum Discs	7
Disc P-1	7
Disc H-1	7
Disc S/N 124	14
Disc S/N 132	14
Stainless Steel Discs	14
Disc 2 and Disc B	14
Disc S/N 104	38
Disc S/N 107	38
Tantalum Discs	38
Disc S/N 143	38
Disc S/N 158	38
Distortion Measurements	38
SECTION B. EVALUATION OF SKYLAB AND FINAL GROUND CHARACTERIZATION METALS MELTING DISCS	58
SPECIMEN PROCESSING	58
RESULTS	58
Aluminum Discs	58

TABLE OF CONTENTS
(Continued)

	Page
Front Surface S/N 130	66
Back Surface S/N 130	67
Front Surface S/N 129	67
Back Surface S/N 129	68
Sectioning and Examination	69
Stainless Steel Discs	69
Front Surface S/N 106	69
Back Surface S/N 106	83
Front Surface S/N 110	84
Back Surface S/N 110	85
Sectioning and Examination	85
Tantalum Discs	85
Front Surface S/N 145	98
Back Side of S/N 145	98
Front Surface of Disc S/N 147	99
Back Side of S/N 147	100
Sectioning and Examination	101
SECTION C. CONCLUSIONS	107

LIST OF ILLUSTRATIONS

		Page
Figure A-1.	Sectioning Plan - M551	6
Figure A-2.	Front Surface of P-1	8
Figure A-3.	Section P-1 at Tracer Region	8
Figure A-4.	Front Surface H-1.	9
Figure A-5.	Section Through Cut Region - H-1	10
Figure A-6.	Surface of Cut on Inside - H-1	10
Figure A-7.	Surface of Cut - H-1	11
Figure A-8.	Pore in Section at Base Metal Interface - H-1. . .	12
Figure A-9.	Section Through Ramp Region - H-1.	12
Figure A-10.	Pores in Ramp Section - H-1.	13
Figure A-11.	Section Through Crack Near Weld Start.	13
Figure A-12.	Enlargement of Longitudinal Crack at Weld Start - H-1.	15
Figure A-13.	Pore at Inside Edge of Weld - H-1.	15
Figure A-14.	Section Through Full Penetration Region - H-1. . .	16
Figure A-15.	Section Through Partial Penetration Region - H-1.	16
Figure A-16.	Section Through Upper Left Surface of Partial Penetration Weld - H-1	17
Figure A-17.	Section Near Top Surface Partial Penetration Weld - H-1	17
Figure A-18.	Section Through Partial Penetration Region - H-1.	18
Figure A-19.	Section Through Dwell Region - H-1	18
Figure A-20.	Cracks in Dwell Region - H-1	19

LIST OF ILLUSTRATIONS
(Continued)

		Page
Figure A-21.	Molybdenum Traces on Surfaces of Dwell Region - H-1.	20
Figure A-22.	Cracks Near Top of Dwell Region - H-1.	21
Figure A-23.	Chord Section in Dwell Region - H-1.	21
Figure A-24.	Electron Probe Scans of Region Shown in Figure A-21.	22
Figure A-25.	Electron Probe Scans of Region Shown in Figure A-16.	23
Figure A-26.	Front Surface - S/N 124.	24
Figure A-27.	Section Through Partial Penetration Region - S/N 124.	25
Figure A-28.	Enlarged Areas of Partial Penetration Region - S/N 124.	26
Figure A-29.	Section Through Dwell Region - S/N 124	27
Figure A-30.	Section Through Crack in Dwell Region - S/N 124.	27
Figure A-31.	Chord Section Through Dwell Region - S/N 124 . . .	28
Figure A-32.	Structures in Dwell Region - S/N 124	29
Figure A-33.	Front Surface - S/N 132.	31
Figure A-34.	Back Surface - S/N 132	32
Figure A-35.	Section Through Cut Region - S/N 132	33
Figure A-36.	Chord Section in Full Penetration Region - S/N 132.	34
Figure A-37.	Front of Disc B Showing Section Locations.	35
Figure A-38.	Back of Disc B Showing Quadrant Design	36

LIST OF ILLUSTRATIONS
(Continued)

		Page
Figure A-39.	Front of Disc 2 Showing Section Locations.	37
Figure A-40.	Front Surface - S/N 104.	39
Figure A-41.	Section Through Cut Region - S/N 104	40
Figure A-42.	Section Through Ramp Section - S/N 104	40
Figure A-43.	Fusion Line Region - S/N 104	41
Figure A-44.	Section Through Full Penetration Region - S/N 104.	41
Figure A-45.	Section at Root of Weld.	42
Figure A-46.	Section Through Partial Penetration Region - S/N 104.	42
Figure A-47.	Fusion Line Region at Shape Change	43
Figure A-48.	Section Through Partial Penetration Region - S/N 104.	43
Figure A-49.	Weld Structures - S/N 104.	44
Figure A-50.	Sections Through Dwell Region - S/N 104.	45
Figure A-51.	Front Surface - S/N 107.	47
Figure A-52.	Back Surface - S/N 107	48
Figure A-53.	Section Through Cut Region - S/N 107	49
Figure A-54.	Chord Section Through Full Penetration Region - S/N 107.	49
Figure A-55.	Front Surface - S/N 143.	50
Figure A-56.	Section Through Region Before Cut - S/N 143. . . .	51
Figure A-57.	Section Through Cut Region - S/N 143	51
Figure A-58.	Bottom Surface of Outside Cut Edge - S/N 143 . . .	51

LIST OF ILLUSTRATIONS
(Continued)

		Page
Figure A-59.	Bottom Surface of Inside Cut Edge - S/N 143. . . .	52
Figure A-60.	Section Through Bridge Broken in Cutting - S/N 143.	52
Figure A-61.	Section Through Partial Penetration Region - S/N 143.	52
Figure A-62.	Section Through Dwell Region - S/N 143	53
Figure A-63.	Chord Section Through Dwell Region - S/N 143 . . .	53
Figure A-64.	Front Surface - S/N 158.	54
Figure A-65.	Back Surface - S/N 158	55
Figure A-66.	Section Through Bridge in Cut Region - S/N 158 . .	56
Figure A-67.	Chord Section Through Full Penetration Region - S/N 158.	56
Figure A-68.	Section Through Dwell Region - S/N 158	56

LIST OF ILLUSTRATIONS
(Continued)

		Page
Figure B-1.	Front Surface - S/N 130.	61
Figure B-2.	Back Surface - S/N 130	62
Figure B-3.	Front Surface - S/N 129.	63
Figure B-4.	Back Surface - S/N 129	64
Figure B-5.	Sectioning Plan - S/N 129 and 130.	65
Figure B-6.	Sections Through Cut Region.	70
Figure B-7.	Contour at Base Metal Interface Cut Region - S/N 129.	71
Figure B-8.	Section Through Full Penetration Region - S/N 129 Skylab	72
Figure B-9.	Section Through Partial Penetration Region - S/N 129 Skylab	72
Figure B-10.	Chord Section in Full Penetration Region - S/N 129.	73
Figure B-11.	Microstructure in Chord Section - S/N 129.	73
Figure B-12.	Structures in Full Penetration Region - S/N 129 Skylab	74
Figure B-13.	Sections Through Dwell Region of S/N 129 and 130.	75
Figure B-14.	Structures in Dwell Region - S/N 129 Skylab. . . .	76
Figure B-15.	Chord Sections of Dwell Region	77
Figure B-16.	Hardness Survey--Aluminum Full Penetration	78
Figure B-17.	Front Surface - S/N 106.	79
Figure B-18.	Back Surface - S/N 106	80
Figure B-19.	Front Surface - S/N 110.	81
Figure B-20.	Back Surface - S/N 110	82
Figure B-21.	Sectioning Plan - S/N 106 and 110.	86

LIST OF ILLUSTRATIONS
(Continued)

		Page
Figure B-22.	Section Through Cut Region - S/N 106 Skylab. . . .	87
Figure B-23.	Chord Section Through Full Penetration Region - S/N 106 Skylab	87
Figure B-24.	Cross Section Through Full Penetration Region. . .	88
Figure B-25.	Structures in Full Penetration Region - S/N 106 Skylab	89
Figure B-26.	Radial Section of Dwell Regions.	90
Figure B-27.	Contour of Top Fusion Line Areas in Dwell Region - S/N 106 Skylab.	91
Figure B-28.	Internal Microstructures in Dwell Region - S/N 106 Skylab	92
Figure B-29.	Hardness Survey--Stainless Steel Full Penetration Weld	93
Figure B-30.	Front Surface - S/N 145.	94
Figure B-31.	Back Surface - S/N 145	95
Figure B-32.	Front Surface - S/N 147.	96
Figure B-33.	Back Surface - S/N 147	97
Figure B-34.	Sectioning Plan - S/N 145 and 147.	102
Figure B-35.	Section Through Cut Region - S/N 145 Skylab. . . .	103
Figure B-36.	Section Through Bridge in Cut Region - S/N 145 Skylab	103
Figure B-37.	Weld Sections in Full Penetration Region - S/N 145 Skylab	104
Figure B-38.	Section Through Partial Penetration Region - S/N 145 Skylab	105
Figure B-39.	Chord Section in S/N 145 Skylab.	105
Figure B-40.	Sections Through Dwell Region.	106

LIST OF TABLES

Page

Table A-1. Distortion Measurements. 57

Table B-1. Thickness Measurements -- M551 59

Table B-2. Distortion Measurements -- M551. 60

CONTRACTOR REPORT

CHARACTERIZATION OF METALS MELTING DISCS SKYLAB EXPERIMENT M551

SUMMARY

Sixteen discs from the metals melting experiment were examined to provide data on the possible effects of zero gravity on molten metals. Three of the discs, one each of 2219 aluminum, austenitic stainless steel and tantalum, were processed on Skylab. The remaining discs were processed in the normal earth gravitational field. Examinations were conducted with careful visual and radiographic methods, dimensional checks, and metallographic techniques. A large number of features were observed and documented for comparative purposes and for study by other investigators. Although the individual discs contain a variety of features, few of these appear to be useful in demonstrating a pronounced effect of zero gravity in the experiment. The cut and weld shapes obtained and the microstructures observed were typical of normal electron beam processing. Weld defects were not as useful in studying gravity effects as anticipated. Porosity was infrequent only along surface interfaces in the aluminum samples. Cracks occurred only in predictable locations in the aluminum at the weld start in the dwell area, and at the point where a molybdenum tracer was used. The tracer technique itself was overshadowed by the pronounced mixing occurring during welding.

Significant findings were as follows:

(1) The distribution of aluminum oxide on the full penetration weld surface was entirely different in the Skylab and ground characterization specimens.

(2) Weld-base metal surface contours appear to be generally flatter in the Skylab specimens. Further study of these contours should be made including the data available from other investigators.

INTRODUCTION

This report covers the work conducted at Battelle-Columbus in support of Skylab experiment M551 Metals Melting. The report covers characterization of both ground-based and Skylab-processed specimens during the period from May 15, 1972, through December 4, 1973.

The work was conducted in three phases concerned with (A) Planning, (B) Ground-Based Characterization, and (C) Skylab Specimen Characterization. Inputs made during Phase A were reflected in the experimental details that have evolved and are reported elsewhere. This report covers the details of Phases B and C and is organized into three sections. Section A covers the evaluation of ground characterization samples available prior to the Skylab flight. Section B covers characterization of the Skylab specimens and a post flight series of ground characterization specimens. Finally, conclusions covering all aspects of the program are presented.

The Battelle effort under this program was only a portion of the total effort conducted both by NASA and other contractors. For completeness, some data and information from other sources are included in this report. The reader will find much related information in other reports on this experiment.

SECTION A. EVALUATION OF GROUND CHARACTERIZATION SAMPLES - M551

During Phase B, the evaluation procedures proposed in Phase A were studied and proven out by examination of ten ground characterization discs. The procedures generally involved visual, nondestructive, and metallographic examinations. The discs examined in this program can be classed in three groups:

(1) Preliminary - Phase B

(2) Ground Based - Phase B

(3) Skylab - Phase C

Only the Preliminary-Phase B group is discussed in this section, since Group 2, Ground Based-Phase B were processed after the Skylab flight. Also, interpretation of the data is limited in this section. Instead, most information is presented as observations made.

MATERIALS

The discs included in the Preliminary-Phase B study are listed below:

Identification	Material	Remarks
2	Stainless Steel	Quadrant Design
B	Stainless Steel	Quadrant Design
P-1	2219 Al	Mo Coating Evaluation
H-1	2219 Al	Final Design
S/N 124	2219 Al	Final Design
S/N 104	Stainless Steel	Final Design
S/N 143	Tantalum	Final Design
S/N 132	2219 Al	Final Design
S/N 107	Stainless Steel	Final Design
S/N 158	Tantalum	Final Design

Procedures

The evaluation procedures proposed in Phase A were studied and applied as required. The visual appearance of the front and back disc surfaces was recorded photographically at 1X. A low power examination using a binocular microscope at magnifications in the range of 7 to 30X also was made. Written descriptions of this visual examination will be prepared for the final Phase B and Phase C specimens.

Radiographic exposures were taken with Norelco-MG-150 equipment on the aluminum and stainless steel and with General Electric - OX250 equipment on the tantalum. The exposure conditions are tabulated below:

Material	Voltage KVP	Current ma.	Time min.	Focal Length inch.	Film Type(a)
AL	40	5	5	46	M
	47	5	5	46	M
SS	110	5	5	46	AA & M(b) (c)
Ta	210	8	3	51	AA(b)
	250	8	3	51	AA(b)

(a) Kodak Designation.
(b) With Lead Screens.
(c) Films Exposed Together.

Generally two exposures were required to provide the proper density for intrepretation because of the thickness variation in the disc.

Other nondestructive inspection methods, penetrant and ultrasonics, were not found useful in examination of these discs.

Measurements were taken of the disc thickness with appropriate micrometers, and on some discs dial indicator readings were made to determine the out of plane distortion. The procedure for these later measurements was as follows:

(1) Set up disc in a lathe chuck and adjust to have the front disc surface perpendicular to the rotation axis.

(2) Check region near center of disc with dial indicator and readjust as necessary.

(3) Establish zero reading on center region.

(4) Record readings at distance of 1/4 inch from weld centerline on either side of weld every 30 degrees.

The discs were marked for sectioning with scribe lines at the appropriate points. The basic pattern for sectioning is shown in Figure A-1. Sectioning was accomplished using a water cooled abrasive wheel, 0.040 inch-thick. Sections cut for other investigators were marked and returned to MSFC. The nomenclature used for sectioning and sample designation is listed below:

(1) 0 degree is target.

(2) Looking at front surface, angle is measured counterclockwise.

(3) All discs are identified with a disc number.

(4) All radial sections are designated by the angle of the plane examined.

(5) All chord sections are designated by the included angle.

(6) All photographs will have a negative number and magnification shown as follows (AAA-20X).

(7) Direction of view of radial planes will be indicated as, +, looking in direction of weld finish or, -, looking in direction of weld start.

Sections for examination were mounted and polished using conventional metallographic procedures. Sections were examined in both the as polished condition and after etching. The etchants normally used on each base material were as follows:

(1) Aluminum - 60H_2O_2-30HNO_3-20 Ethyl Alcohol, 15 drops HF

(2) Stainless Steel - 97HCL, 3HNO_3-1/2 gram $CuCl_2$

(3) Tantalum - 30 Lactic,-40HNO_3-40HF

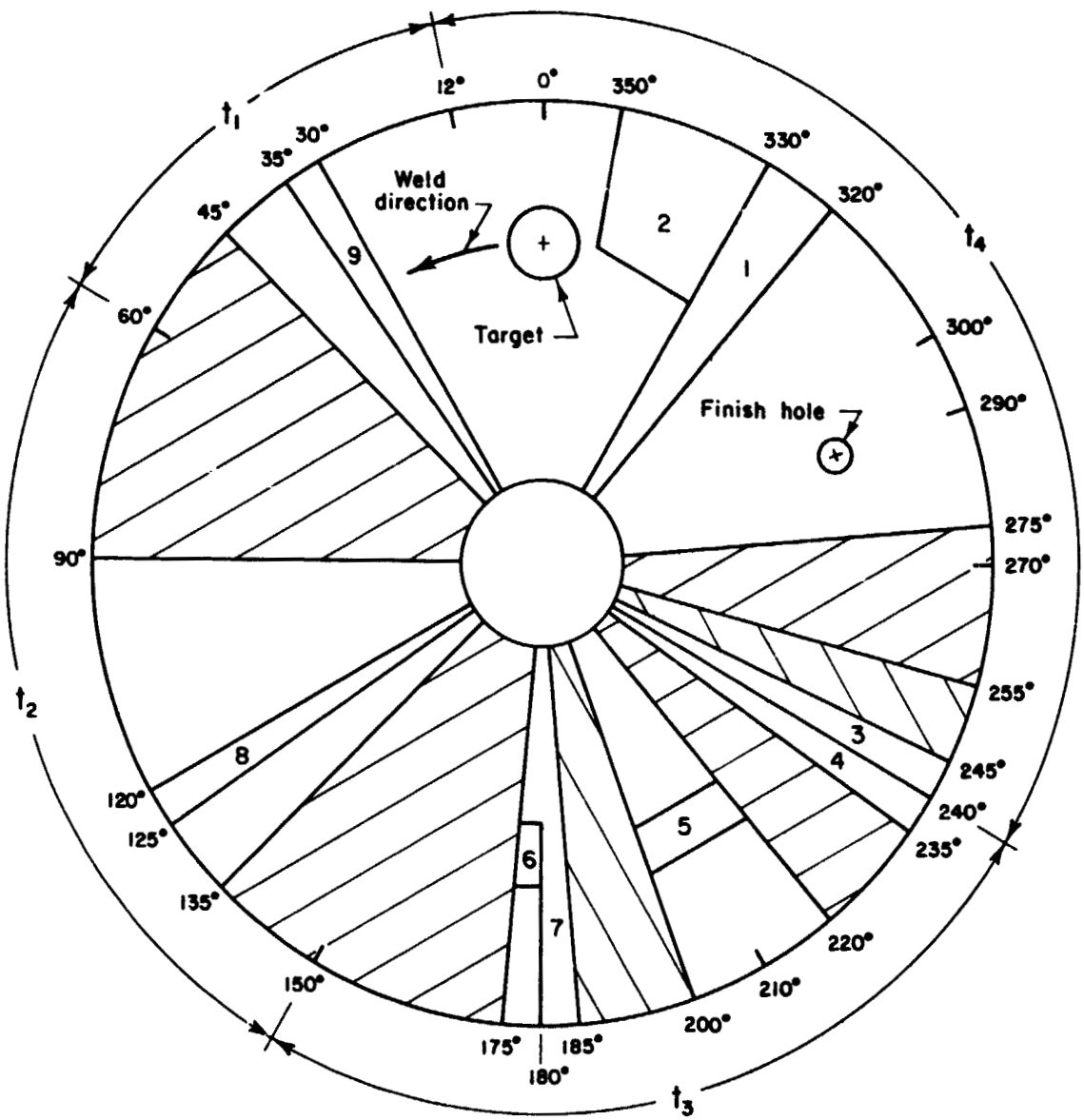

FIGURE A-1. SECTIONING PLAN - M551

Numbered Sections - BCL

▨ - MSFC ▧ - UK

T_1 - Cut
T_2 - Ramp
T_3 - Full penetration
T_4 - Partial penetration/dwell

All photomicrographs identified as etched were prepared with these etches unless a different etchant is indicated.

Electron probe microanalysis was used as appropriate to identify phases present in the microstructure.

RESULTS

Results of the preliminary Phase B studies are presented in sections containing the data developed on each specimen. The specimens have been grouped by material except for the distortion measurements.

Aluminum Discs

Four aluminum discs were examined. Three of these were of the final disc design and one was a disc used to develop molybdenum coating techniques.

Disc P-1

No defects were noted in the radiograph except cr. er carcks at the weld stops and dwells. Figure A-2 shows the appearance of this disc as received. The black area is a molybdenum spray coating used for a tracer. A section through the weld zone in the area of the tracer is shown in Figure A-3. No adverse effects of the tracer on the weld region were noted in this section.

Disc H-1

The radiograph showed longitudinal weld cracks near the weld start (125° to 135°), and near the molybdenum tracer (225° to 235°). Cracks in the dwell crater also were apparent. All of these cracks also were visible on the weld surface. Figure A-4 shows the front surface of Disc H-1. The rectangular cutouts were examined at Battelle. The cross hatch wedge sections were sent to MSFC for examination.

Figures A-5 through A-10 show the appearance and microstructural details in the cut region. Several areas on the cut surfaces indicate the presence of a contaminant or reaction zone. This has probably come from material vaporized from the surface under the weld disc. The very wide cut that resulted in this disc is

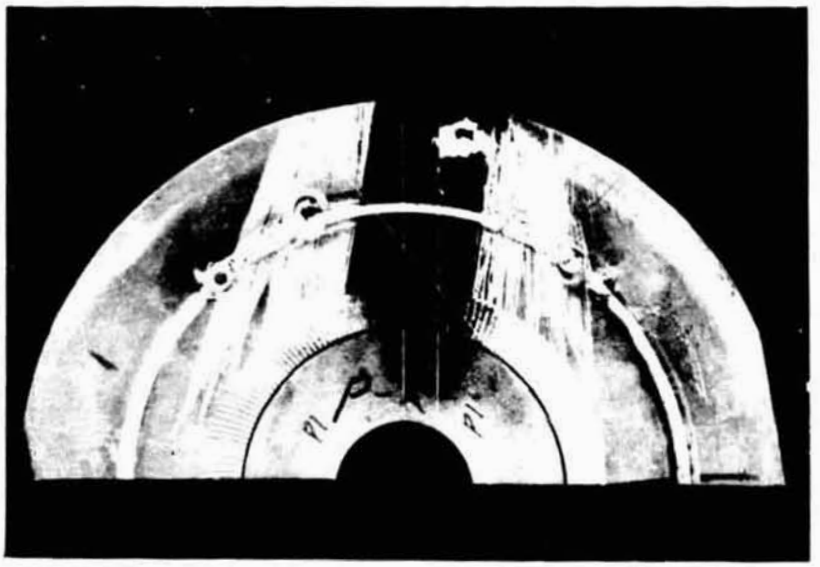

2G905-0.5X

FIGURE A-2. FRONT SURFACE OF P-1

Etched 5G265-20X

FIGURE A-3. SECTION P-1 AT TRACER REGION

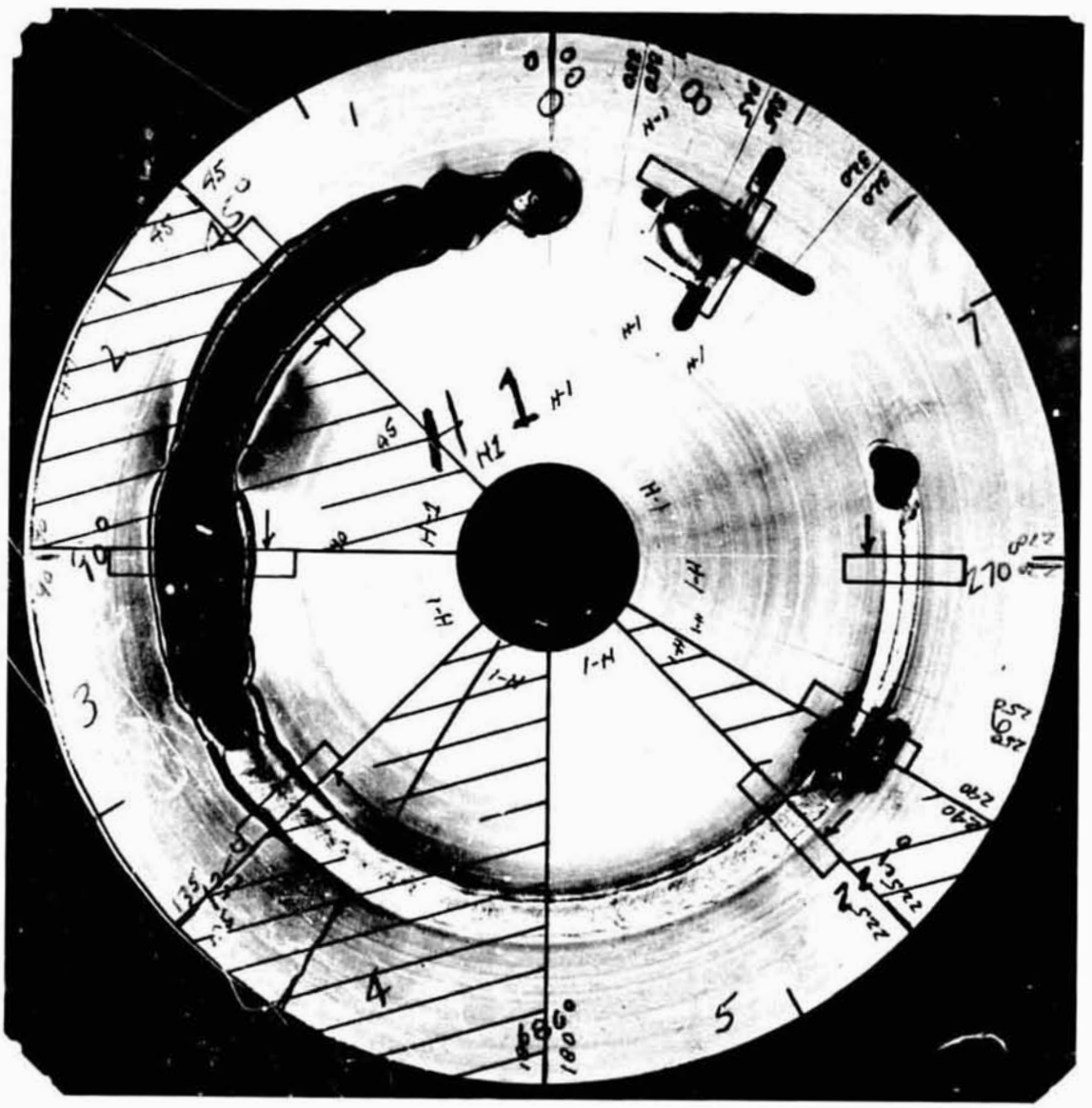

2G906-1X

FIGURE A-4. FRONT SURFACE H-1

45°(-) Etched 5G264-20X

FIGURE A-5. SECTION THROUGH CUT REGION -H-1

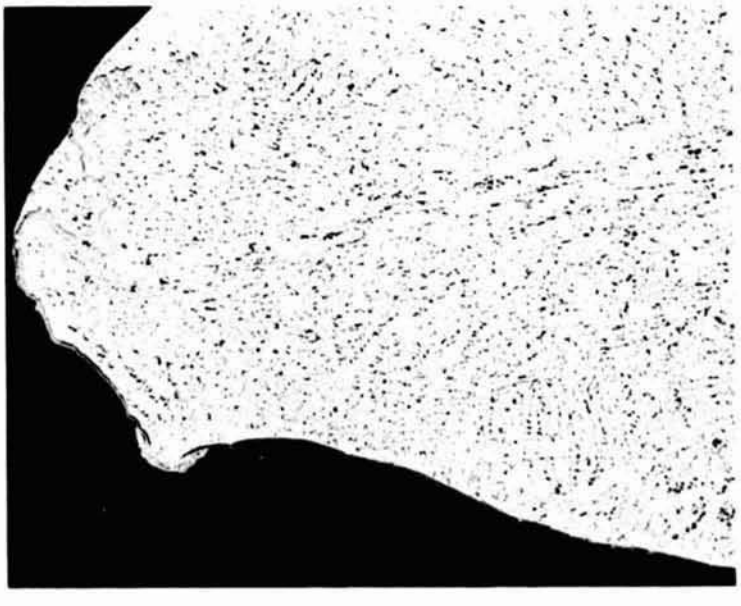

45°(-) Etched 5G254-100X

FIGURE A-6. SURFACE OF CUT ON INSIDE -H-1

45°(-) Etched 5G255-250X

a. Enlarged area of Figure A-6

45°(-) Etched 5G256-250X

b. Bottom surface of cut on outside

FIGURE A-7. SURFACE OF CUT -H-1

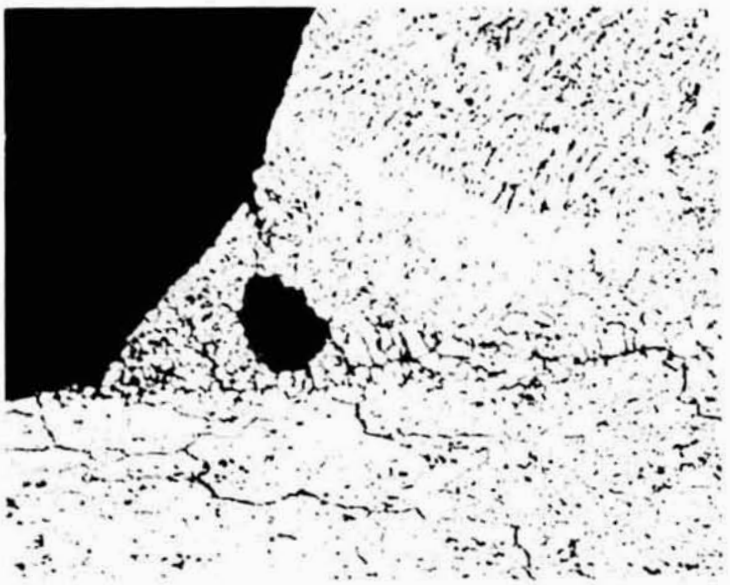

45°(-) Etched 5G253-100X

FIGURE A-8. PORE IN SECTION AT BASE METAL INTERFACE H-1

90°(+) Etched 5G263-20X

FIGURE A-9. SECTION THROUGH RAMP REGION -H-1

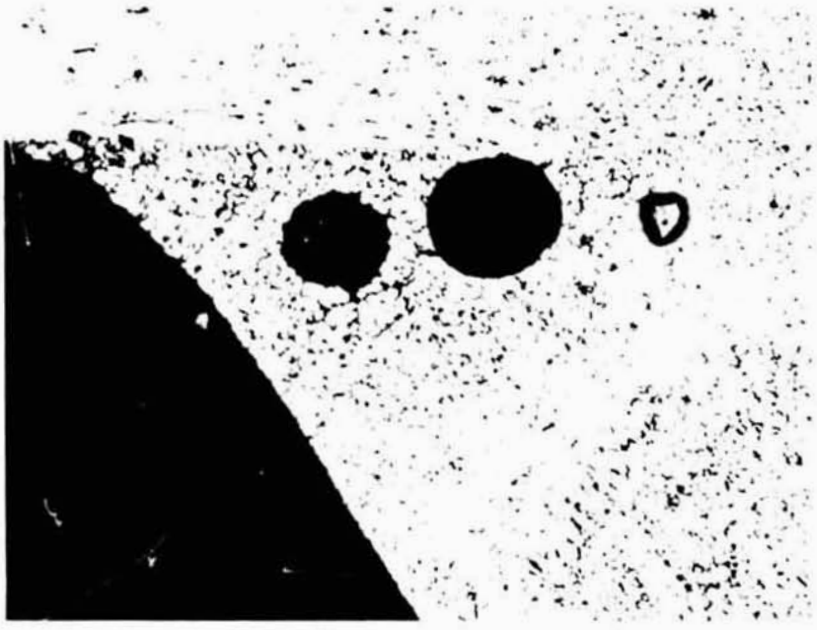

90°(+) Etched 5G252-100X

FIGURE A-10. PORES IN RAMP SECTION -H-1

135°(-) Etched 5G262-20X

FIGURE A-11. SECTION THROUGH CRACK NEAR WELD START

indicative of an electron-beam power level favoring excessive penetration.

The details shown in Figures A-11 through A-23 are provided for future comparisons of structures and defects. Figures A-24 and A-25 illustrate the technique available to identify phases present in the regions containing the molybdenum tracer.

Disc S/N 124

Figures A-26 through A-32 show the appearance of this disc and selected macro- and microstructures.

Disc S/N 132

Figures A-33 through A-36 show additional features of an aluminum disc.

Stainless Steel Discs

Four stainless steel discs were examined. Two were of an early quadrant design and the last two of the final design.

Disc 2 and Disc B

Figures A-37 through A-39 show the front and back surfaces of Disc B and Disc 2. The quadrant thickness of these discs is tabulated below:

Region	Thickness, inch "B"	"2"
Cut	0.027	0.026
Full penetration	0.097	0.049
Partial Penetration	0.168	0.123
Dwell	0.258	0.248

A large number (about fifty) macro and microphotographs were taken of sections from these discs. They are available, but not shown herein because of later changes in material and disc design.

135°(-) Etched 5G250-100X

FIGURE A-12. ENLARGEMENT OF LONGITUDINAL CRACK AT WELD START - H-1

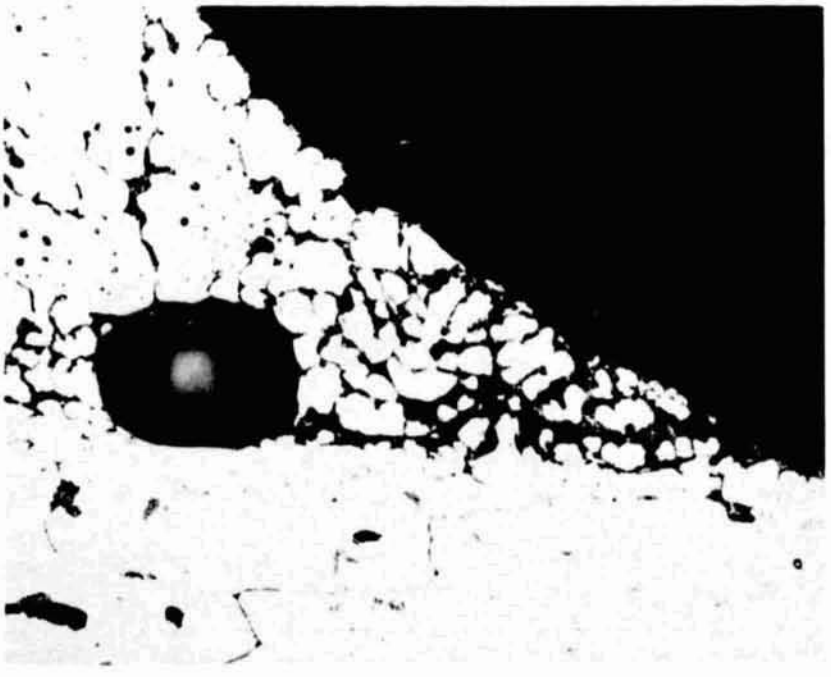

135°(-) Etched 5G251-500X

FIGURE A-13. PORE AT INSIDE EDGE OF WELD - H-1

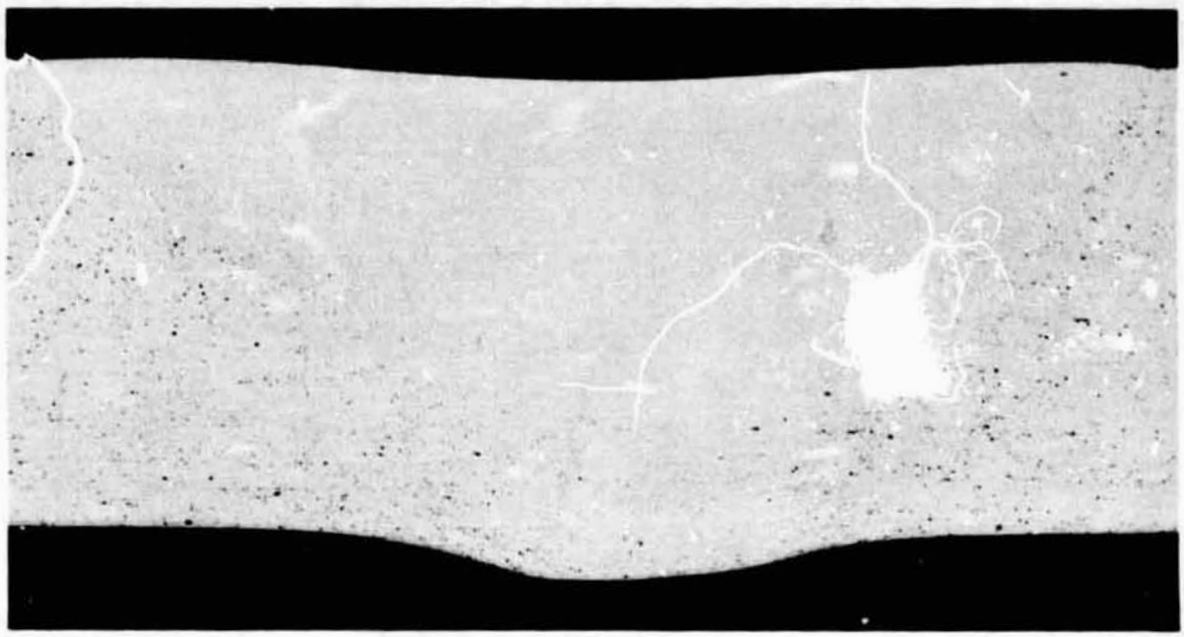

225°(-) Etched 5G261-20X

FIGURE A-14. SECTION THROUGH FULL PENETRATION REGION- H-1

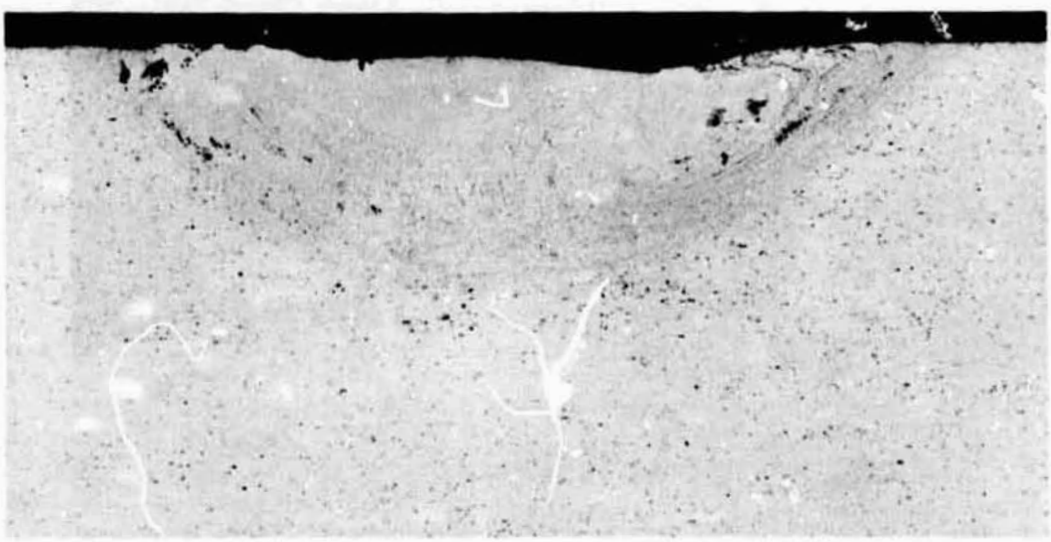

240°(+) Etched 5G259-20X

FIGURE A-15. SECTION THROUGH PARTIAL PENETRATION REGION- H-1

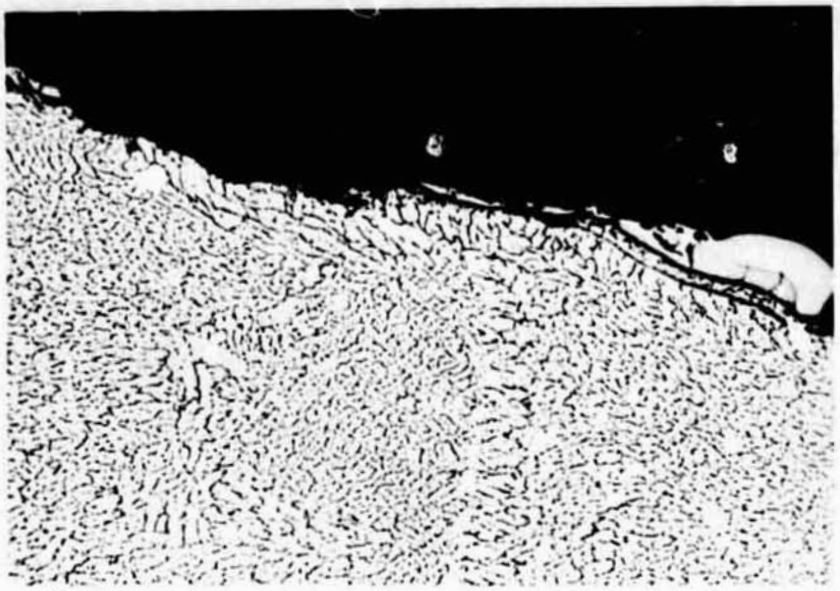

240° (+) Etched 5G248-250X

FIGURE A-16. SECTION THROUGH UPPER LEFT SURFACE OF PARTIAL PENETRATION WELD- H-1

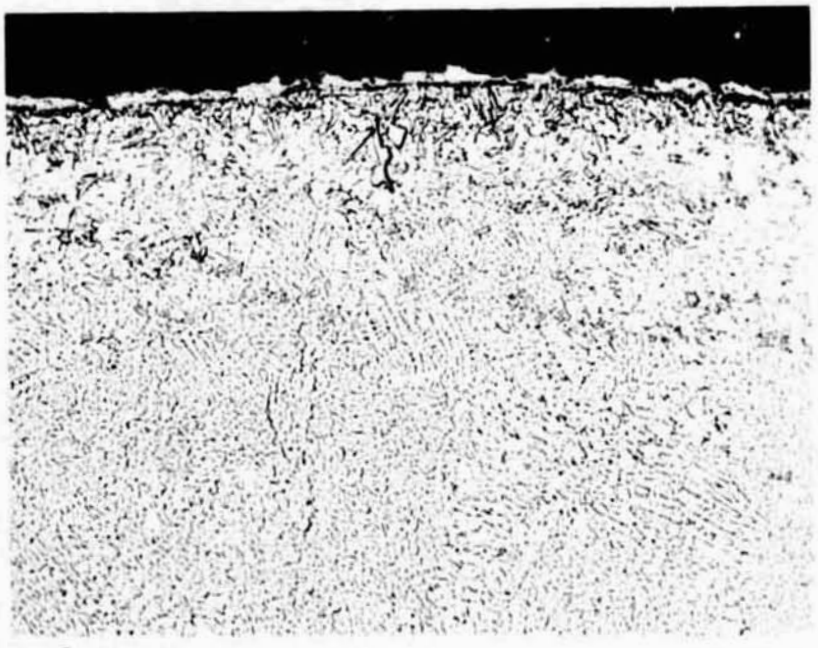

240° (+) Etched 5G249-250X

FIGURE A-17. SECTION NEAR TOP SURFACE PARTIAL PENETRATION WELD- H-1

270°(-) Etched 5G260-20X

FIGURE A-18. SECTION THROUGH PARTIAL PENETRATION REGION-H-1

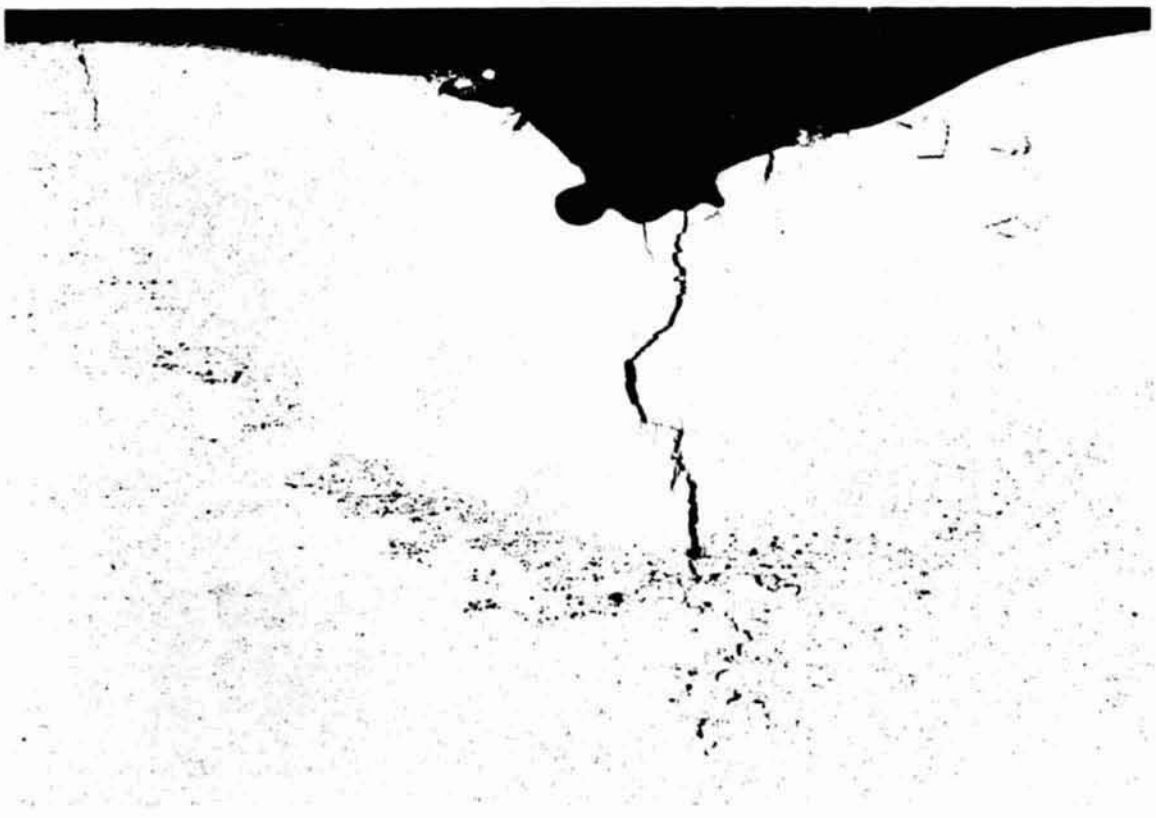

335°(-) Etched 5G258-20X

FIGURE A-19. SECTION THROUGH DWELL REGION - H-1

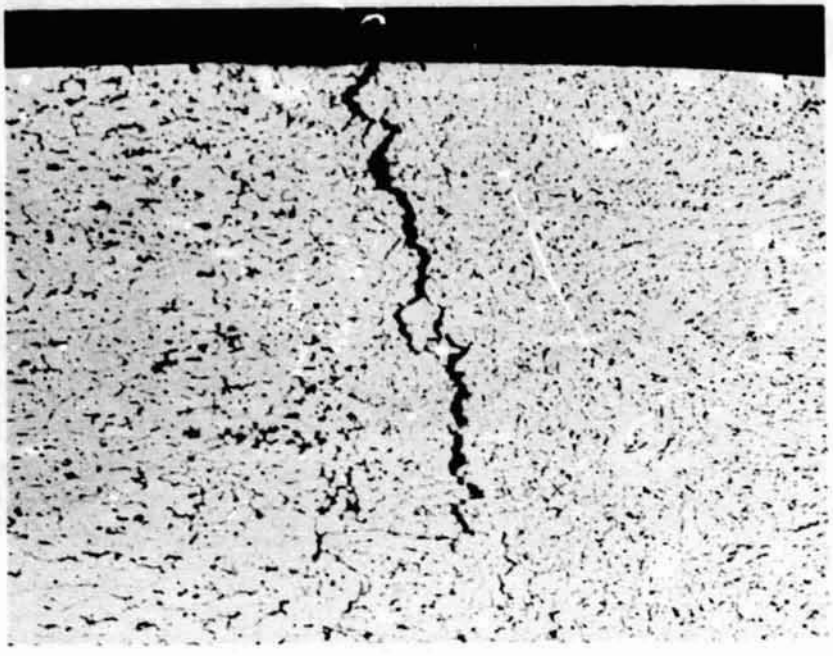

335°(-) Etched 5G245-100X

a. Crack near left edge in Figure A-19

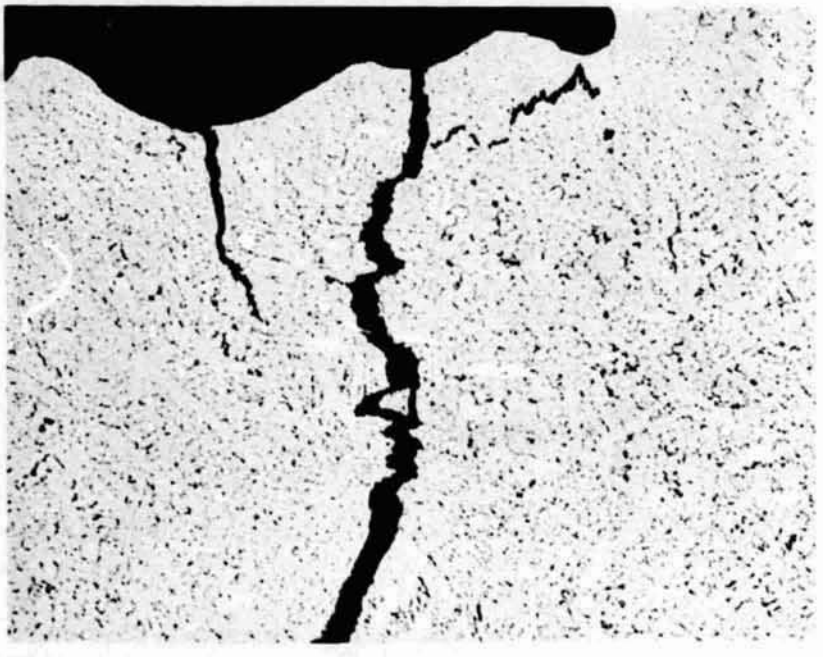

335°(-) Etched 5G244-100X

b. Main crack near center in Figure A-19

FIGURE A-20. CRACKS IN DWELL REGION- H-1

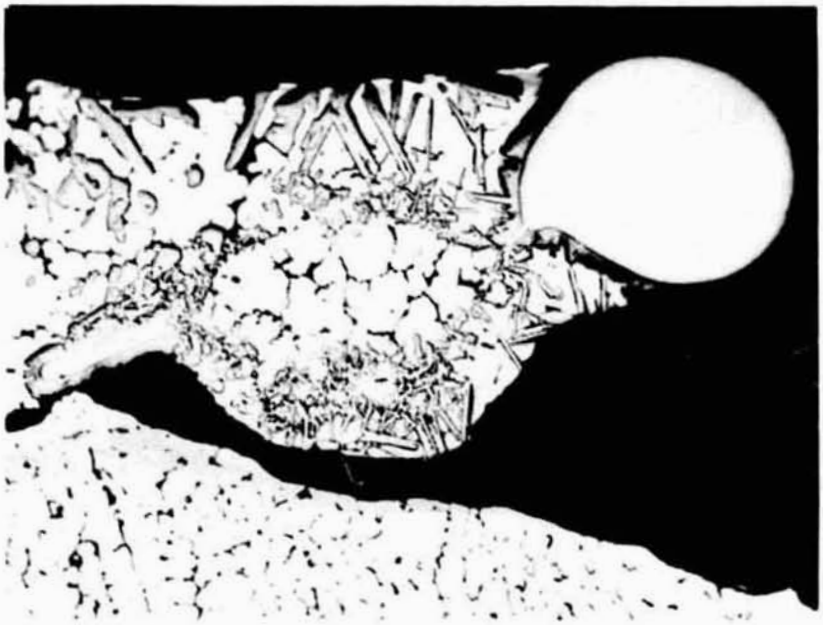

335°(-) Etched 5G246-250X

a. Near Left center in Figure A-19

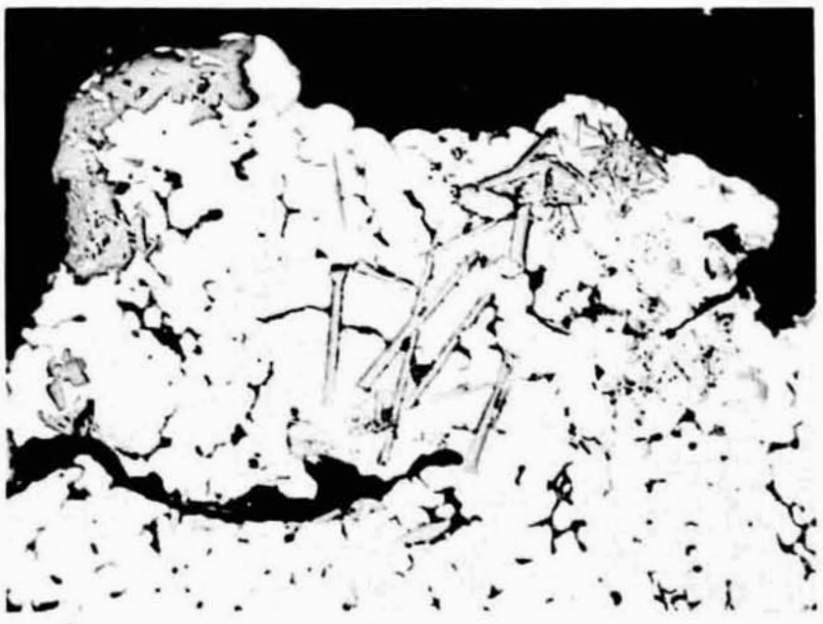

335°(-) Etched 5G247-500X

b. Near right center in Figure A-19

FIGURE A-21. MOLYBDENUM TRACES ON SURFACES OF DWELL REGION- H-1

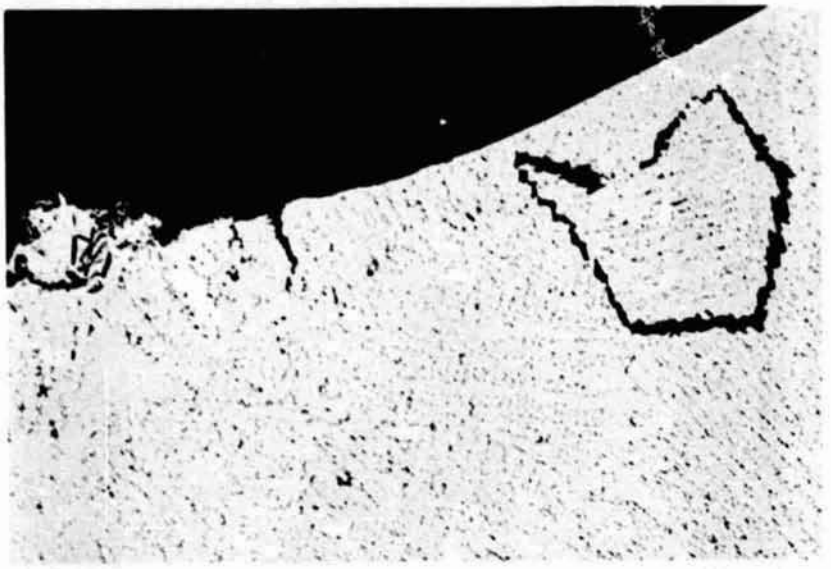

335°(-) Etched 5G243-100X

FIGURE A-22. CRACKS NEAR TOP OF DWELL REGION- H-1

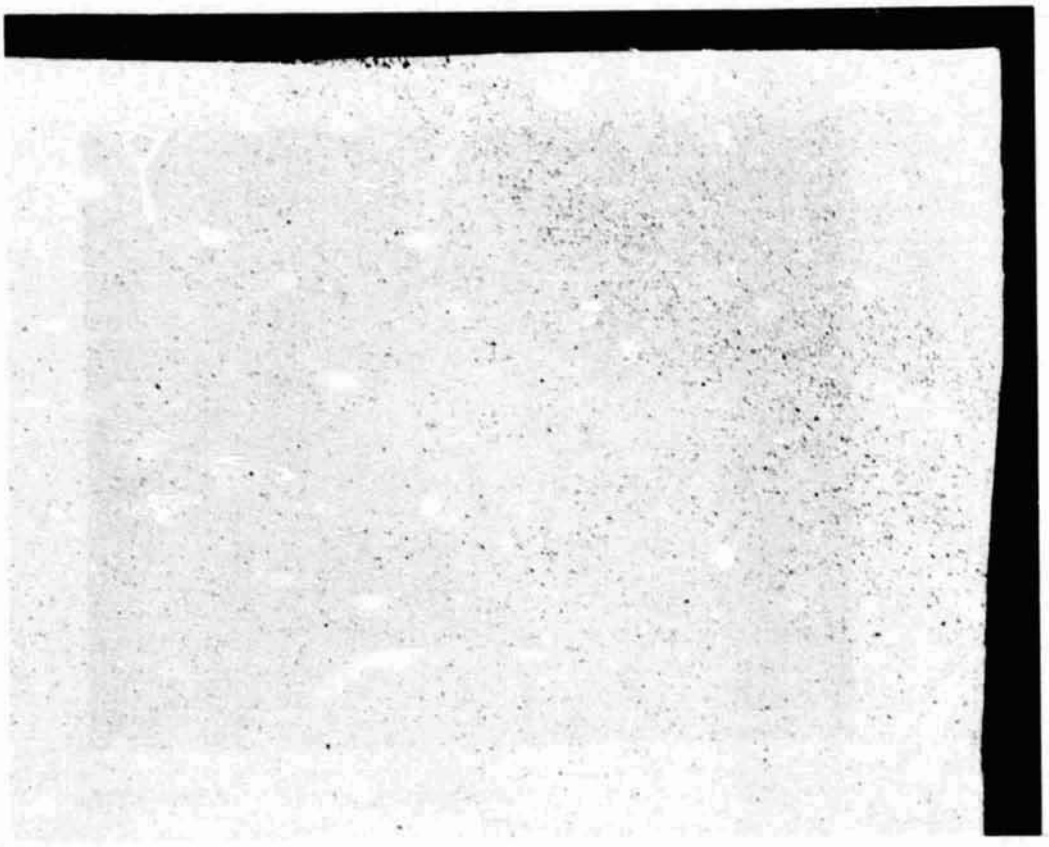

340°-335° Etched 5G257-20X

FIGURE A-23. CHORD SECTION IN DWELL REGION- H-1

335°(-) Aluminum 11299-300X

335°(-) Molybdenum 11300-300X

FIGURE A-24. ELECTRON PROBE SCANS OF REGION SHOWN IN FIGURE A-21 - LARGE PARTICLE AT LEFT CENTER ADJACENT TO END OF CREVICE - H-1

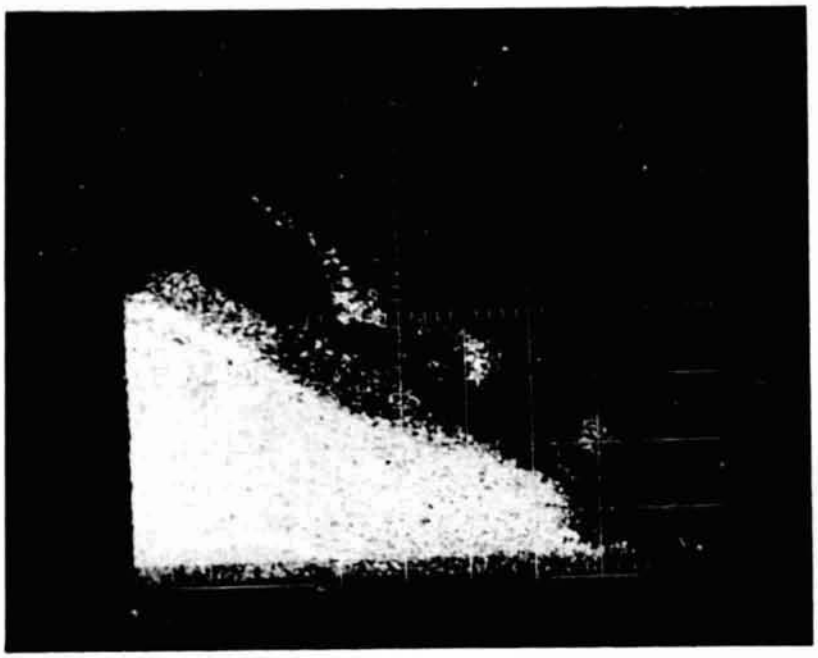

240° (+) Aluminum 11301-300X

240° (+) Molybdenum 11302-300X

FIGURE A-25. ELECTRON PROBE SCANS OF REGION SHOWN IN FIGURE A-16 - LARGE PARTICLE AT TOP RIGHT SURFACE -H-1

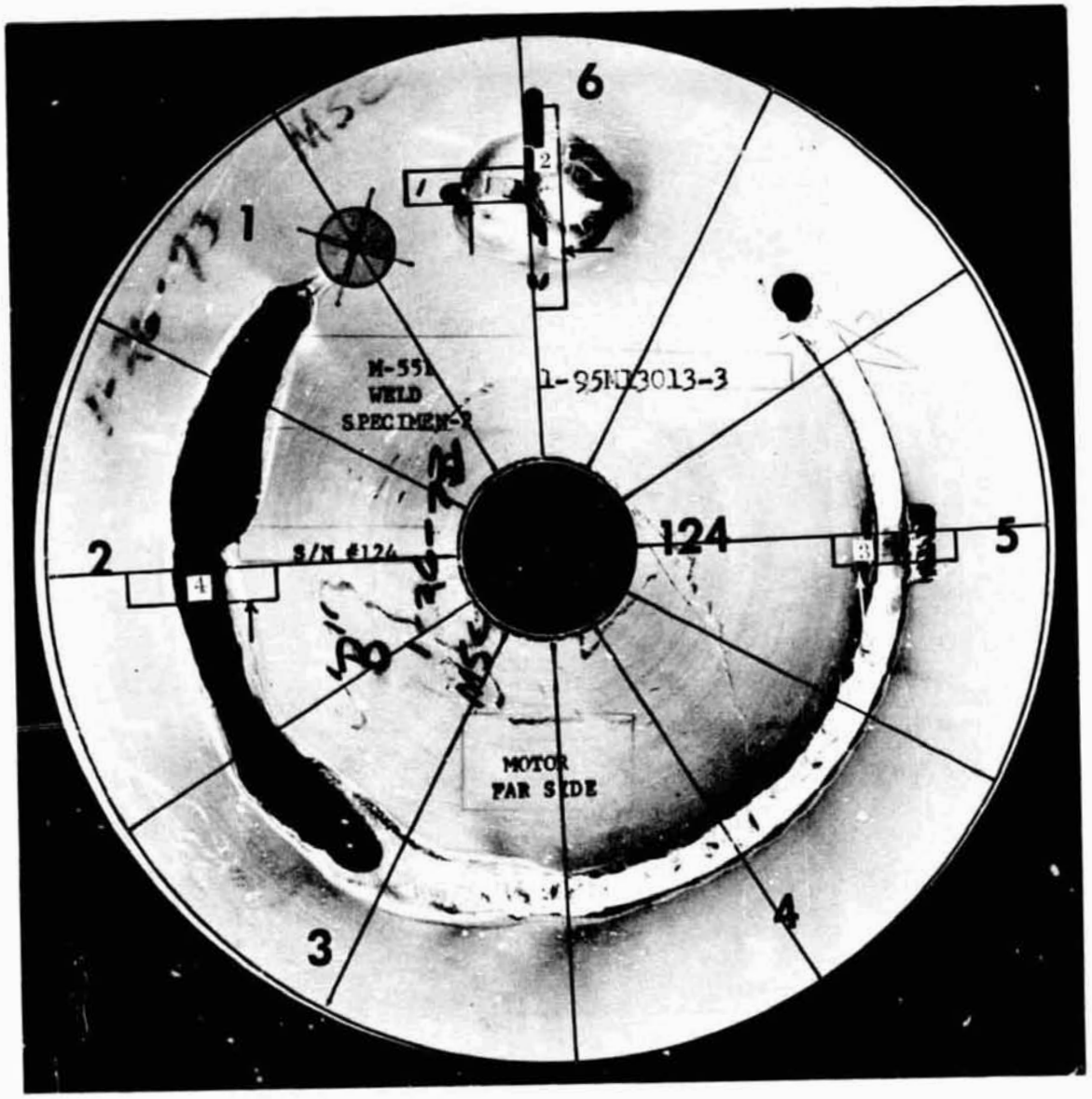

Aluminum

5G443-1X

FIGURE A-26. FRONT SURFACE - S/N 124

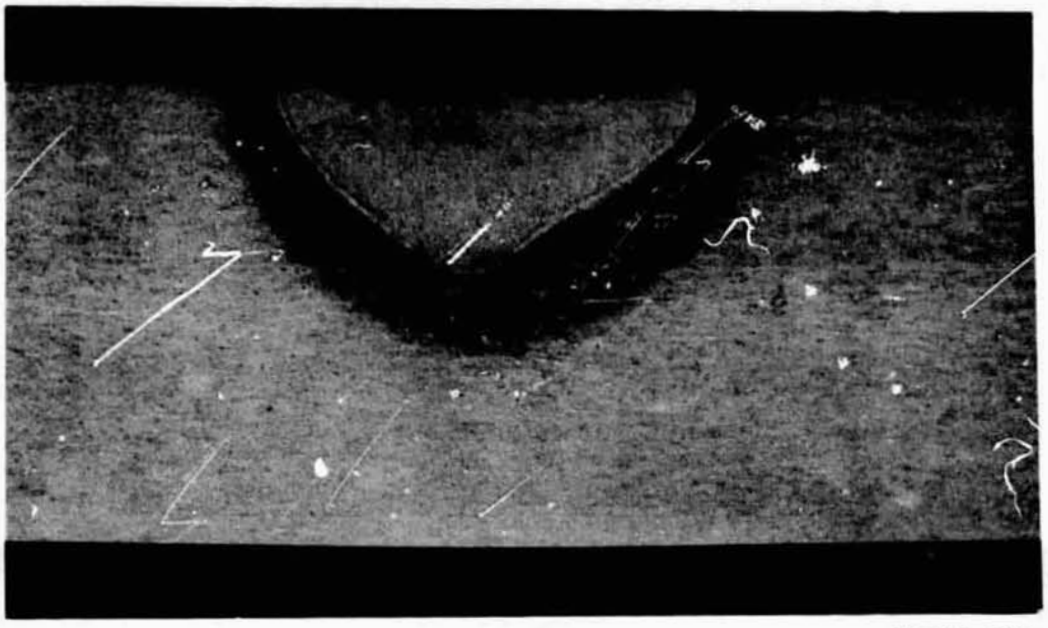

240°(-) Etched 7G483-10X

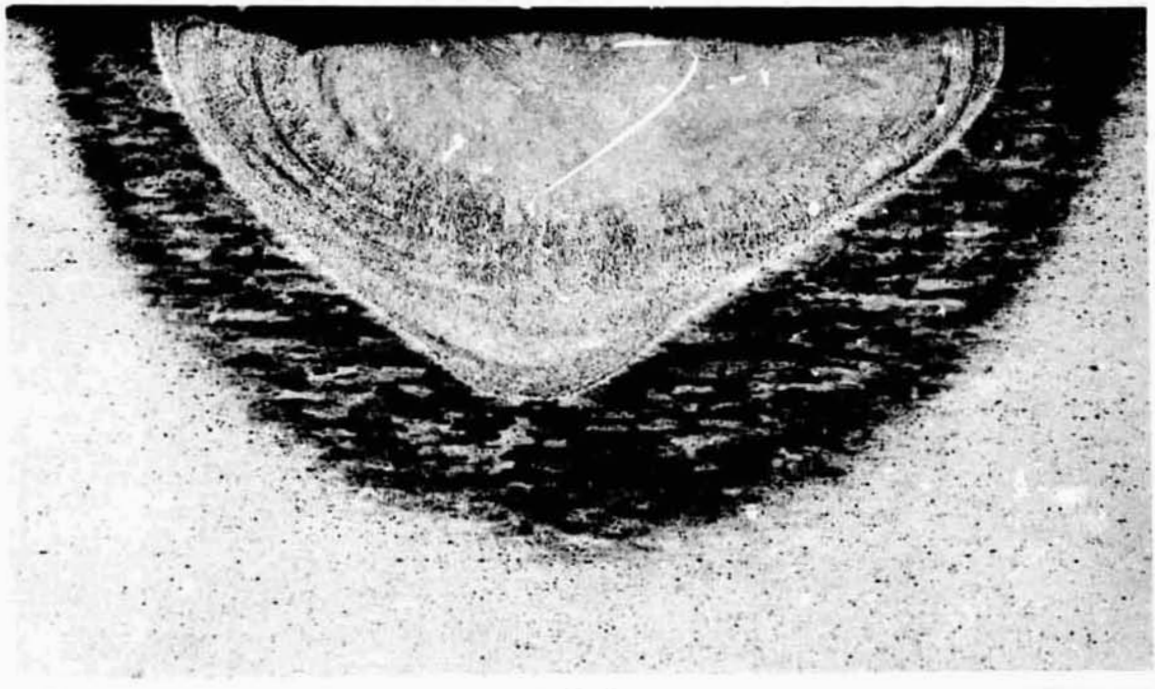

240°(-) Etched 7G485-20X

FIGURE A-27. SECTION THROUGH PARTIAL PENETRATION REGION - S/N 124

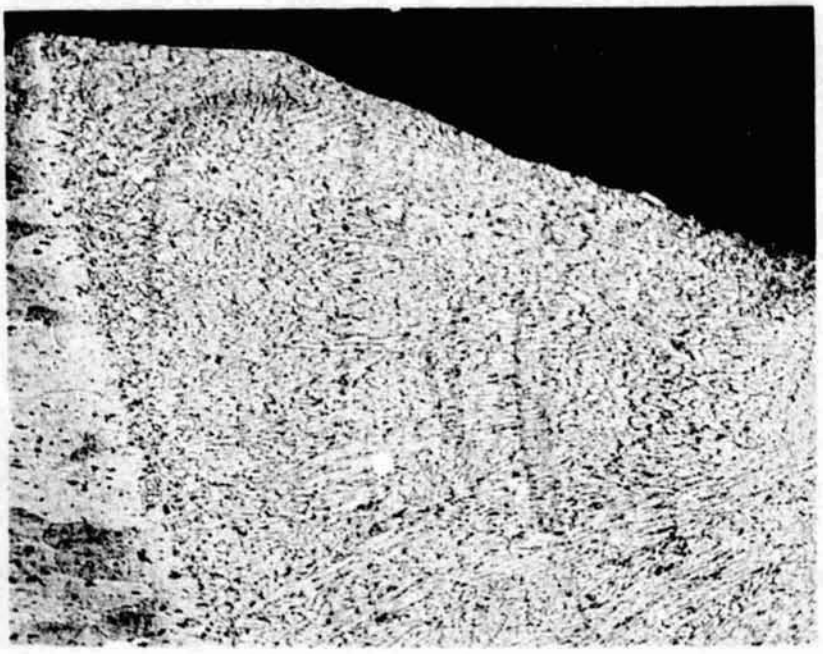

240°(-) Etched 7G486-100X

a. Left fusion line

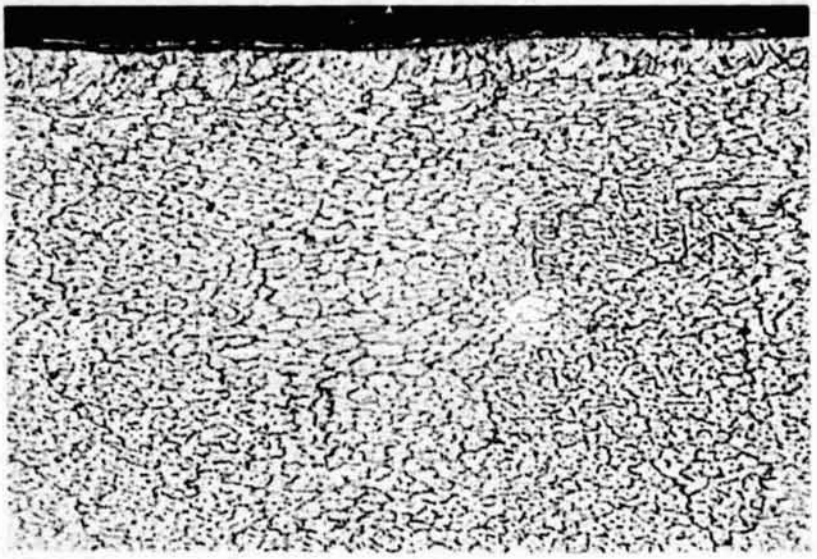

240°(-) Etched 7G487-250X

b. Weld surface

FIGURE A-28. ENLARGED AREAS OF PARTIAL PENETRATION REGION S/N 124

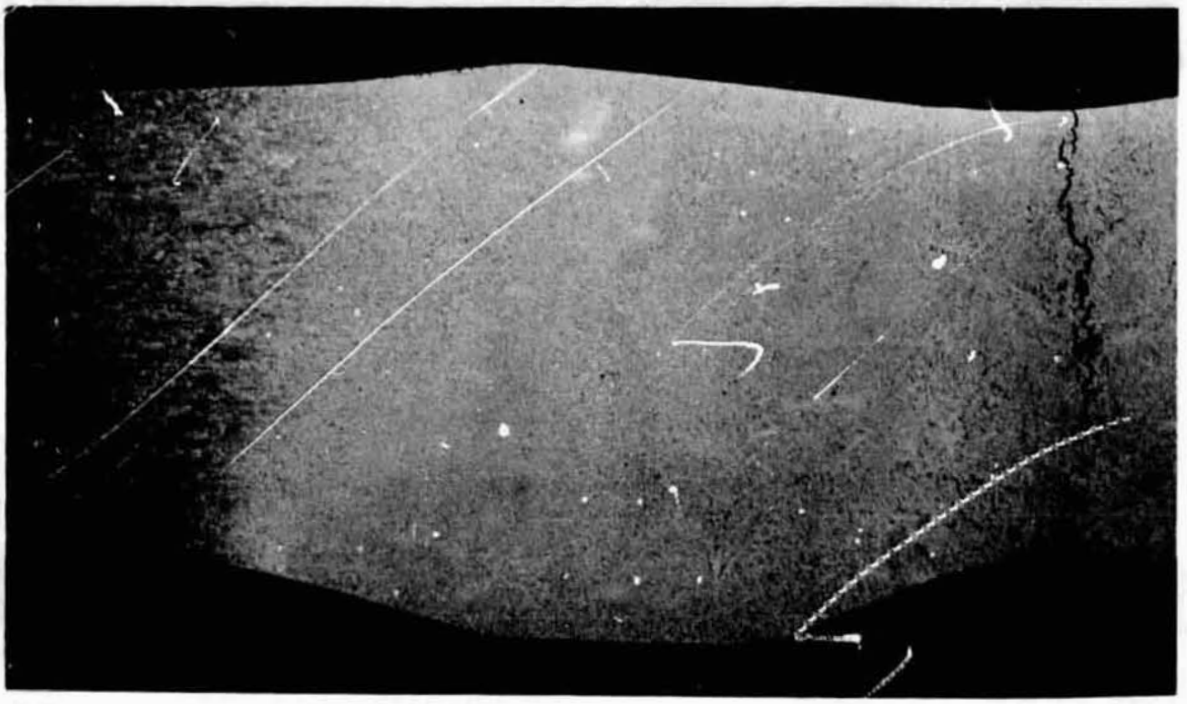

290° (+) Etched 7G481-10X

FIGURE A-29. SECTION THROUGH DWELL REGION S/N 124

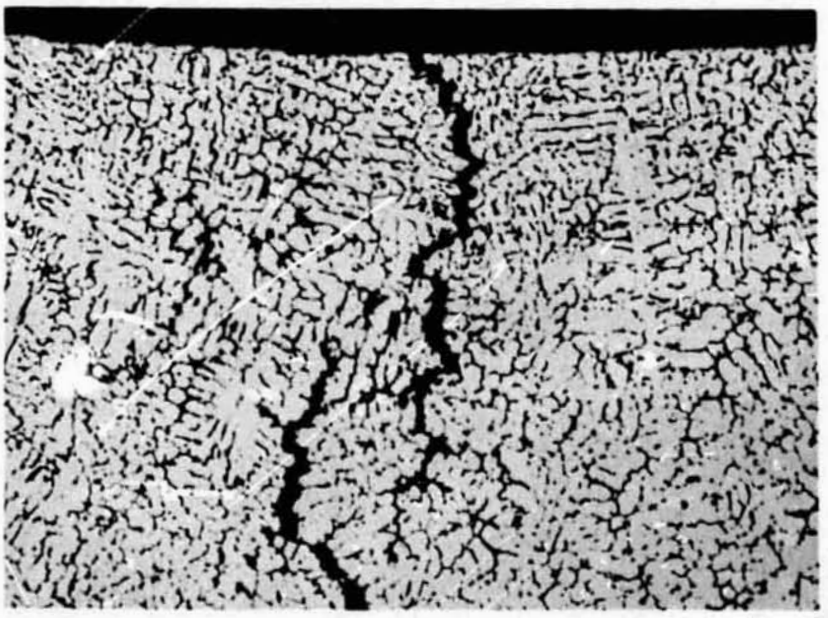

290° (+) Etched 7G482-10CX

FIGURE A-30. SECTION THROUGH CRACK IN DWELL REGION -- S/N 124

350°-330° Etched 7G476-10X

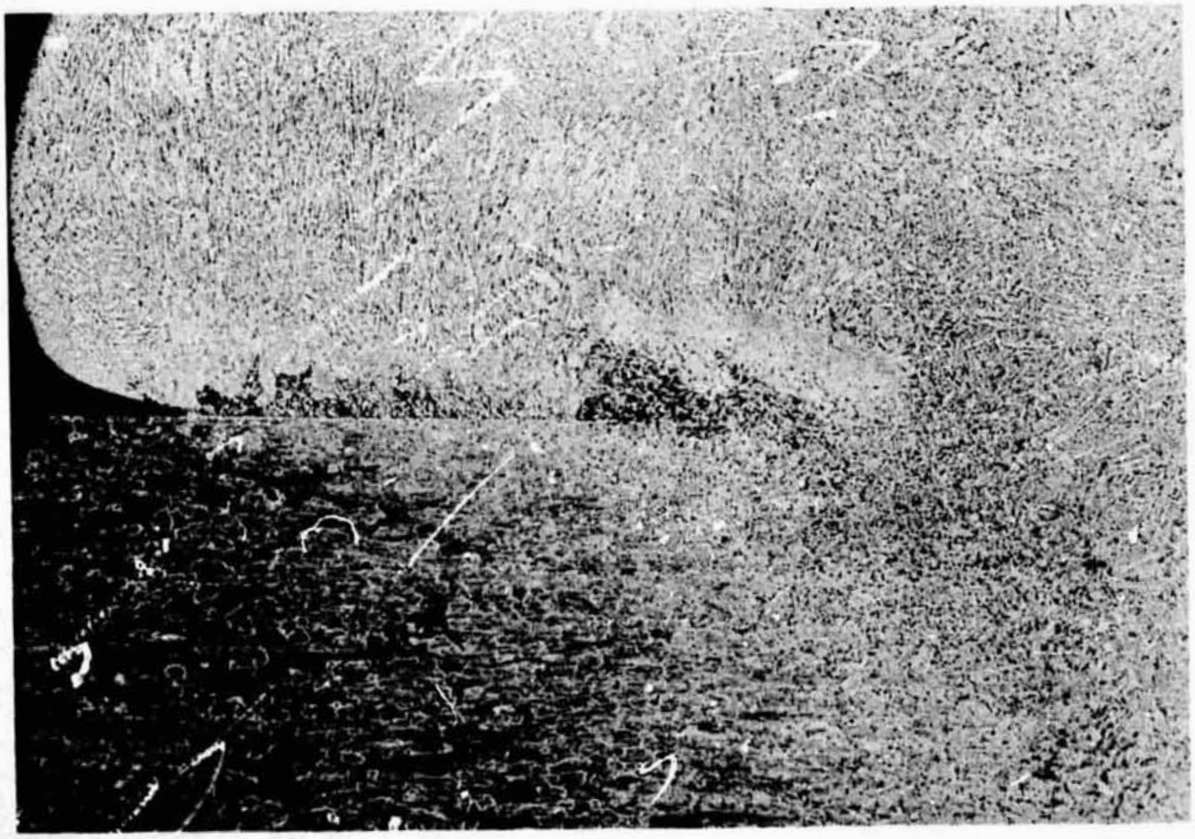

~ 340° Etched 7G477-20X

FIGURE A-31. CHORD SECTION THROUGH DWELL REGION S/N-124

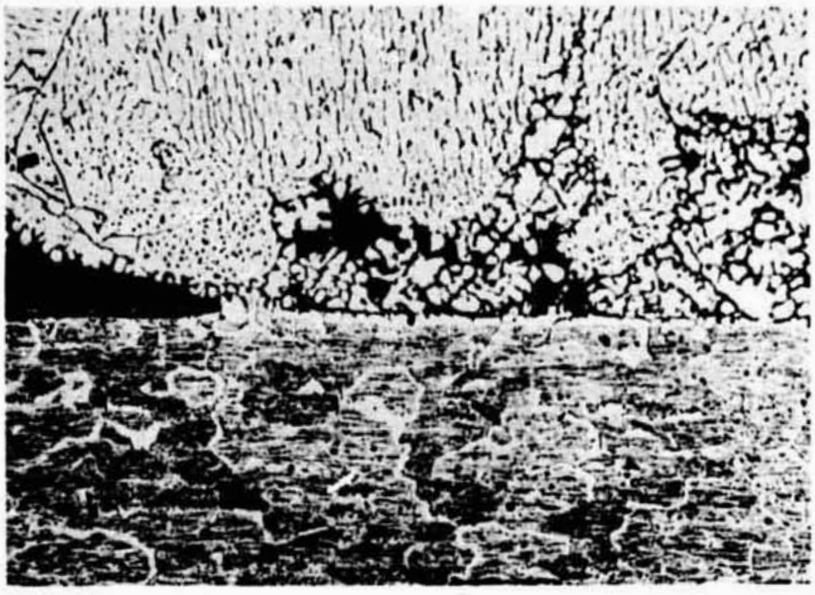

~340° Etched 7G478-100X

a. Weld metal-base metal interface

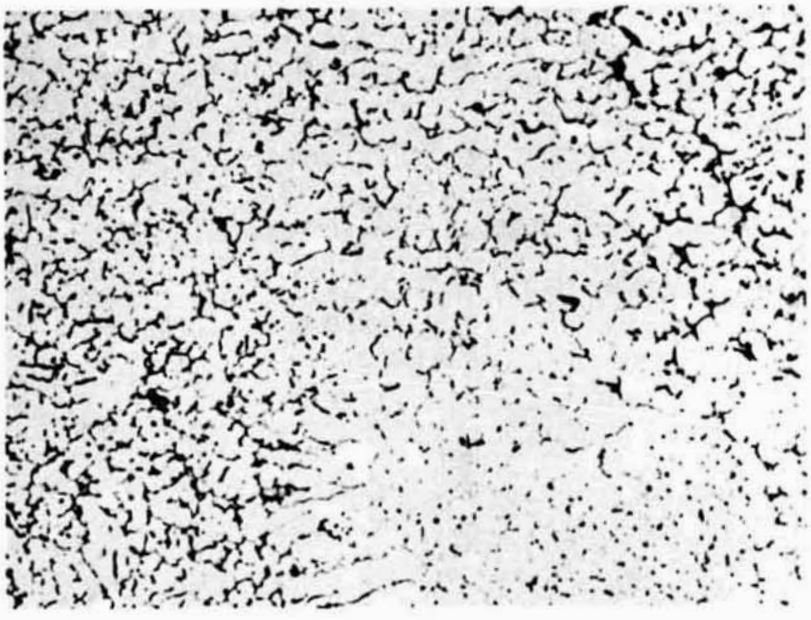

~335° Etched 7G479-100X

b. Internal microstructure

FIGURE A-32. STRUCTURES IN DWELL REGION S/N 124

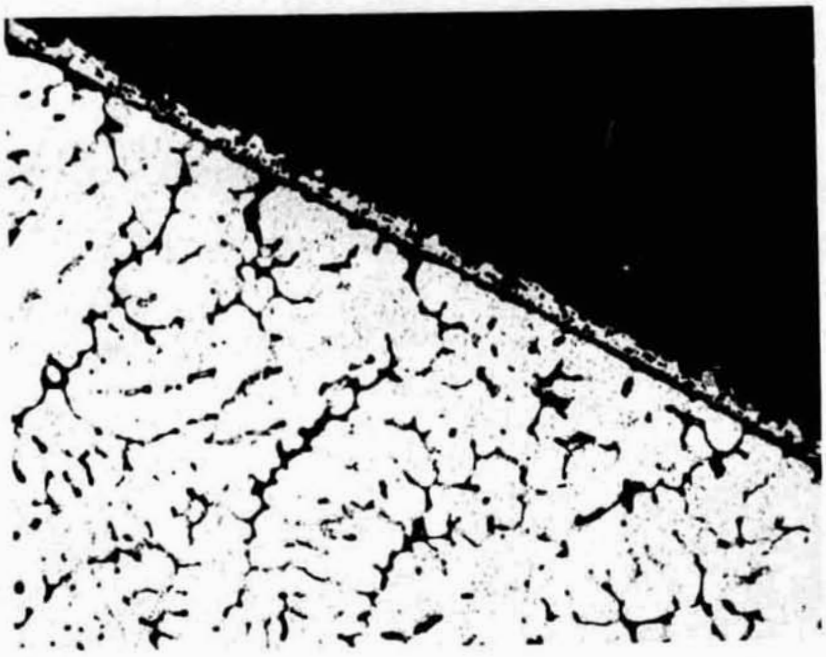

~330° Etched 7G480-250X

c. Surface microstructure

FIGURE A-32. (Continued)
STRUCTURES IN DWELL REGION
S/N 124

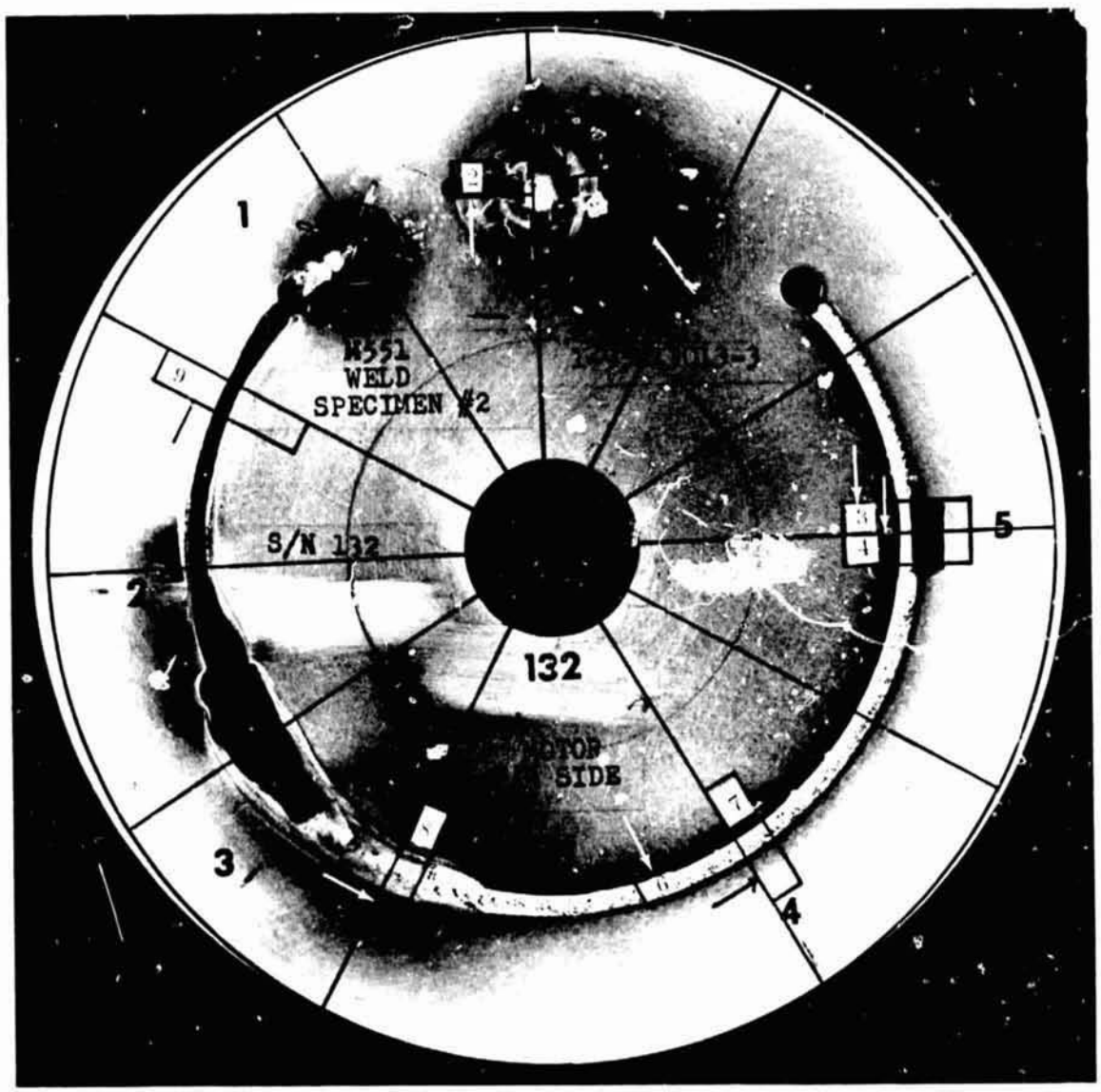

7G515-1X

FIGURE A-33. FRONT SURFACE -S/N 132

7G512-1X

FIGURE A-34. BACK SURFACE - S/N 132

40°(-) Etched 7G518-20X

a. Cut Region

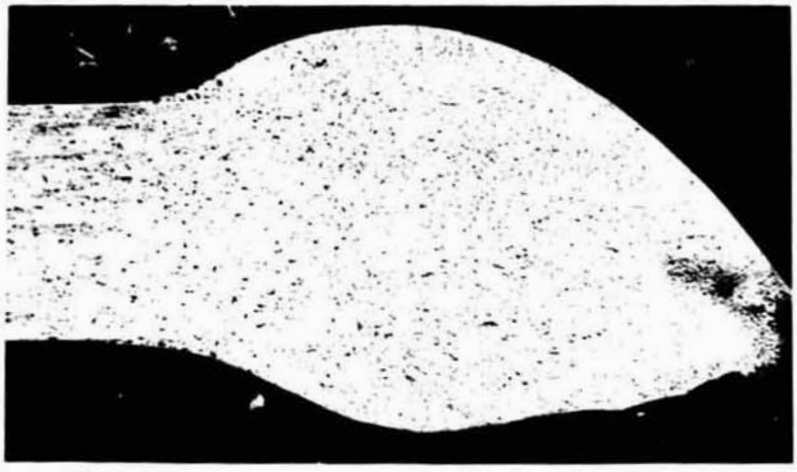

40°(-) Etched 7G519-50X

b. Outside Region

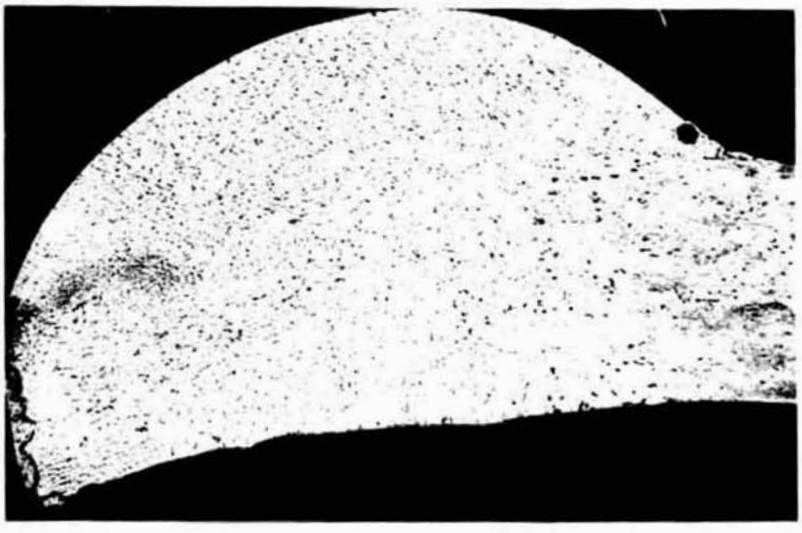

40°(-) Etched 7G520-50X

c. Inside Bead

FIGURE A-35. SECTION THROUGH CUT REGION - S/N 132

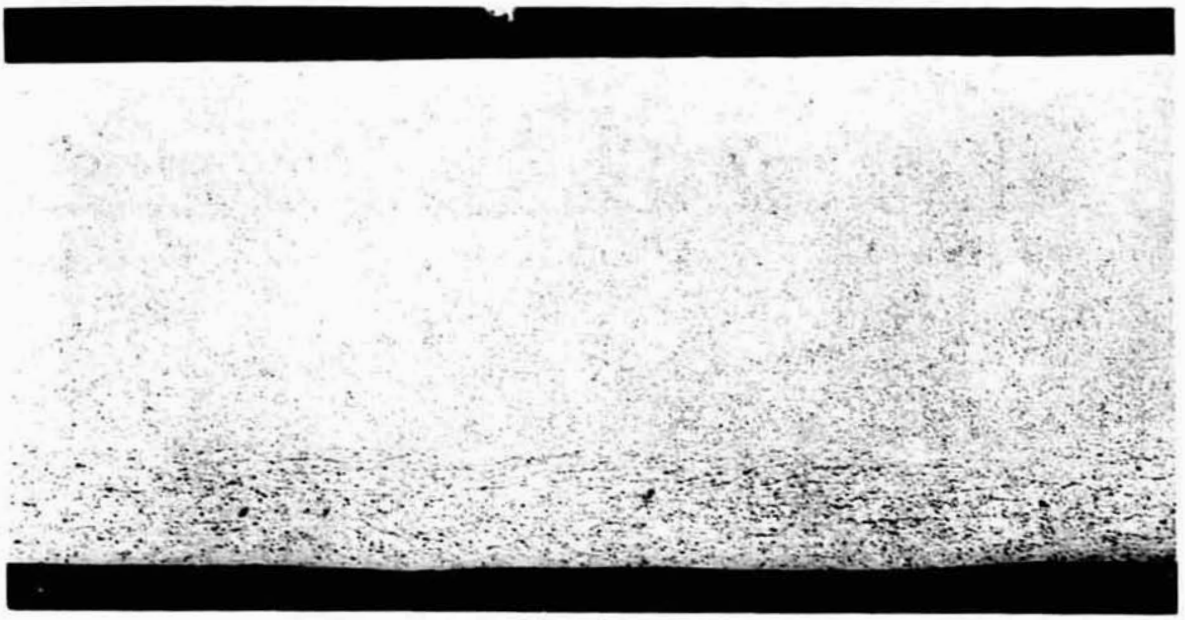

165°-180° Etched 7G516-2

a. Complete section

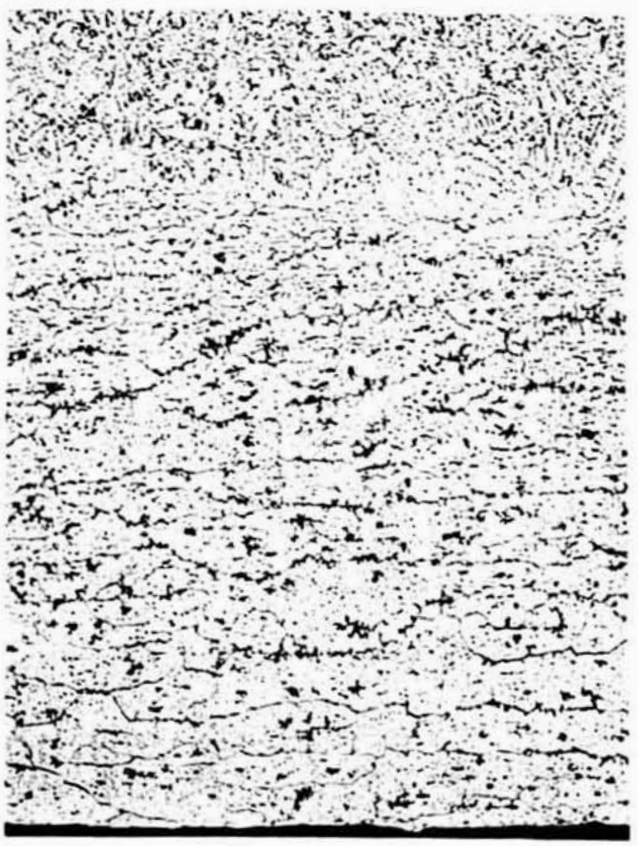

~170° Etched 7G517-100X

b. Bottom finish line

FIGURE A-36. CHORD SECTION IN FULL PENETRATION REGION S/N 132

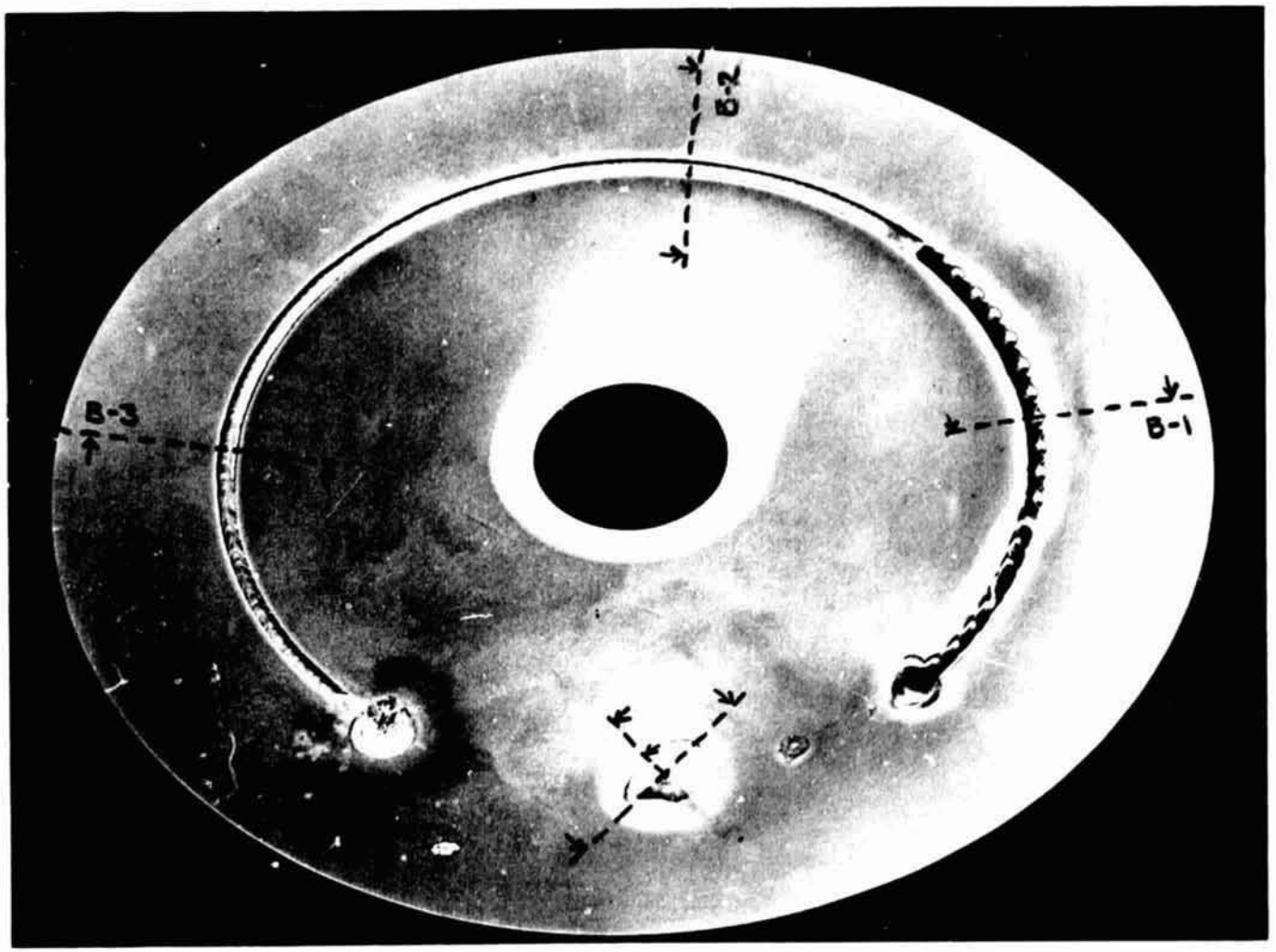

5112-n/X

FIGURE A-37. FRONT OF DISC B SHOWING SECTION LOCATIONS

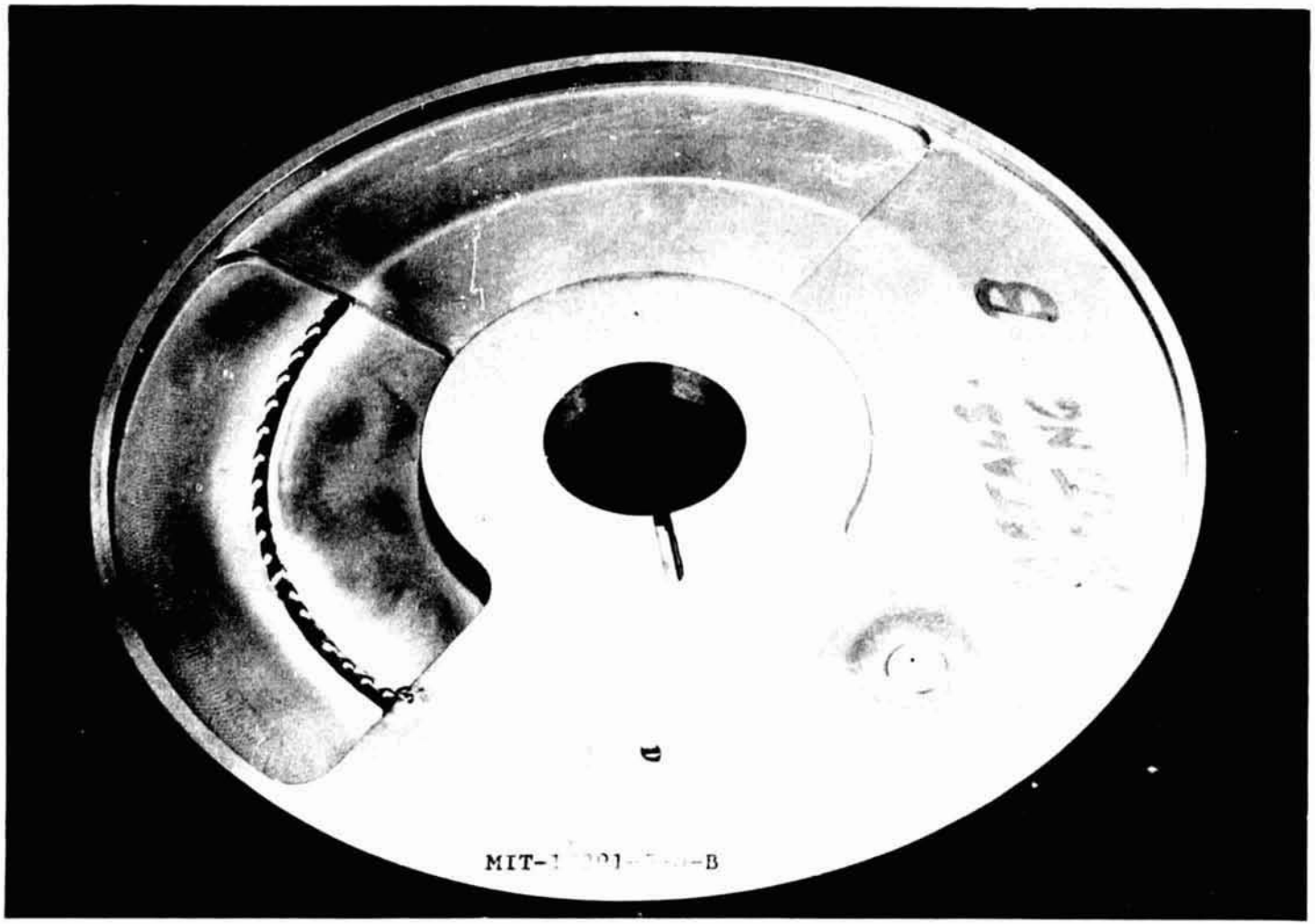

5111-n/X

FIGURE A-38. BACK OF DISC B SHOWING QUADRANT DESIGN

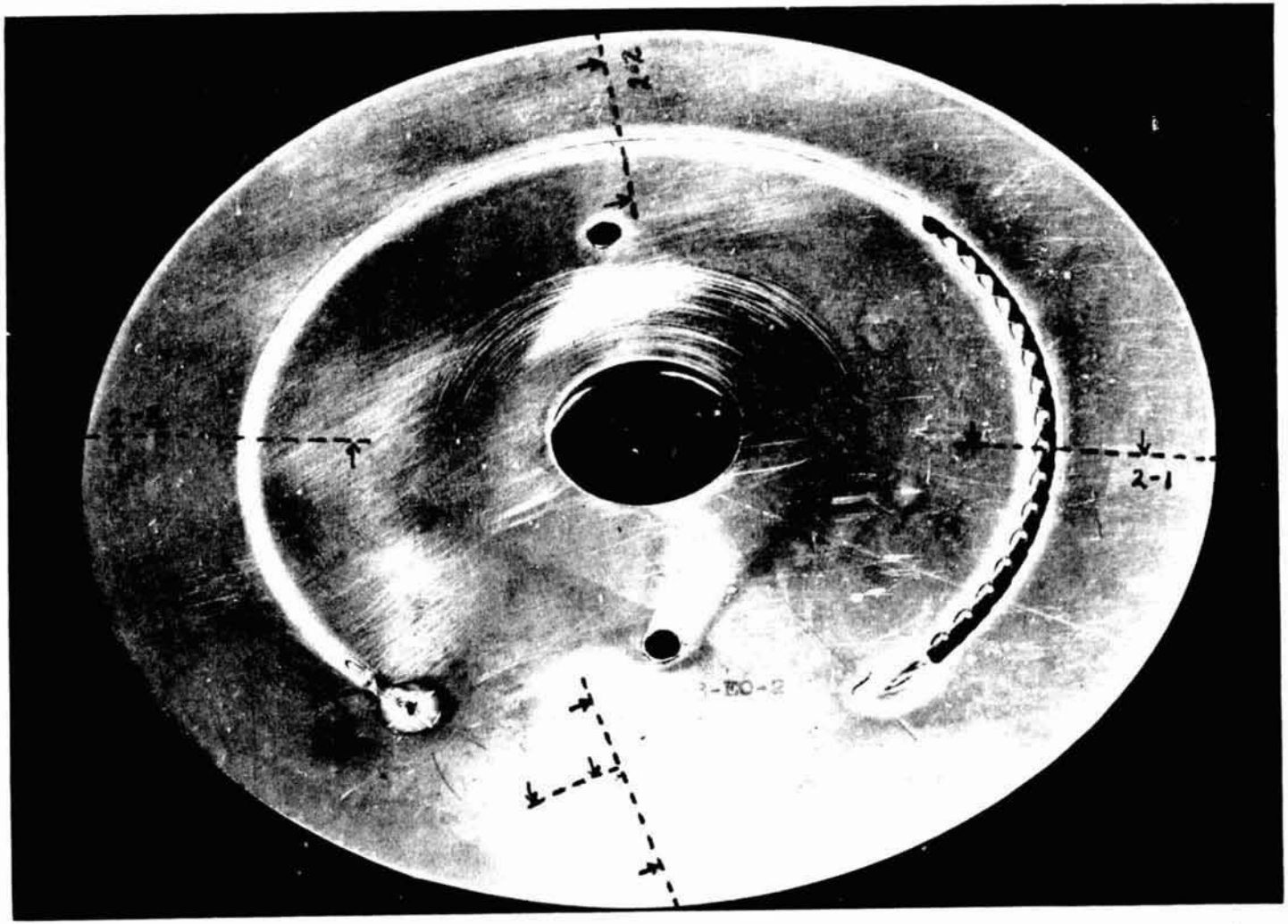

5113-n/X

FIGURE A-39. FRONT OF DISC 2 SHOWING SECTION LOCATIONS

Disc S/N 104

Figures A-40 through A-50 show the front surface and transverse sections through the various regions of a stainless steel disc.

Disc S/N 107

Figures A-51 through A-54 show additional features of a stainless steel disc.

Tantalum Discs

Two tantalum discs, both of the final design, were examined.

Disc S/N 143

This disc is shown in Figure A-55. Sectioning was limited by the extensive cutting that occurred. Figures A-56 through A-63 show the sections examined.

Disc S/N 158

Figures A-64 through A-68 show features of this disc and selected sections taken.

Distortion Measurements

The distortion measurements are given in Table A-1. Distortion in the cut region was greater than in other regions.

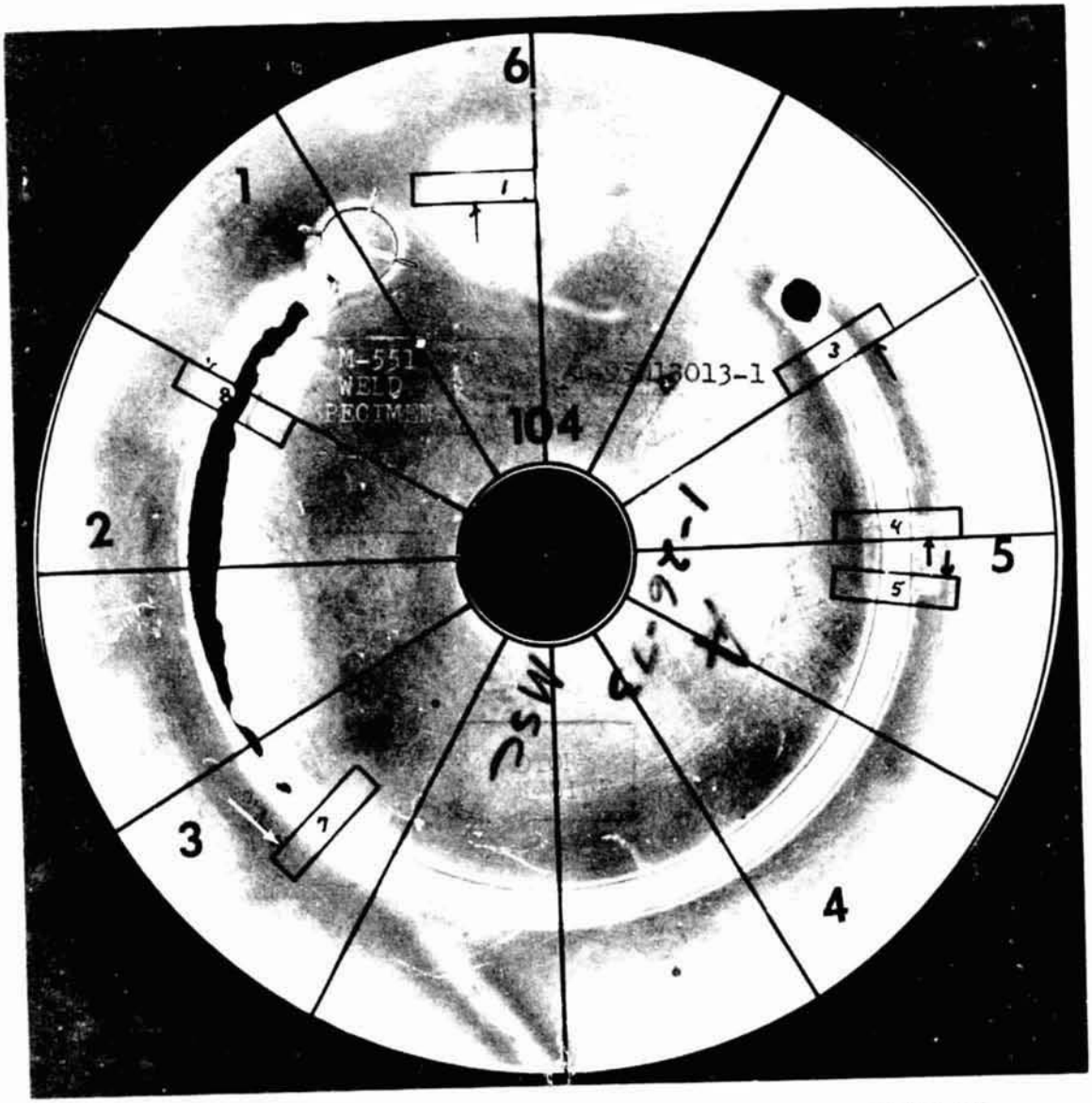

5G442-1X

FIGURE A-40. FRONT SURFACE - S/N 104

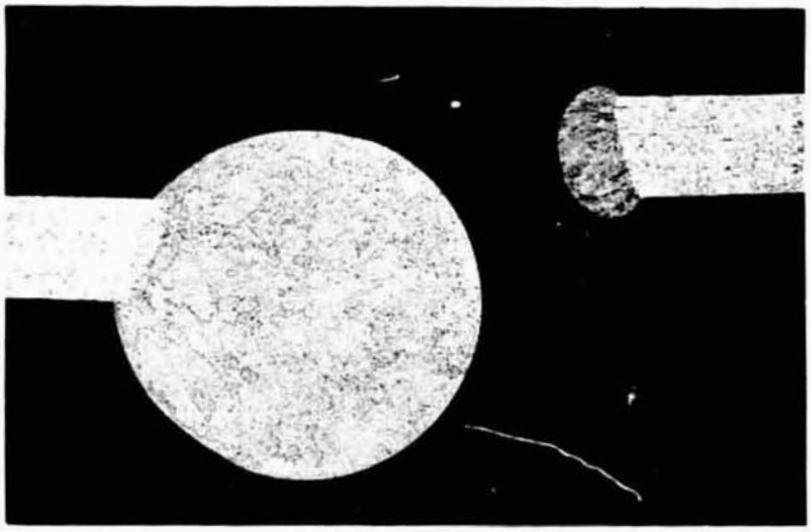

30°(+) Etched 7G500-20X

FIGURE A-41. SECTION THROUGH CUT REGION - S/N 104

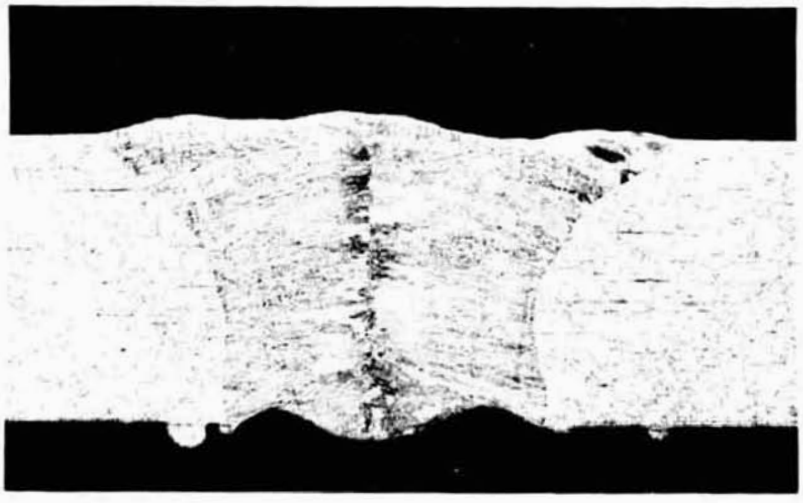

105°(+) Etched 7G498-20X

FIGURE A-42. SECTION THROUGH RAMP REGION - S/N 104

105° (+) Etched 7G481-10X

FIGURE A-43. FUSION LINE REGION
S/N 104

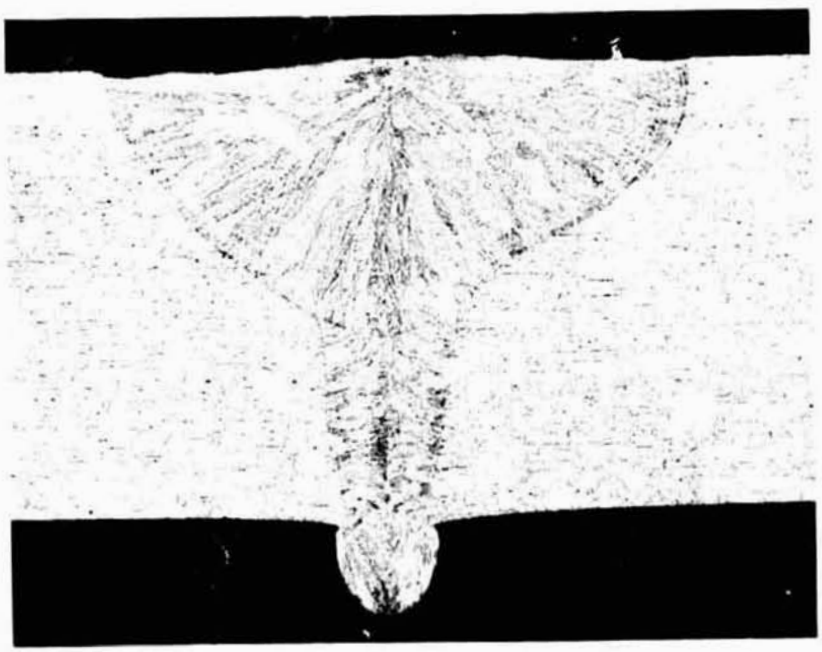

235° (-) Etched 7G496-20X

FIGURE A-44. SECTION THROUGH FULL
PENETRATION REGION
S/N 104

235° (-) Etched 7G497-100X

FIGURE A-45. SECTION AT ROOT OF WELD

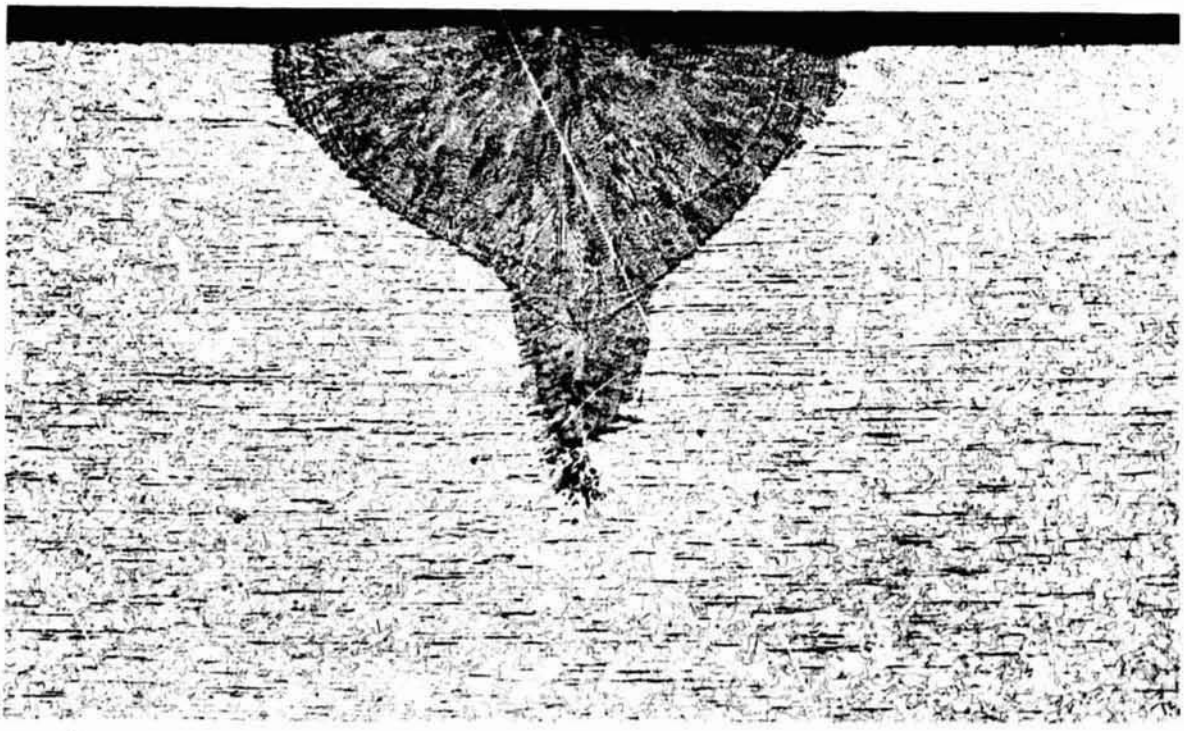

240° (+) Etched 7G494-20X

FIGURE A-46. SECTION THROUGH PARTIAL PENETRATION REGION - S/N 104

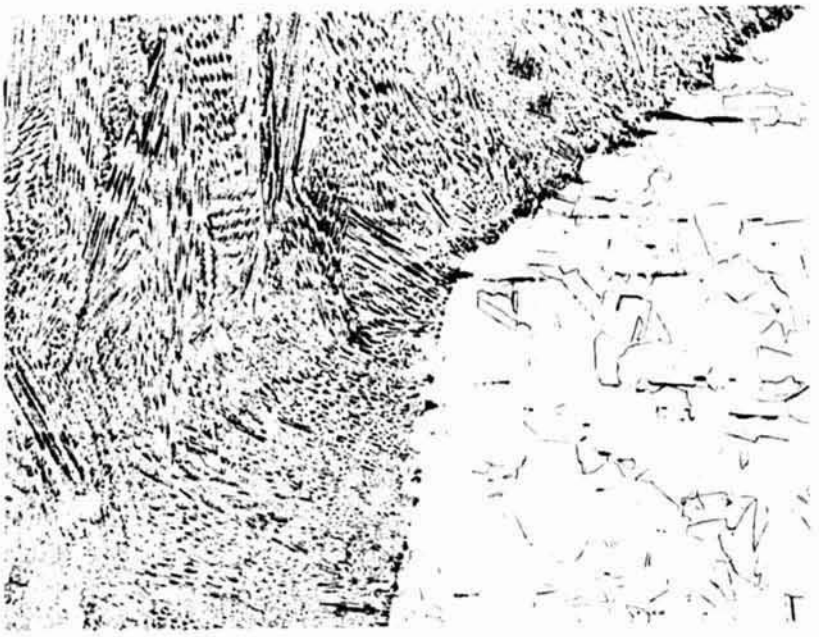

240° (+) Etched 7G495-100X

FIGURE A-47. FUSION LINE REGION AT SHAPE CHANGE

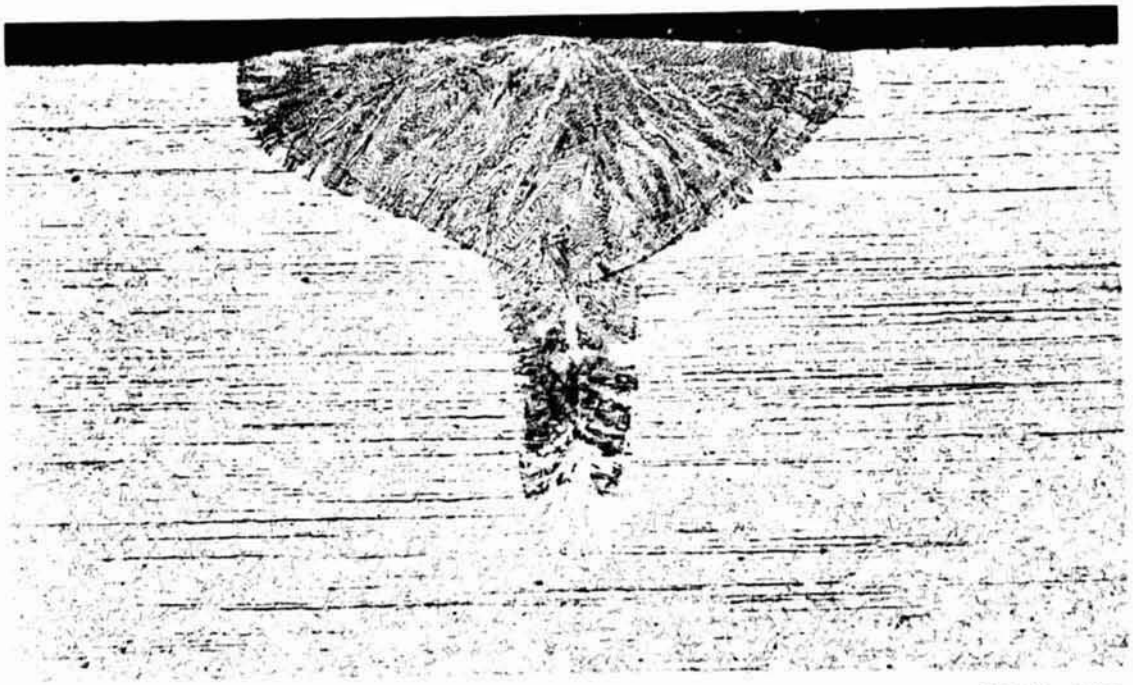

270° (+) Etched 7G491-20X

FIGURE A-48. SECTION THROUGH PARTIAL PENETRATION REGION S/N 104

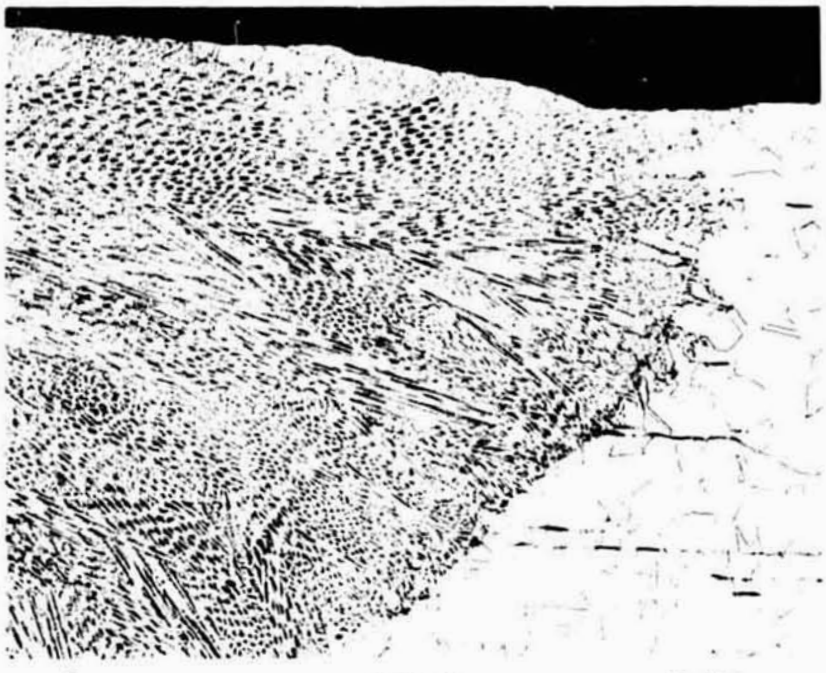

270°(+) Etched 7G493-100X

a. Fusion Line at Top

270°(+) Etched 7G492-100X

b. Root of Weld

FIGURE A-49. WELD STRUCTURES - S/N 104

345°-330° Etched 7G488-20X

a. Chord Section

FIGURE A-50. SECTIONS THROUGH DWELL REGION - S/N 104

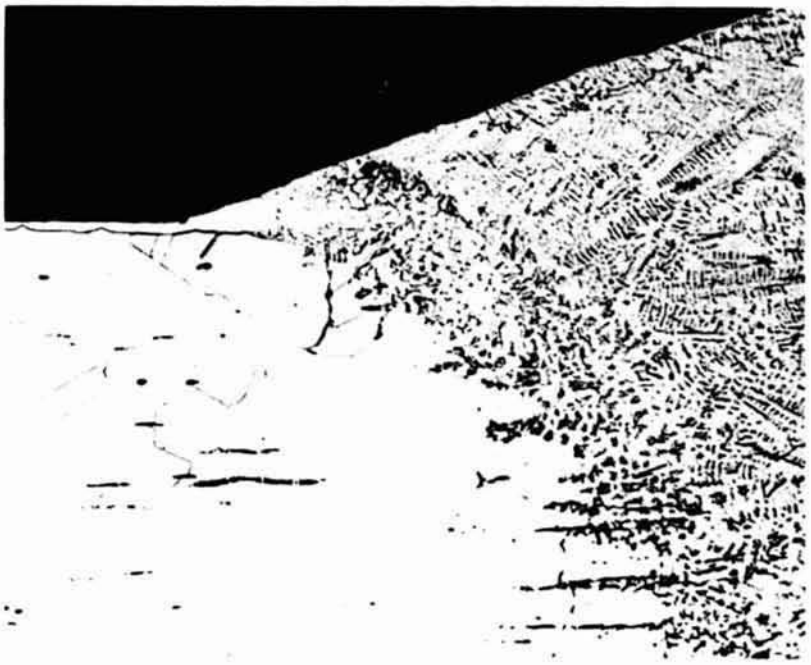

-345° Etched 7G489-100X

b. Top Edge Fusion Line

-340° Etched 7G490-250X

c. Typical Weld Microstructure

FIGURE A-50. (Continued)
SECTIONS THROUGH DWELL REGION
S/N 104

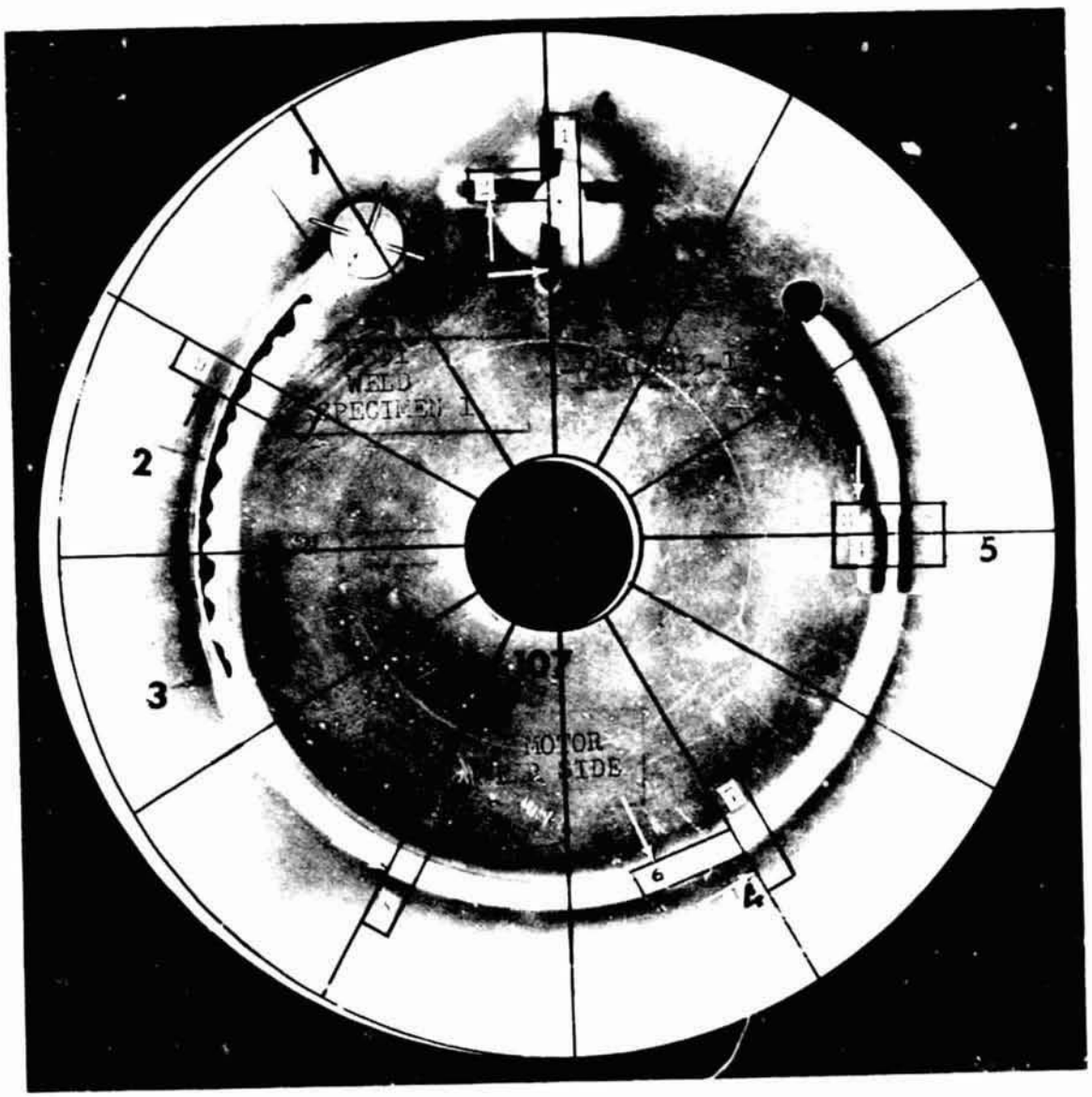

7G511-1X

FIGURE A-51. FRONT SURFACE - S/N 107

7G510-1X

FIGURE A-52. BACK SURFACE - S/N 107

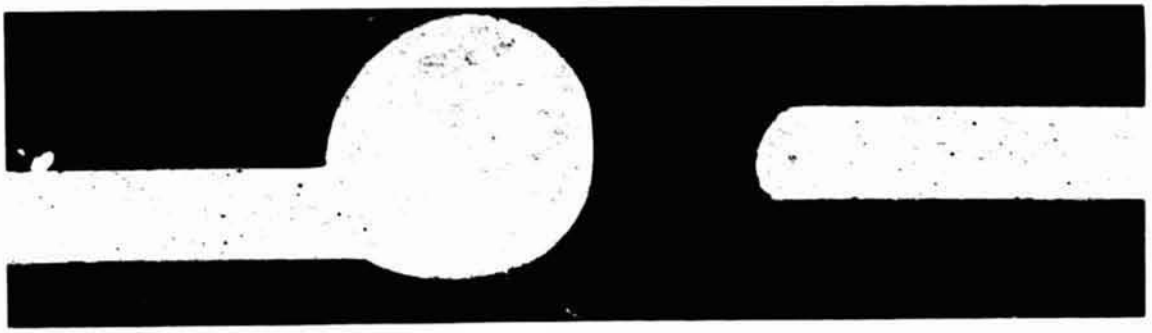

35°(+) Etched 7G522-20X

FIGURE A-53. SECTION THROUGH CUT REGION S/N 107

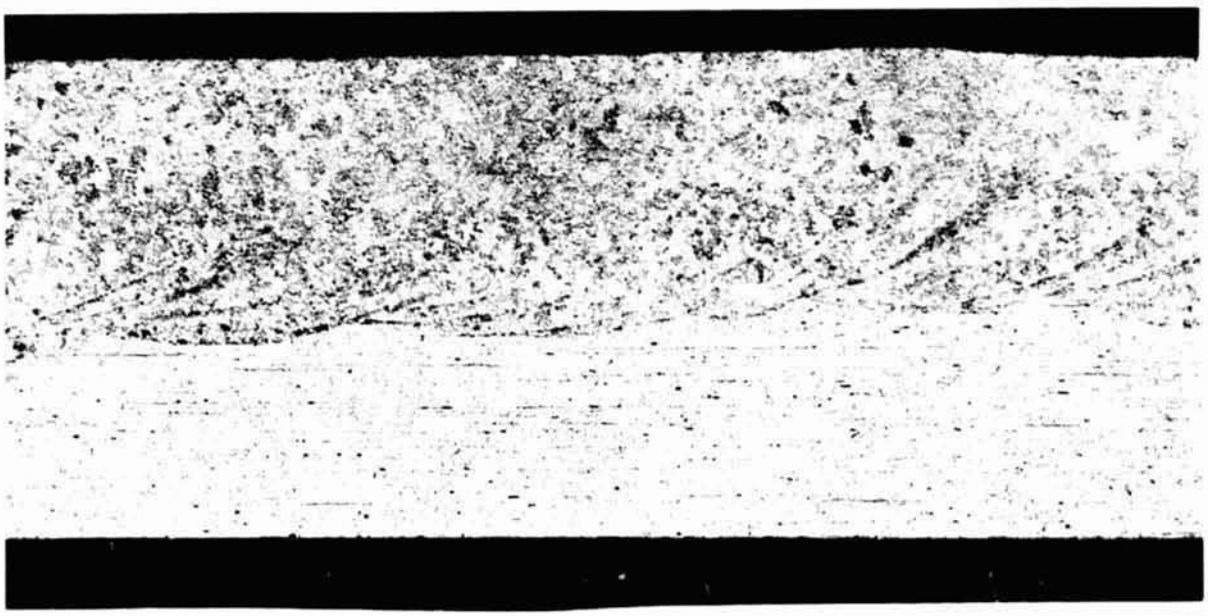

160°-180° Etched 7G521-20X

FIGURE A-54. CHORD SECTION THROUGH FULL PENETRATION REGION - S/N 107

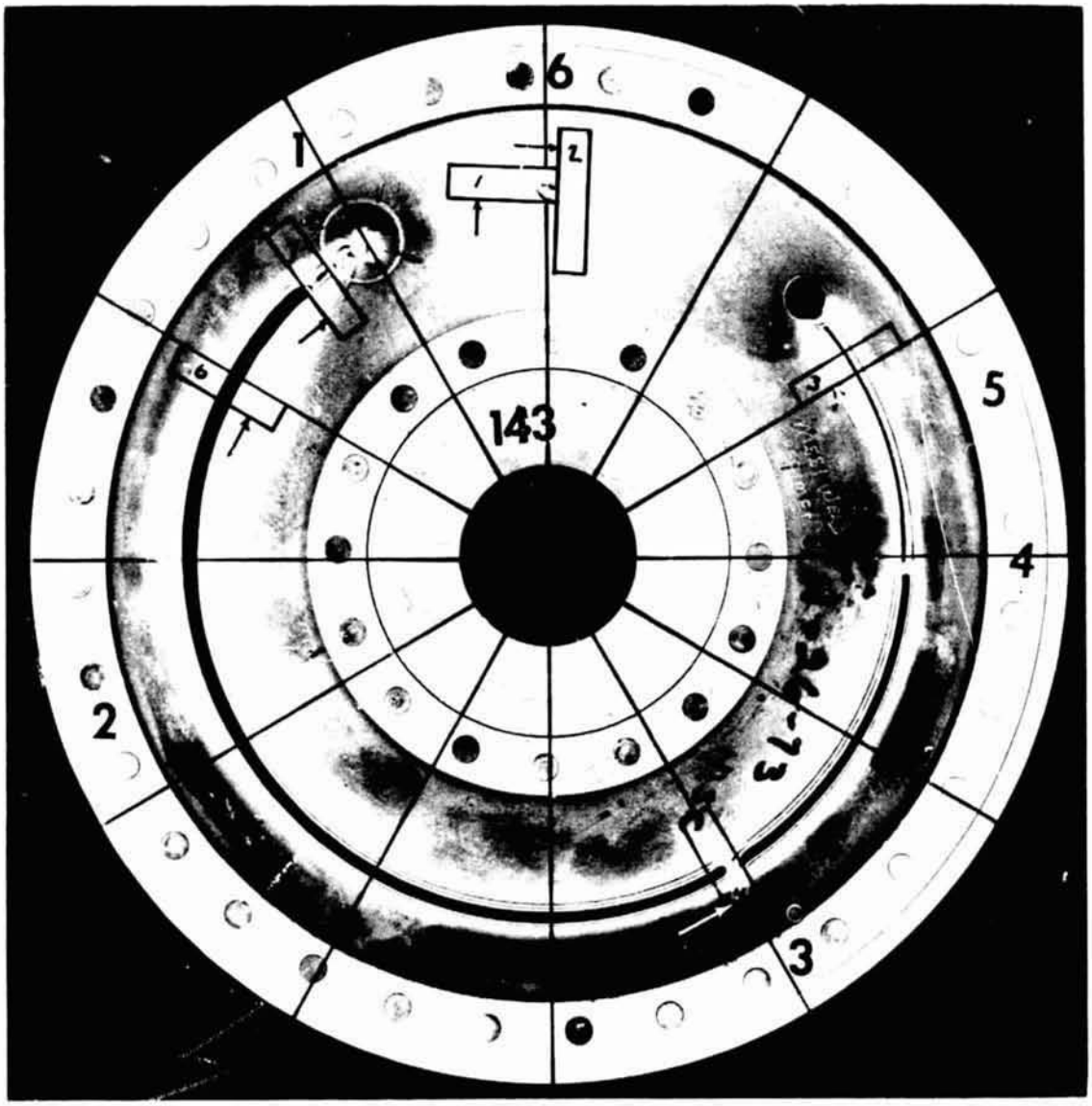

5G444-1X

FIGURE A-55. FRONT SURFACE - S/N 143

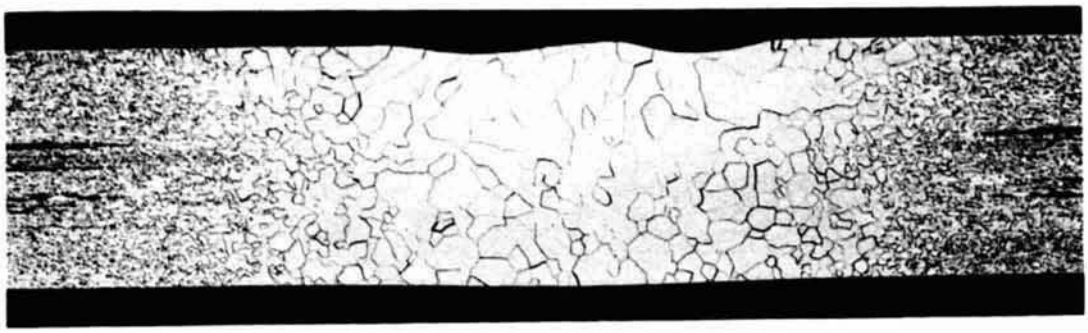

15°(-) Etched 7G509-20X

FIGURE A-56. SECTION THROUGH REGION BEFORE CUT S/N 143

35°(-) Etched 7G506-20X

FIGURE A-57. SECTION THROUGH CUT REGION S/N 143

350°(-) Etched 7G507-100X

FIGURE A-58. BOTTOM SURFACE OF OUTSIDE CUT EDGE S/N 143

35°(-) Etched 7G508-250X

FIGURE A-59. BOTTOM SURFACE OF INSIDE CUT EDGE S/N 143

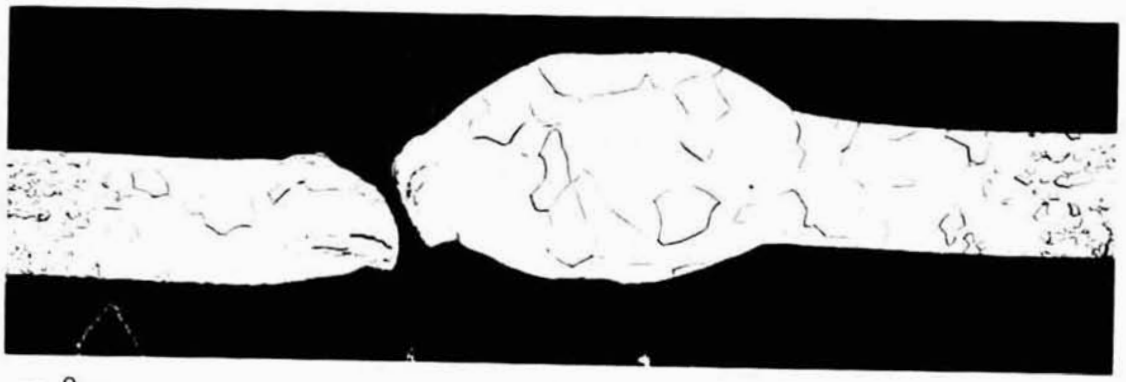

175°(+) Etched 7G504-20X

FIGURE A-60. SECTION THROUGH BRIDGE BROKEN IN CUTTING S/N 143

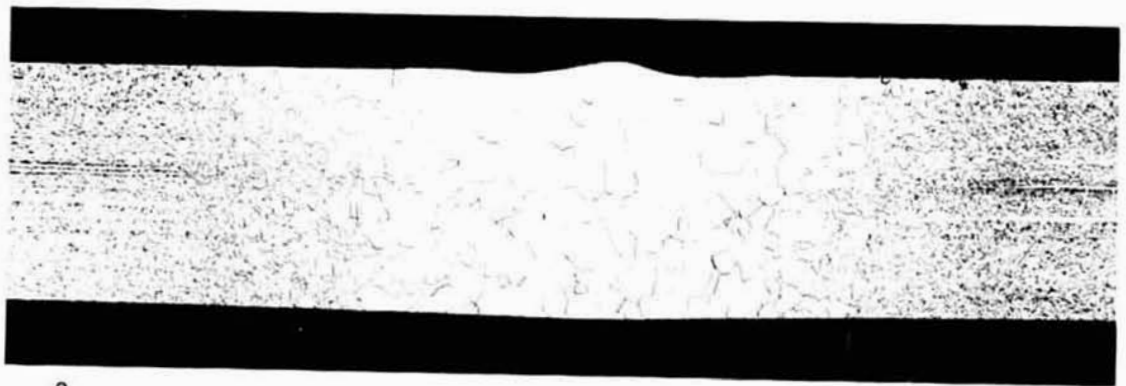

270°(+) Etched 7G503-20X

FIGURE A-61. SECTION THROUGH PARTIAL PENETRATION REGION S/N 143

325° (-) Etched 7G502-1

FIGURE A-62. SECTION THROUGH DWELL REGION S/N 143

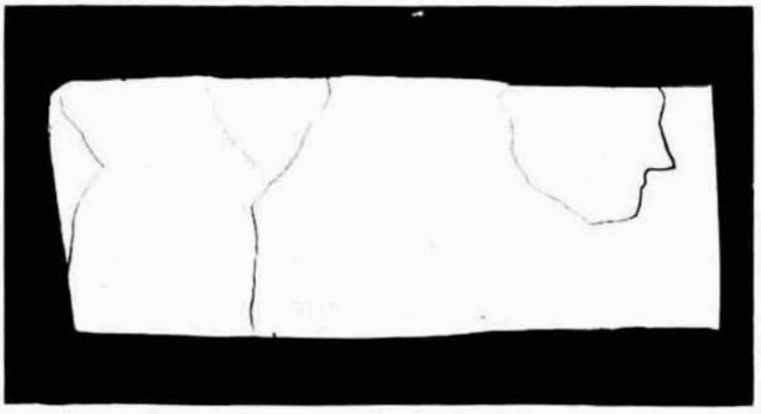

330°-325° Etched 7G501-20X

FIGURE A-63. CHORD SECTION THROUGH DWELL REGION S/N 143

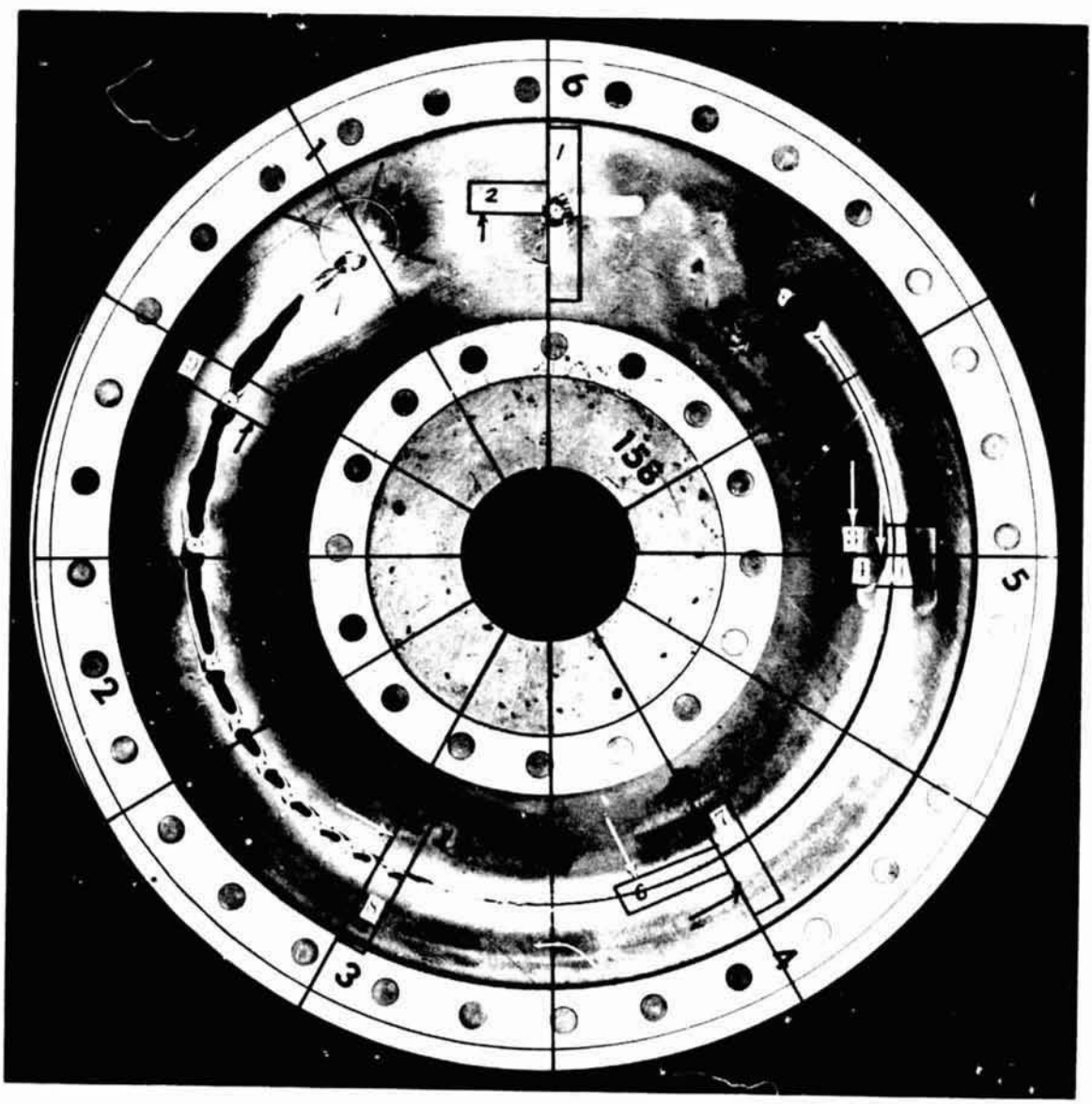

7G515-1X

FIGURE A-64. FRONT SURFACE S/N 158

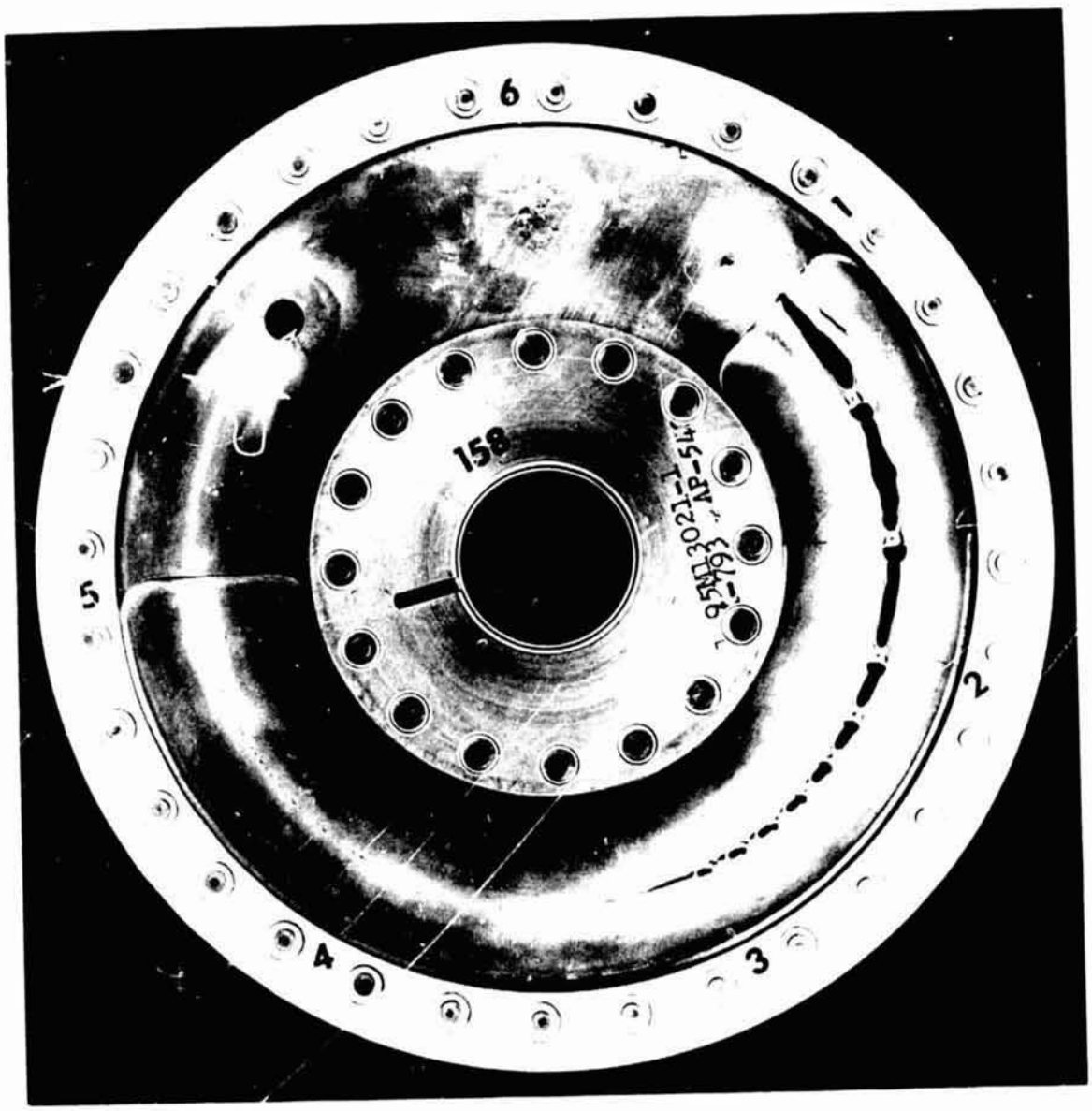

7G514-1X

FIGURE A-65. BACK SURFACE S/N 158

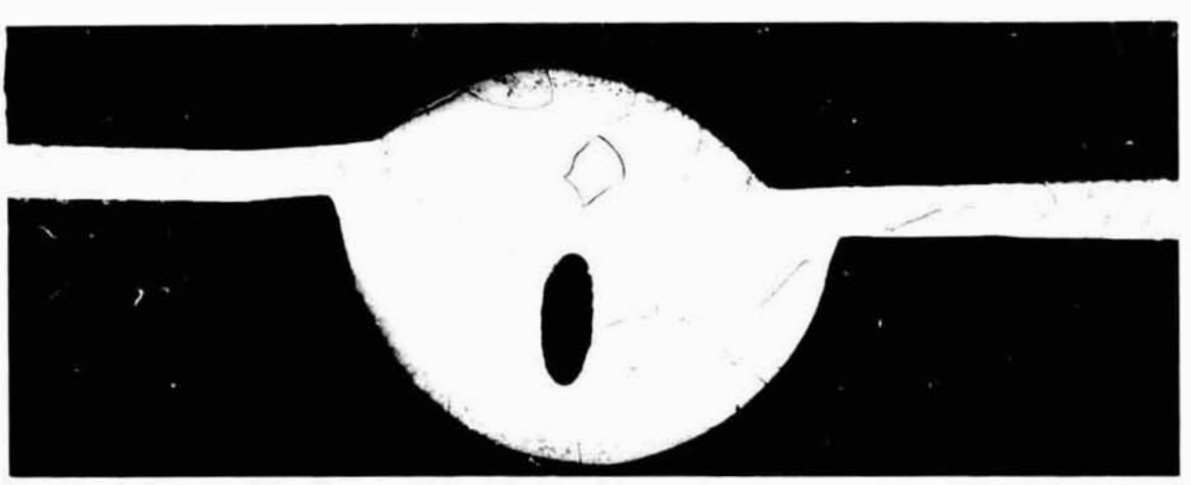

35°(-) Etched 7G526-20X

FIGURE A-66. SECTION THROUGH BRIDGE IN CUT REGION S/N 158

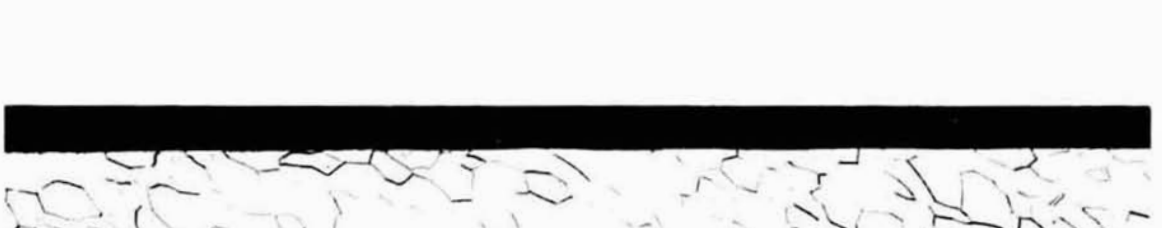

160°-180° Etched 7G525-20X

FIGURE A-67. CHORD SECTION THROUGH FULL PENETRATION REGION S/N 158

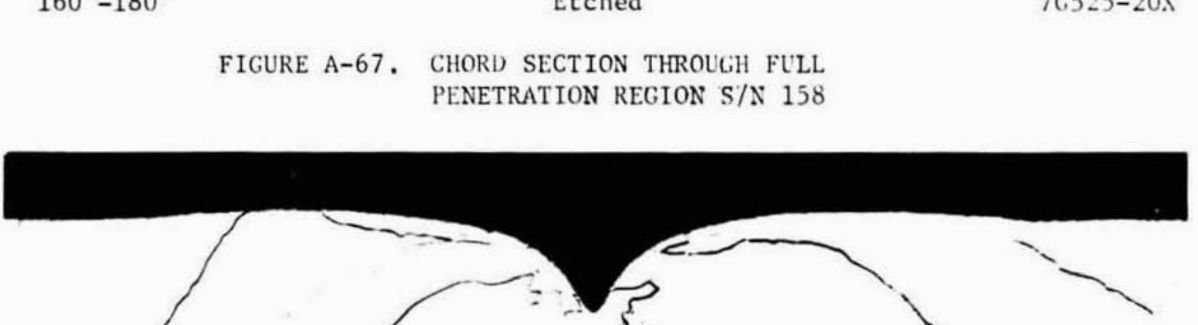

330°(-) Etched 7G523-20X

FIGURE A-68. SECTION THROUGH DWELL REGION S/N 158

TABLE A-1. DISTORTION MEASUREMENTS

Location, degrees	Distortion, inch x 10^{-3}(a)					
	Aluminum S/N 132		Stainless Steel S/N 107		Tantalum S/N 158	
	In	Out	In	Out	In	Out
0	-2	-2	0	+3	0	+1
30	-2	-23	+5	+6	+2	+2
60	+3	-32	+8	+16	0	0
90	(b)	-28	+5	+11	0	0
120	+1	-13	+2	+2	0	0
150	+1	-1	+2	+4	0	+2
180	+4	+4	+1	+4	0	+2
210	+2	-1	-1	+4	0	0
240	0	-8	-2	+4	0	0
270	-3	-11	-1	+4	0	0
300	-4	-8	+1	+3	+1	0
330	(b)	(b)	0	+3	0	+1

(a) + = distortion toward electron gun

- = distortion away from electron gun

(b) No measurement, probe in cut or dwell region.

SECTION B. EVALUATION OF SKYLAB AND FINAL GROUND CHARACTERIZATION METALS MELTING DISC

A review meeting on this experiment held at MSFC was attended on July 19. Skylab specimens S/N-106, S/N-129, and S/N 145 were hand carried to Battelle following that meeting. A post flight series of ground characterization specimens, S/N-110, S/N 130 and S/N 147 were received at Battelle in August. Sections from the Skylab samples for examination at MSFC and others were returned to MSFC on July 26. Similar sections from the post flight ground characterization samples were returned to MSFC September 10.

SPECIMEN PROCESSING

Processing of the specimens at Battelle has followed the procedures previously developed and demonstrated in processing ground characterization samples. Visual examinations, thickness and distortion measurements, radiographic inspection, sectioning, and metallographic examinations were conducted.

RESULTS

Results of the thickness and distortion measurements are shown in Tables B-1 and B-2. Good agreement with intended dimensions was observed except for the two tantalum discs. The thickness variation in the cut and ramp regions of these discs may have influenced the extent and nature of cutting. The distortion measurements appear to indicate generally similar behavior in the Skylab and ground characterization samples. The radiographic inspection revealed the same defects that could be detected visually. No abnormal conditions were shown up in the radiographs. Additional results follow in separate sections on each material.

Aluminum Discs

Samples S/N 129 (Skylab) and S/N 130 (ground) are shown in Figures B-1 through B-4. The most significant difference in appearance is the change in the surface along the full penetration region. The skylab samples (Figure B-3) exhibits a bright center region free of oxide. In contrast, the ground characterization sample (Figure B-1) is covered with small oxide particles. These particles

TABLE B-1. THICKNESS MEASUREMENTS - M551

Location in Degrees	Thickness, Inch					
	Aluminum		Stainless Stee		Tantalum	
	S/N 129	S/N 130	S/N 106	S/N 110	S/N 145	S/N 147
0-30	.025	.024	.026	.025	.022	.018
30-60	.025	.024	.025	.025	.020	.018
150-180	.120	.119	.121	.120	.038	.036
180-210	.119	.119	.121	.120	.037	.036
210-240	.119	.119	.121	.119	.037	.036
240-270	.249	.246	.250	.249	.063	.063
270-300	.249	.246	.249	.248	.063	.063
300-330	.249	.247	.249	.248	.063	.063
330-360	.248	.247	.248	.248	.063	.063

TABLE B -2. DISTORTION MEASUREMENTS-M551

Location in degrees	Distortion, inch x 10^{-3}(a)											
	Aluminum				Stainless Steel				Tantalum			
	S/N 129		S/N 130		S/N 106		S/N 110		S/N 145		S/N 147	
	In	Out	In	Out	In	Out	In	Out	In	Out	In	Out
0	-2	0	+2	0	-4	0	-1	0	-6	0	-5	0
30	+1	+12	+7	+23	-9	+6	-1	-1	+4	+6	+4	-2
60	-3	+15	+3	+27	-9	+10	-1	+12	-4	+1	-7	-3
90	0	+20	+6	+22	-3	+7	-5	+3	-8	-5	-10	-7
120	0	+17	+5	+12	-7	-1	-10	-9	-10	-6	-11	-8
150	-1	+7	+3	+5	-7	-3	-6	-7	-10	-5	-11	-7
180	-4	0	+3	+6	-8	-4	-5	-3	-10	-7	-10	-7
210	-5	+1	+5	+13	-8	-1	-4	+1	-10	-7	-10	-8
240	-5	+4	+5	+15	-7	+3	-2	+5	-9	-7	-9	-7
270	-3	+4	+5	+12	-4	+4	0	+6	-8	-6	-7	-7
300	-1	+2	+4	+7	-2	+4	+1	+5	-7	-7	-5	-4
330	-2	+4	+4	0	-4	+1	(b)	-4	-8	-6	-6	-1

(a) + = distortion toward electron gun
- = distortion away from electron gun

(b) No measurement, probe in cut or dwell region.

7G843-1X

FIGURE B-1. FRONT SURFACE S/N 130

7G844-1X

FIGURE B-2. BACK SURFACE S/N 130

7C837-1X

FIGURE B-3. FRONT SURFACE S/N 129

70838-1X

FIGURE B-4. BACK SURFACE S/N 129

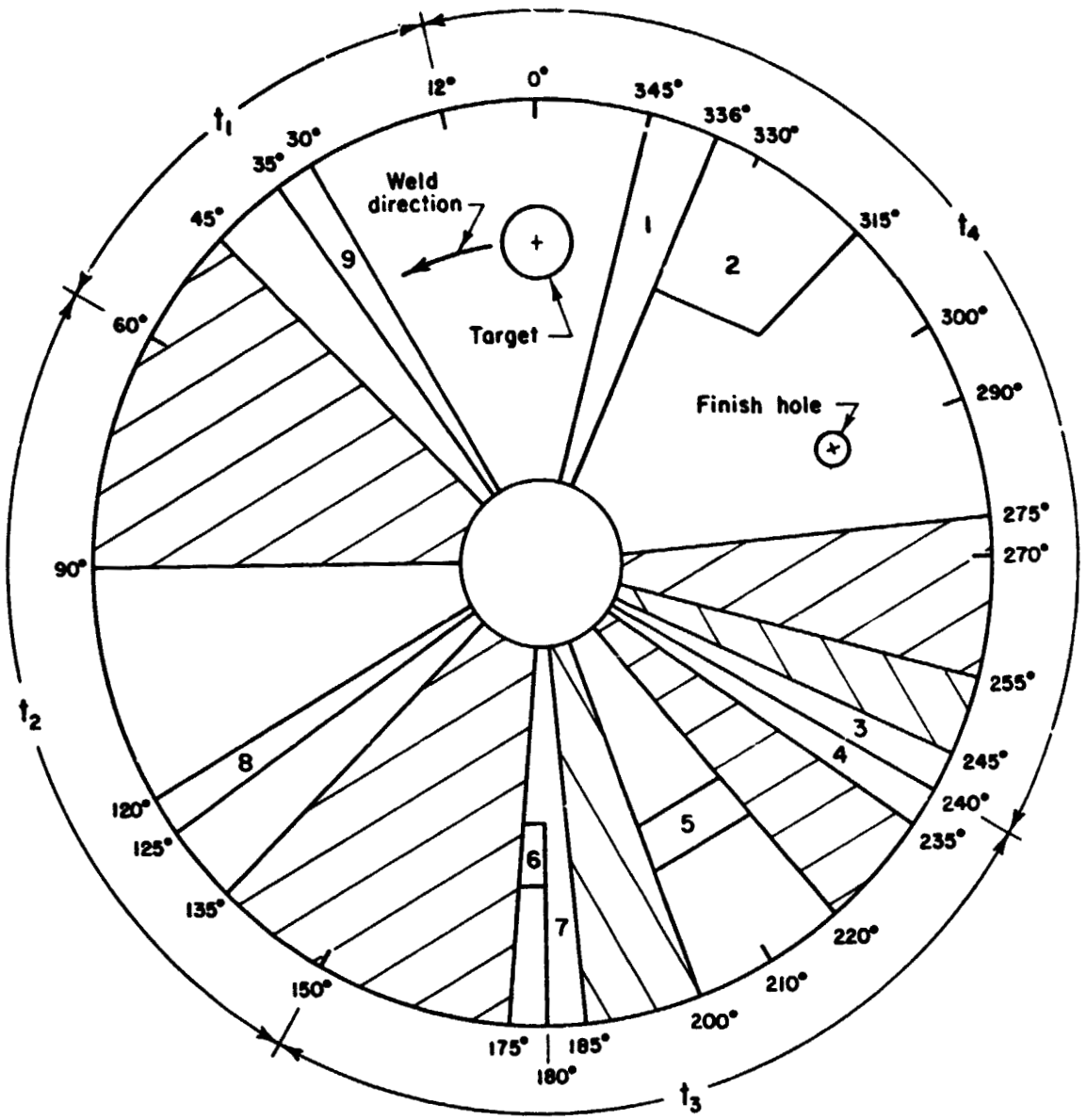

Numbered Sections - BCL

▨ - MSFC ▧ - UK

T_1 - Cut T_3 - Full penetration

T_2 - Ramp T_4 - Partial penetration/dwell

FIGURE B-5. SECTIONING PLAN S/N 129 & 130

are believed to be transported from the back surface of the disc. Initially, both surfaces of the aluminum are covered with a thin film of aluminum oxide. The oxide on the front surface is removed from the weld center by impingement of the electron beam. Oxide on the back surface is not subject to the same conditions and is free to interact with the molten aluminum weld pool.

Comments made during the visual examination of the aluminum discs follow.

Front Surface S/N 130

At 0 degrees, the target shows good positioning of the electron beam; almost exactly dead center. There is a short weld region on the tungsten which is not contaminated by aluminum which did flow back onto the outer edge of the target for a short distance. A short length of weld then exists up to the point where cutting starts. There is a shrinkage crack in the termination of this short length of weld. The initial width of the cut region is 6 millimeters. For most of the rest of the cut. the cut narrows to approximately 2 millimeters in width. Material from the cut region formed a bead on either side of the cut. This bead is much heavier on the inside edge of the cut. Several more massive accumulations of molten metal exist along the cut region. One at about 20 degrees, one at about 70 degrees, and one at 95 degrees. The region between about 80 and 100 degrees is very erratic in appearance with the cut width varying considerably and a very massive ball of molten material on the inside edge, as mentioned previously at 95 degrees. Welding starts at about 100 degrees with only a very slight indication of a starting crack. Weld ripples are fairly pronounced although the surface is quite molted with a brownish spot-type deposit in the center region with a dark appearance on the outer region of the weld. The weld continues fairly uniform in appearance until the molybdenum tracer region is reached. Initially, at that point, there is a depression in the weld surface and numerous small hairline cracks are apparent in this area. Once the weld passes by the tracer region, it again assumes a uniform appearance with clear surface ripples and very little evidence of the brown spotty material in the center. The center region for the remainder of the weld is basically bright and clean; the brown material appears to have remained along the edges of the weld. The weld terminates in the finish hole with some slight cracking in the weld center. The initial weld width is 8 mm; it then narrows to 6 mm (full penetration) then to 4 mm (partial penetration). The dwell region was focused slightly to the inside and beyond the intended 330 degrees. The bulk of the dwell which is basically circular in appearance, is completely outside of the two legs of the molybdenum target. The dwell extends

under these two legs but does not appear to have reacted with either leg very much. There are a number of shrinkage cracks in the center of the dwell region, which is depressed. In general, the dwell periphery is raised above the surface of the plate being approximately even with the surface at the top. The center of the dwell is quite bright with the outer fringes of the molten zone appearing with a light brownish surface coloring. The dwell measures 15 x 12 mm.

Back Surface S/N 130

At the target, there is nothing of significance. The cut area looks much like the top surface but is not as smooth nor is there as much molten metal attached below the plate surface as on the top. The inner surface is much dirtier than it is on the top. When welding starts, there is no evidence of the hot tear on the under surface. The initial width of the weld on the under surface is quite wide, measuring approximately 8 millimeters. At about 140 degrees, the width narrows to about 5 millimeters and stays essentially at that width throughout the remainder of the full penetration section. Throughout this region, the under surface is somewhat erratic in appearance. There is a small crack evident at the termination of the full penetration weld. There is no indication of welding on the partial penetration region except that the area around the termination hole is slightly discolored. A slight indication of the existence of this region can be seen without magnification. There is no difference in the surface appearance when looked at through the microscope.

Front Surface S/N 129

At zero degrees, the target shows evidence of aluminum material which has run back onto the target area for a distance of about 3-1/2 millimeters. The initial weld area, which is solid, is approximately 7 millimeters in length. At this point, the cutting action begins as intended. The initial width of the cut region is 6 millimeters. Throughout the rest of the cut, the kerf narrows to approximately 2 millimeters in width. Material from the cut region has formed a bead on either side of the cut. This bead is heavier on the inside edge of the cut. At about 80 degrees, there is the first large ball of material which occurs on the inside edge. At about 90 degrees, there is a large ball of material collected on the outside edge of the cut. At 120 degrees, welding starts. For the initial portion of the weld, there is a hot tear along the weld

centerline. The initial upper surface of the weld is relatively rough. The hot tearing condition continues until about 150 degrees. Surface roughness is still apparent and the weld surface is not depressed, but actually raised. At approximately 230 degrees, cracks are again on the upper surface at this point and between this point and 240 degrees there is some depression of the weld surface. Cracks are evident and traces of the molybdenum tracer present in this region are apparent on the weld surface. The first evidence of ripples on the weld surface occurred just beyond 240 degrees. Weld appearance is fairly uniform from this region on to the termination hole. There is a small crater crack at the termination hole. The weld surface ripples are more apparent in the partial penetration region of the plate. Throughout the length of both the cut and weld region, there is apparent continuous cracking of the oxide film on either side of the weld. This film has a brownish appearance. The dwell region appears to be centered approximately 5 degrees off of the intended centerline and about 2 millimeters outside of the intended focal point. There is some cracking evident in the dwell region. The dwell measures 16 millimeters in length in the radial dimension and 20 millimeters in length along the chord dimension. The dwell is oval in shape with a slight depression at the center.

Back Surface S/N 129

At the target, there is nothing of significance. The cut area looks very much like the top surface but is not as smooth and to some degree, looks a little dirtier. Where welding starts, the hot crack is apparent on the undersurface extending from the start of the weld until approximately 150 degrees. Ripples appear to be evident on the under weld surface starting at approximately 180 degrees. These ripples are quite elongated. Small check like indications in the heat affected zone are evident between 210 degrees and about 225 degrees. These are possible heat-affected zone cracks, but this cannot be confirmed visually. The cracks evident on the top surface at about 240 degrees are also evident on the lower surface. From 240 degrees to the weld termination hole, there is no evidence of welding; however, the area around the hole itself is slightly discolored.

In the dwell region there is no absolute evidence that melting occurred through to the back side. This region is slightly different in appearance from the remainder of the plate with the machine markings being not quite as clear. It would appear that the surface of this region has a fine grained structure.

Sectioning and Examination

Both aluminum discs have been sectioned as shown in Figure B-5. All sections were mounted and examined. Macro- and microphotographs showing the significant features of discs S/N 129 and 130 are shown in Figures B-6 through B-15. Figure B-16 shows the results of hardness traverses across the full penetration region of the weld.

Stainless Steel Discs

Samples S/N 106 (Skylab) and S/N 110 (ground) are shown in Figures B-17 through B-20. Comments made during the visual examination follow.

Front Surface S/N 106

At zero degrees, the target shows evidence of having been used to locate the beam with a slight melted region almost exactly on the center. The flow back of the weld appears to extend all the way from the edge of the target back to the center. Another region on one of the grooves appears to contain molten stainless steel which has flowed back in almost a brazing-type flow. The surface of the tungsten shows evidence of having reacted with this stainless steel and also evidence of two cracks -- one on either side of the main weld deposit. A solid weld region extends from the target to the point where the thickness decreases and cutting commences. The appearance of the cut on stainless steel is quite different from that in aluminum. In the stainless steel, the molten metal from the cut region has accumulated periodically in essentially circular type balls. The first ball appears on the inside surface of the cut, followed by a large ball on the outside, another on the inside, and another on the outside. The width of the cut tends to vary considerably ranging between 1 and 2 millimeters. The pattern of the ball deposits being on the inner or outer cut surface is fairly uniform throughout the length of the cut region. At approximately 70 degrees, there is a complete bridge across the cut region. This is followed by one small hole and immediately followed by the start of the full penetration weld. As soon as the weld initiates, surface ripples which are very elongated, are immediately apparent. After an initial variation in the width, the weld is quite uniform in appearance until about 105 degrees. At that point, a rather severe undercut condition develops along the inside edge. This undercut appearance continues essentially unchanged for the remainder of the weld. There is no similar evidence of undercutting on the outside edge of the weld, and no significant variation in weld appearance from the initiation of the

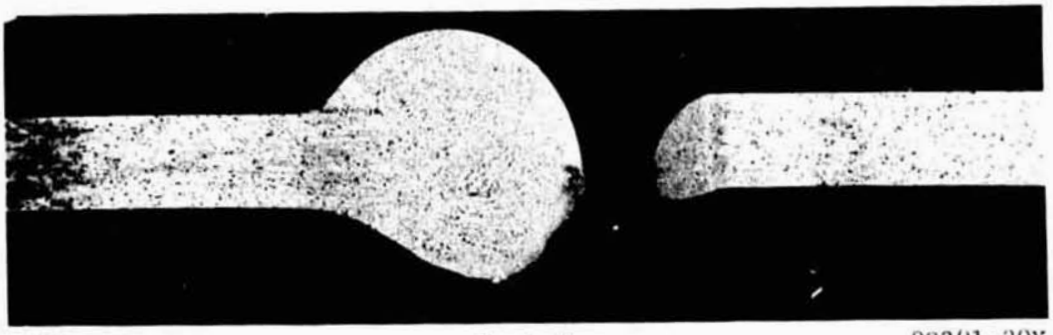

30° (+) Etched S/N 130 Ground 9G301-20X

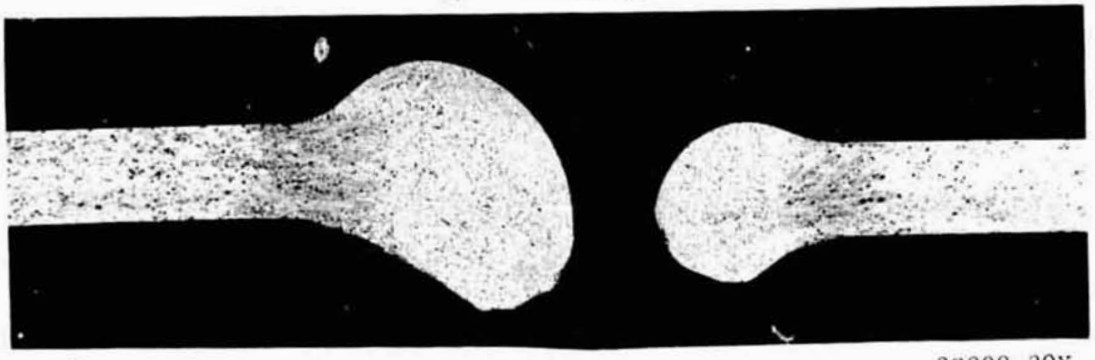

30° (+) Etched S/N 129 Skylab 9G298-20X

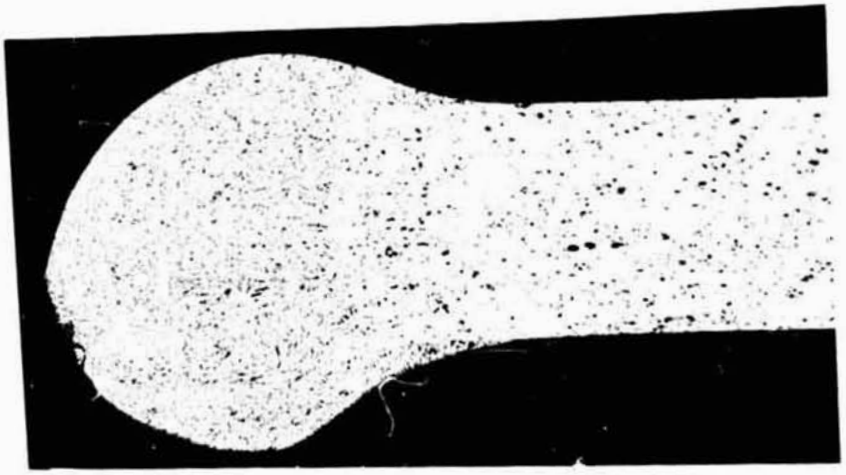

30° (+) Etched S/N 129 Skylab 9G265-50X

FIGURE B-6. SECTIONS THROUGH CUT REGION

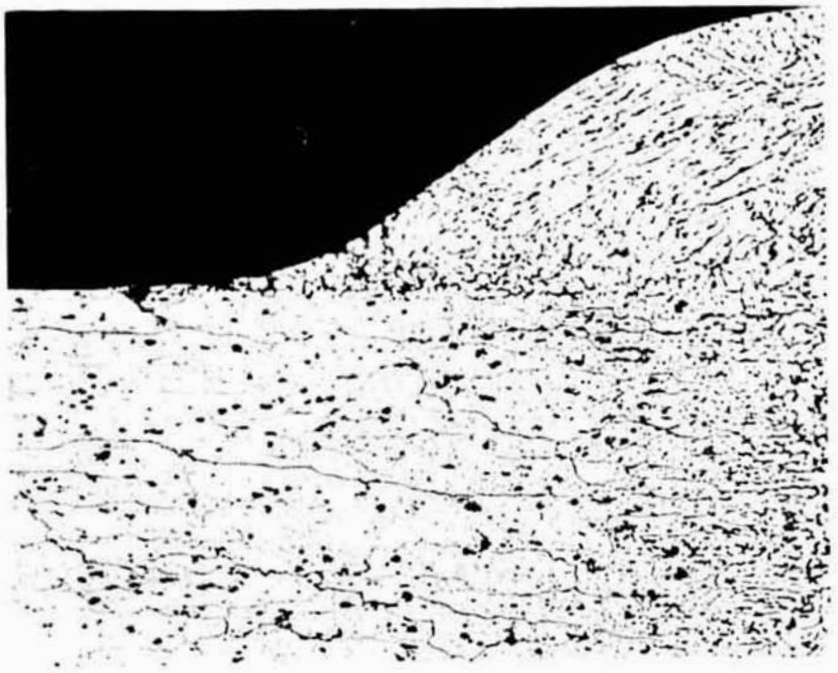

30° (+) Etched 9G266-100X

FIGURE B-7. CONTOUR AT BASE METAL INTERFACE CUT REGION - S/N 129

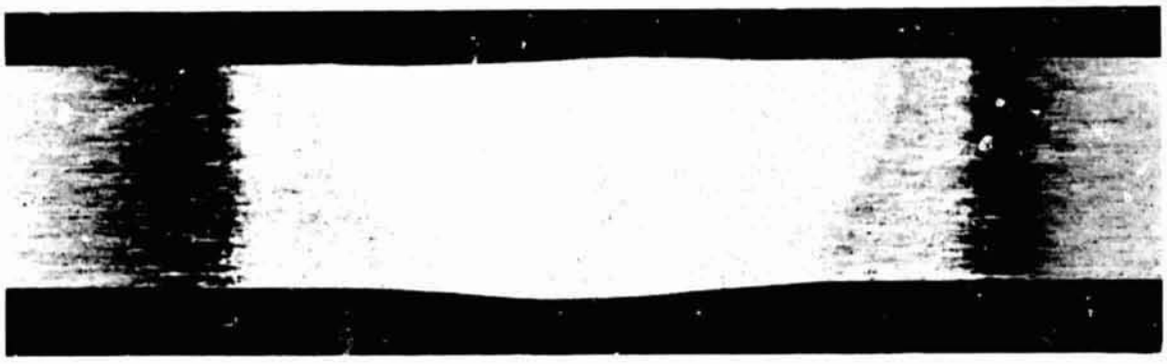

180° (+) Etched 9G297-10X

FIGURE B-8. SECTION THROUGH FULL PENETRATION REGION S/N 129 SKYLAB

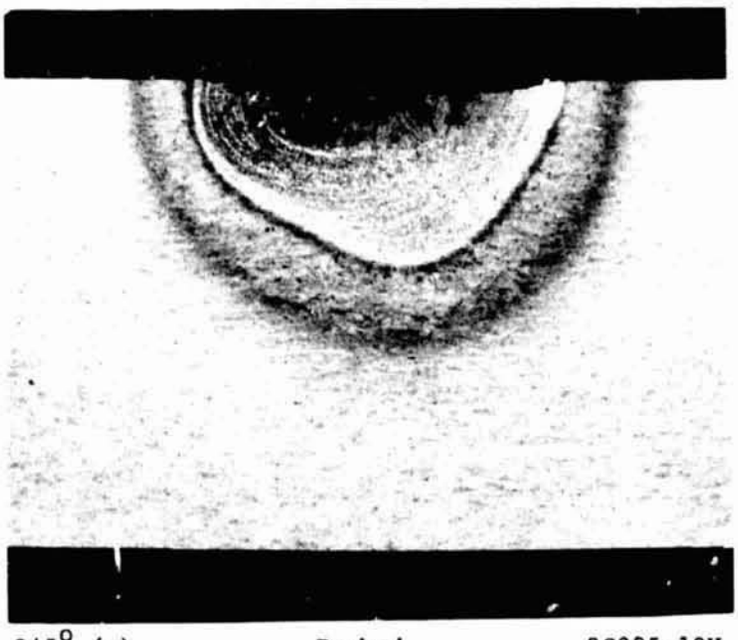

245° (-) Etched 9G295-10X

FIGURE B-9. SECTION THROUGH PARTIAL PENETRATION REGION S/N 129 SKYLAB

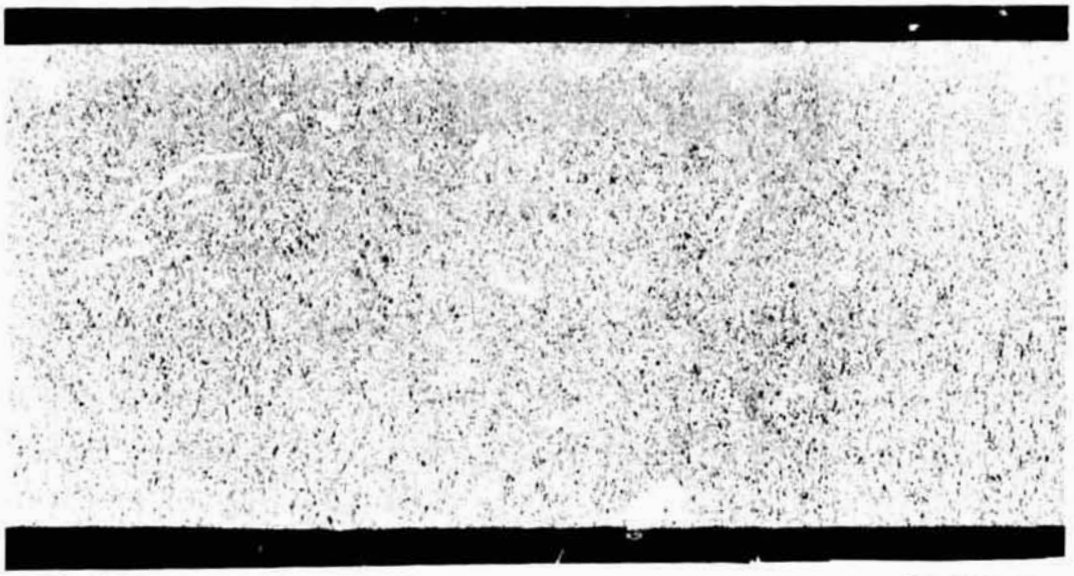

200-220° Etched 9G-296-20X

FIGURE B-10. CHORD SECTION IN FULL PENETRATION REGION - S/N 129

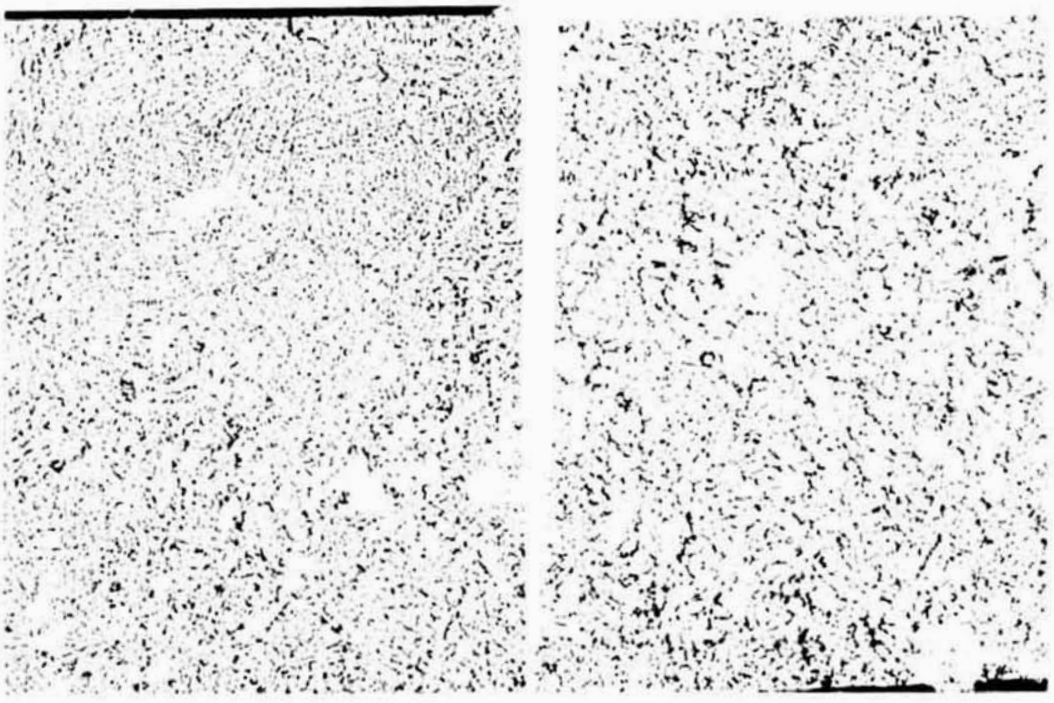

200-220° Etched 9G-261/262-100X

FIGURE B-11. MICROSTRUCTURE IN CHORD SECTION - S/N 129
right-weld Face, left-weld Root

Top Fusion Line

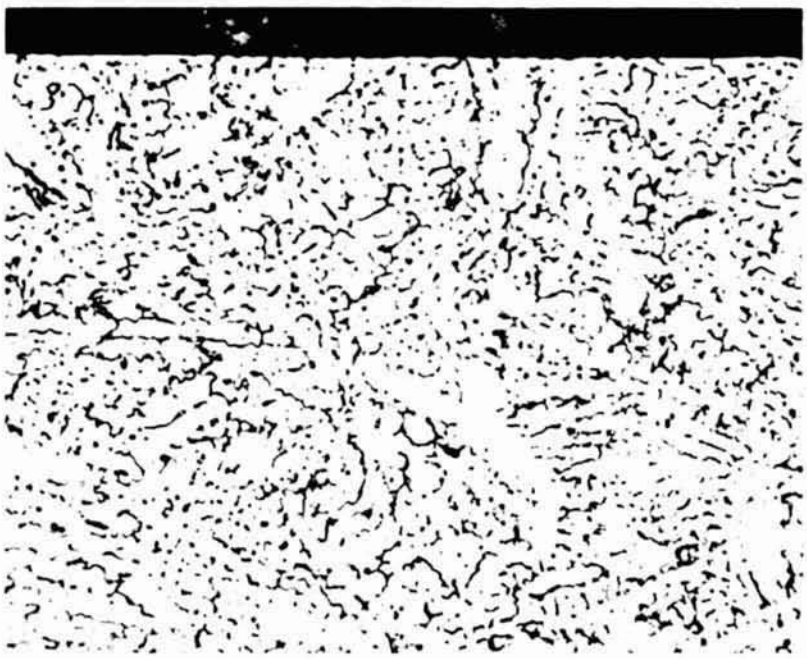

180° (+) Top Surface Etched 9G263,'264-100 and 250X

FIGURE B-12. STRUCTURES IN FULL PENETRATION REGION S/N 129 SKYLAB

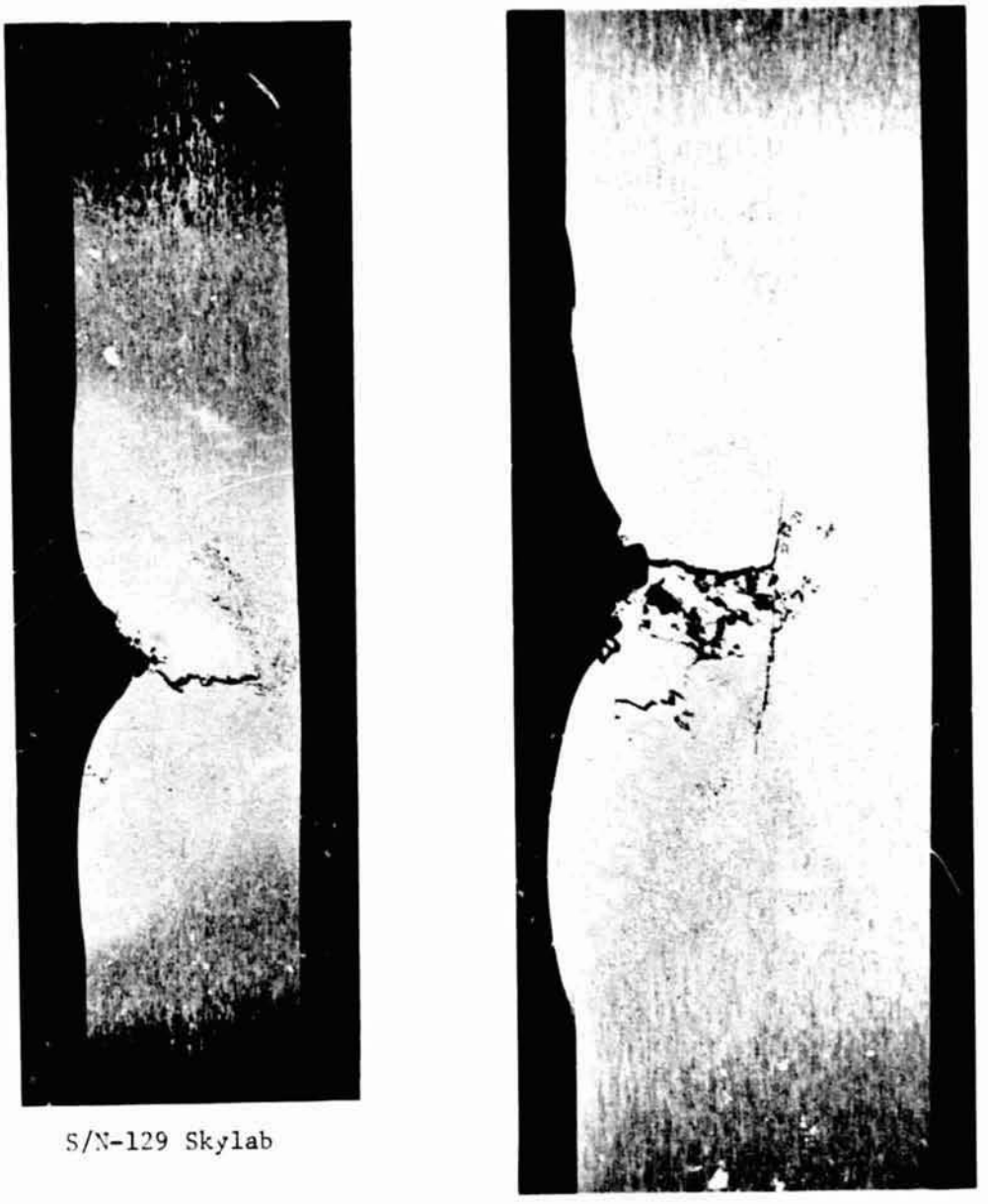

S/N-129 Skylab

S/N-130 Ground

336° (-) Etched 9G293/299-5 & 8 X

FIGURE B-13. SECTIONS THRU DWELL REGION OF S/N 129 and 130

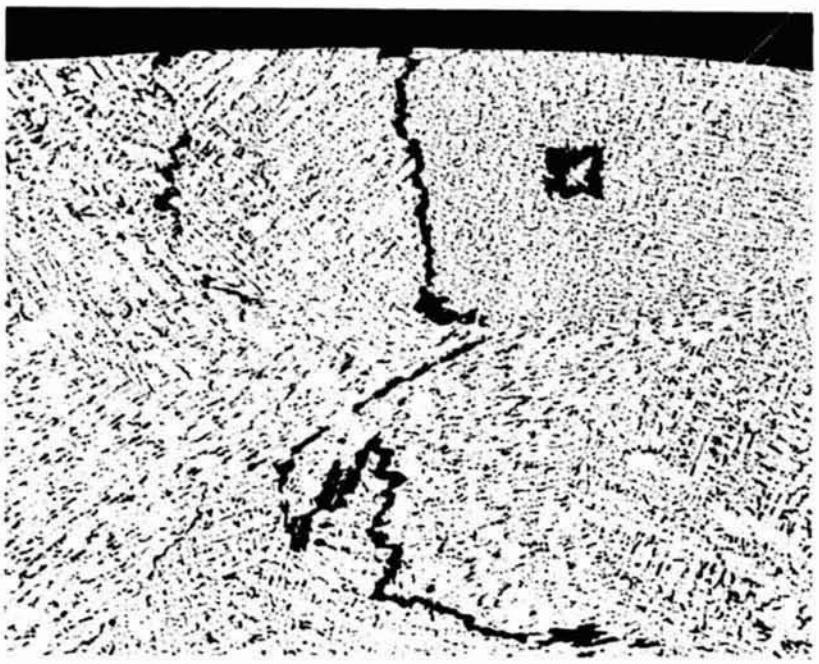

336° (-) Top Surface Area Etched 9G260-100X

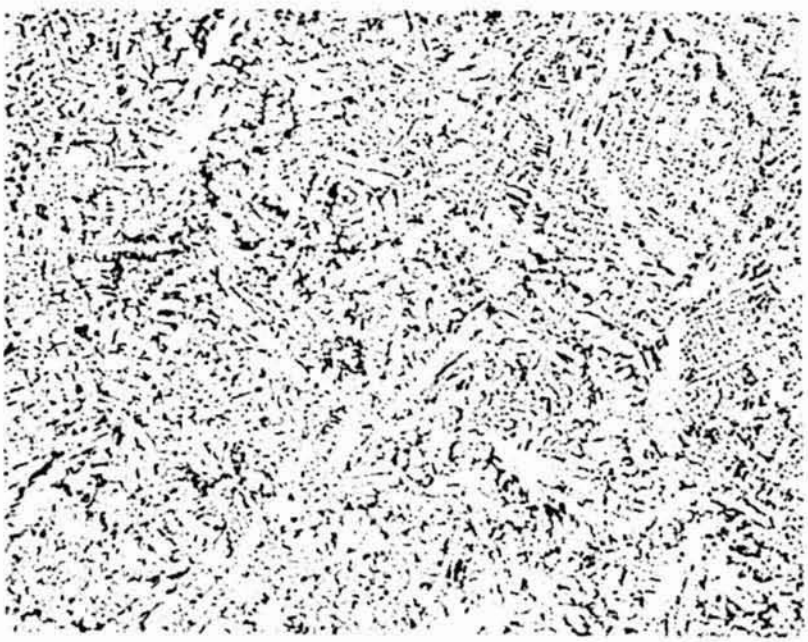

336° (-) Interior Etched 9G258-100X

FIGURE B-14. STRUCTURES IN DWELL REGION S/N 129 SKYLAB

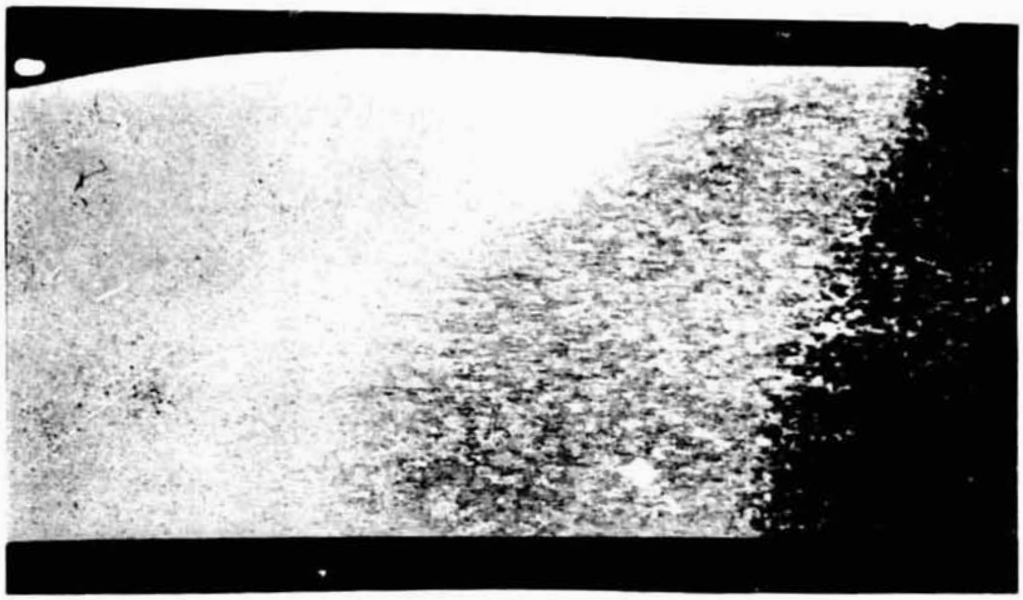

336-315° Etched 9G294-10X
S/N-129 Skylab

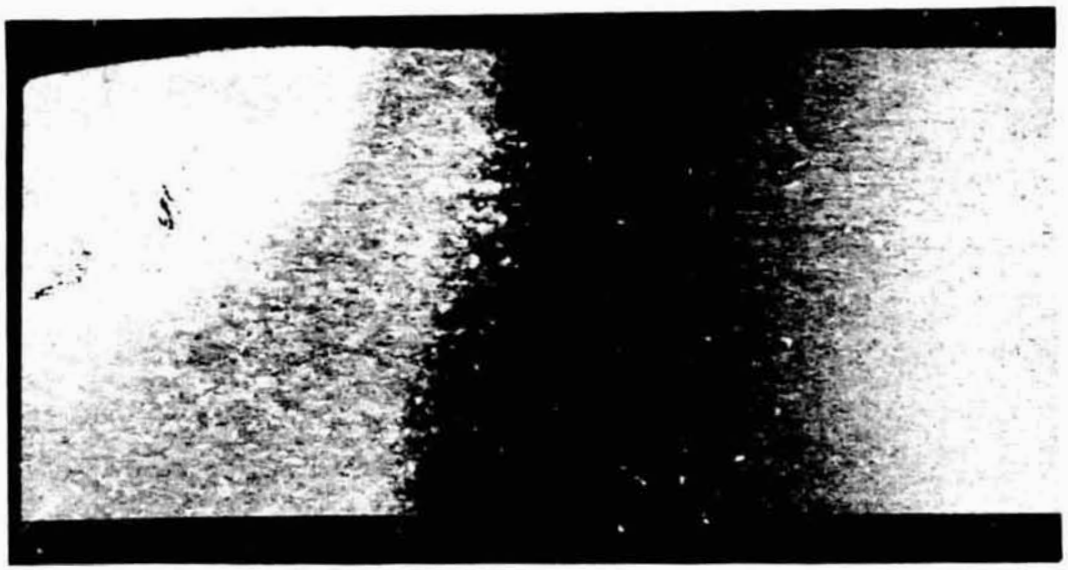

336°-315° Etched 9G300-10X
S/N-130 Ground

FIGURE B-15. CHORD SECTIONS OF DWELL REGION

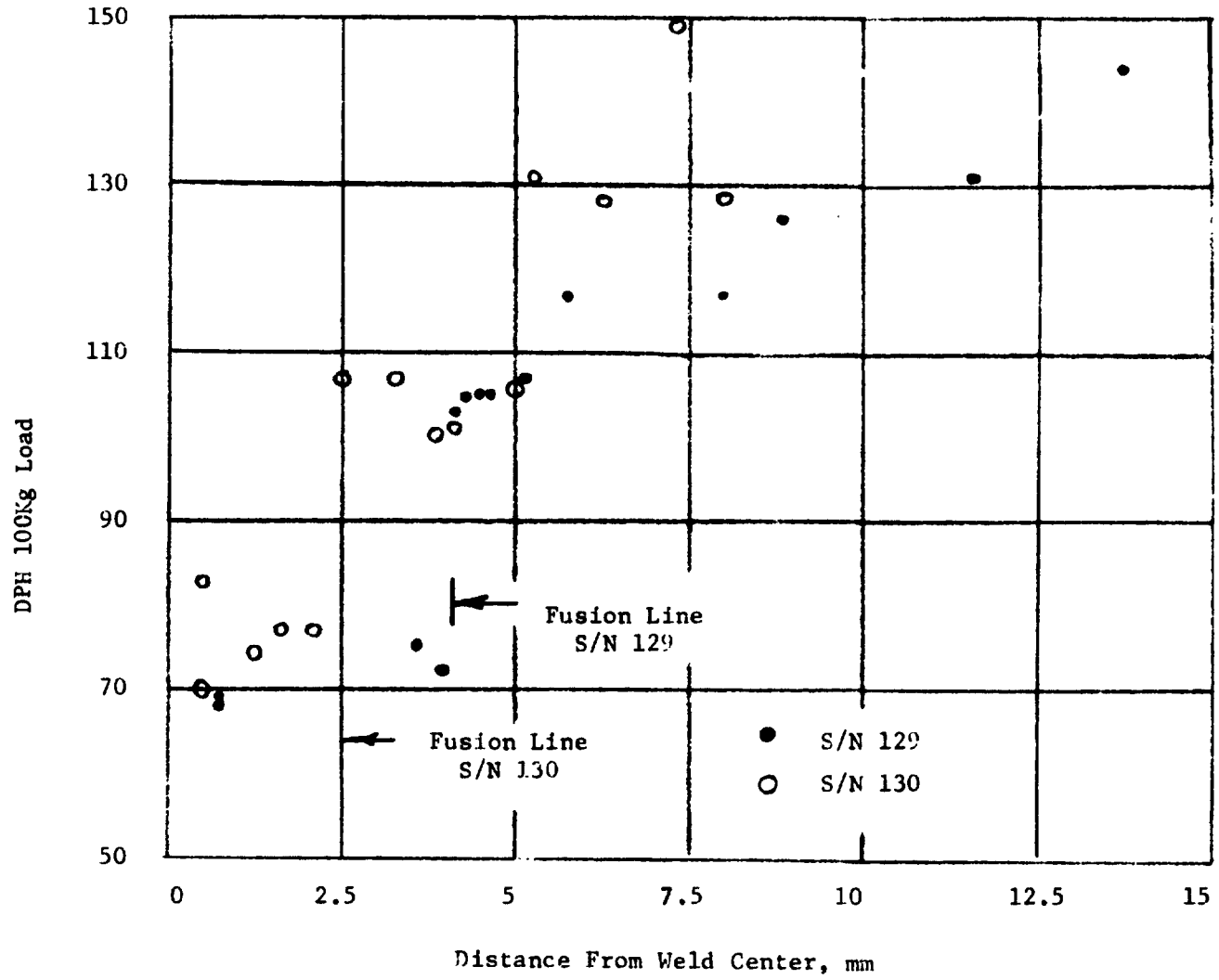

FIGURE B-16. HARDNESS SURVEY-ALUMINUM FULL PENETRATION

7C839-1X

FIGURE B-17. FRONT SURFACE S/N 106

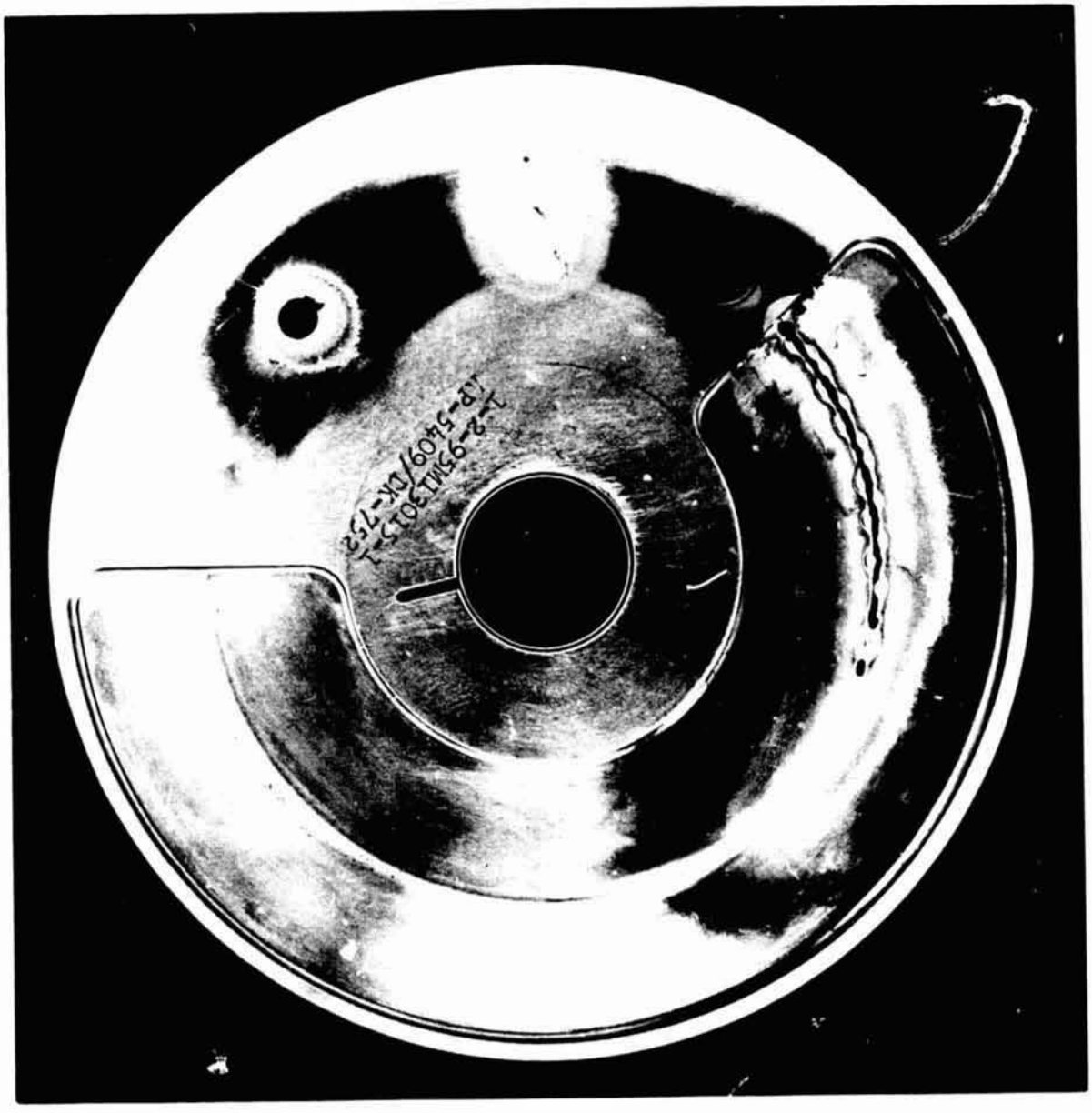

70840-1X

FIGURE B-18. BACK SURFACE S/N 106

7C845-1X

FIGURE B-19. FRONT SURFACE S/N 110

7G846-1X

FIGURE B-20. BACK SURFACE S/N 110

undercut condition until its termination at the hole. There is slight evidence on the opposite side of the hole of the electron beam having been on when the disc was rotated to that point. There are occasional instances where small spatter particles can be seen adhering to the inside edge adjacent to the weld. Surface appearance of the weld is typical for a stainless steel electron-beam joint with evident dendritic patterns at higher magnifications. There is no evidence of any cracking or weld defects other than the undercut. The focal point for the dwell area appears to have been almost exactly at the center of the molybdenum tracer target. It is slightly inside but still within the target region. The dwell is elongated -- the long axis essentially parallel to the radial direction. There is an obvious buildup of material above the surface surrounding the entire dwell region. Solidification ripple patterns are quite evident along this built up region. The center portion of the dwell shows no evidence of ripple patterns for approximately half of the total area. A large cavity and crater are evident at the center of the dwell. The dwell measures approximately 19 millimeters along the long axis and 10 millimeters on the short axis.

Back Surface S/N 106

The target area indicates nothing of significance except slight brownish discoloration. The cut region starts immediately when the thin section is reached. The appearance of the balls along the cut region is quite similar to their appearance on the upper surface, although there is slightly more grayish discoloration on the lower surface. Where the weld commences, a ripple pattern again is immediately evident. The full penetration weld occurs with fairly uniform width penetration from the start of the weld to 120 degrees. At this point, penetration or width of the bead narrows and there is some buildup on the under surface. Full penetration stops at approximately 140 degrees. This situation continues until at approximately 200 degrees there is a single small circular indication of full penetration. It is clear on the under surface where welding has occurred, even in those regions where penetration is not achieved. It would appear that there is a slight drop through on the underside even when penetration is not clearly evident. There is no evidence of the weld on the under surface in the partial penetration region. Some discoloration is evident on the surfaces surrounding the underside of the termination hole. Full penetration was achieved on the dwell but the overall size of the molten spot is much smaller than on the top surface. Its basic appearance is quite similar with evidence of ripple formation on the edges with a single very smooth surface center region which seems to have solidified all at once. Although it is not as obvious, the region of penetration on the lower surface is also

basically oval or oblong in shape. The long axis measured approximately 7 millimeters and the short axis just under 6 millimeters. The general appearance of the contour on the under surface is a very shallow depression with the edges being possibly slightly raised above the original surface.

Front Surface S/N 110

At 0 degrees, the target has been used to locate the beam with a melted region almost exactly on center. Flow back of molten stainless steel has occurred all the way from the edge of the target back to the center. A solid weld region extends from the target to the point where the thickness decreases and the cutting commences. The cut width is 1 mm. In the cut region, the surplus molten metal has accumulated in essentially circular balls. In this specimen, all the balls lie along the inside edge of the cut region. There are 13 of the ball accumulations along this edge. The last of the ball accumulations is slightly beyond degrees, although the actual welding does not start until about 7. degrees. As soon as the weld initiates, the surface ripples which are very elongated are immediately apparent. Undercut along the inside edge is also immediately apparent. Starting at about 130 degrees, the undercut is not as severe and, in fact, may not exist although there is an occasional indication of undercut still along the inside edge. At about 160 degrees, there is a perturbation in the surface appearance related to a mass change as the disc rotates. At the change in thickness going from the thin to the thickest material, there is a change in the bead appearance with the top surface appearing to be more elevated in the partial penetration region. The weld terminated slightly short of the termination hole with a shallow elongated crater. There are occasional instances where small spatter particles can be seen adhering to the inside edge adjacent to the weld. Surface appearance of the weld is typical for stainless steel electron-beam joint. There is no evidence of any cracking or weld defects other than the undercut. The weld width initially is 1-1/2 mm widening to 2.5 mm (full penetration), and then to 3 mm (partial penetration). The focal point for the dwell area appears to be slightly on the inside and slightly beyond the 330 degree position. However, the dwell is fairly well centered on the molybdenum tracer target. The dwell is elongated, the long axis essentially parallel to the radial direction. There is a buildup of material above the surface of the plate in the lower portion of the dwell melt side. The upper portion is depressed below the plate surface. A large cavity and crater are evident at the center of the dwell but slightly toward the top side. The dwell measures approximately 18 millimeters along the long axis and 8 millimeters on the short axis.

Back Surface S/N 110

The target area is completely melted through slightly on the surfaces adjacent to the weld start. Penetration proceeds for a short distance and then stops until the cut region is reached. The cut region starts immediately when the thin section is reached. The appearance of the circular balls along the cut region is quite similar to their appearance on the top surface. Where the weld commences, a ripple pattern again is immediately apparent. Starting at about 145 degrees, there is quite a bit of evidence of spatter adhering to the back surface. The same perturbation noted on the front surface due to the mass shift is also apparent on the back surface. Penetration is continuous throughout the length of the full penetration portion of the plate. At about the same point where spatter first starts, the underside bead contour begins to change getting slightly narrower and somewhat higher than it was in the earlier portion. There is no evidence of the weld on the under surface in the partial penetration region. Full penetration was achieved on the dwell, but the overall size of the molten spot is much smaller than on the top surface. Its basic appearance is quite similar with evidence of ripple formation on the edges with a single very smooth surface center region which appears to have solidified all at once. The outermost edges of the dwell on the under surface are raised slightly above the plate surface everywhere except at the very top. The center region of the dwell is generally depressed. The long axis measures approximately 10 millimeters and the short axis 7 millimeters.

Sectioning and Examination

Both stainless steel discs were sectioned as shown in Figure B-21. All sections were mounted and examined. Macro and microphotographs of significant areas are shown in Figures B-22 through B-28. Hardness traverse results are shown in Figure B-29.

Tantalum Discs

Samples S/N 145 (Skylab) and S/N 147 (ground) are shown in Figures B-30 through B-33. Comments made during visual examinations follow:

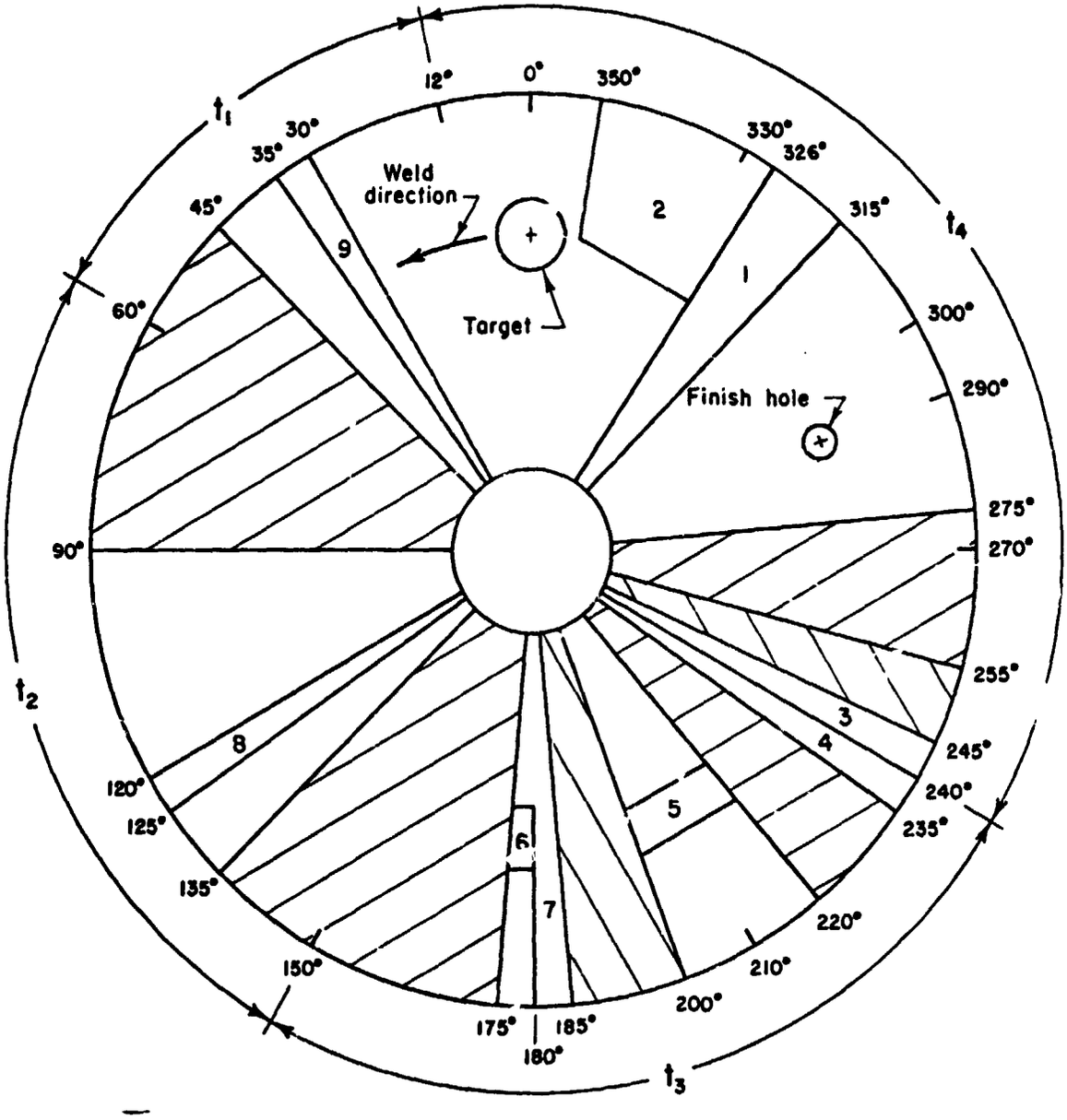

Numbered Sections - BCL

▨ - MSFC ▧ - UK

T_1 - Cut T_3 - Full penetration

T_2 - Ramp T_4 - Partial penetration/dwell

FIGURE B-21. SECTIONING PLAN S/N 106 & 110

35° (+) Etched 9G255-20X

FIGURE B-22. SECTION THRU CUT REGION S/N 106 SKYLAB

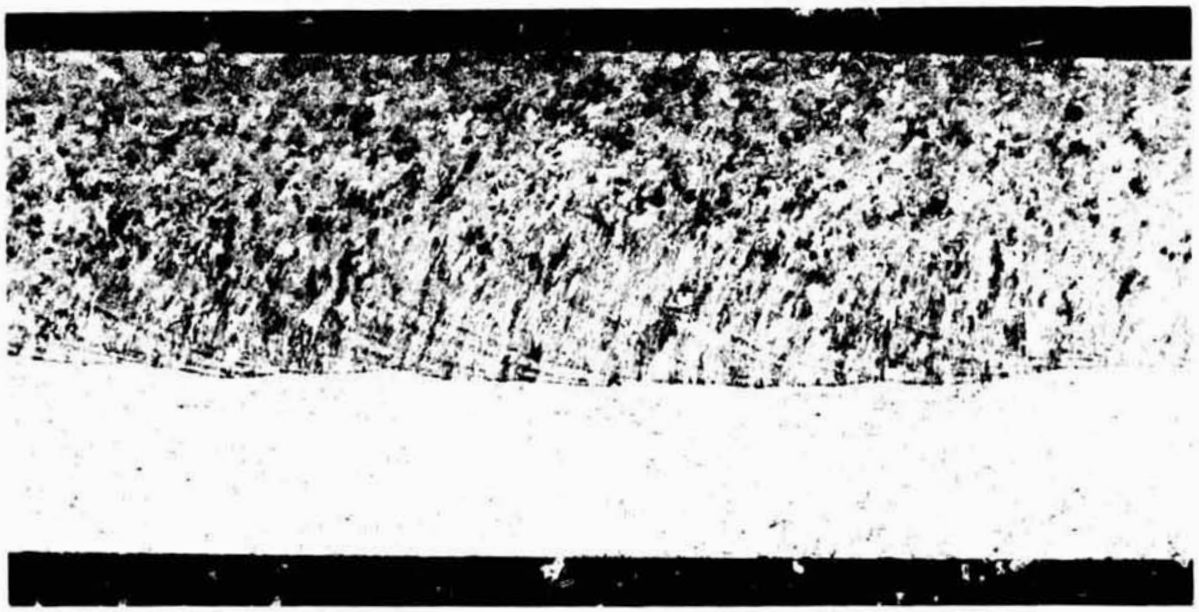

200-220° Etched 9G254-20X

FIGURE B-23. CHORD SECTION THRU FULL PENETRATION REGION S/N 106 SKYLAB
Section is in area of shallow penetration

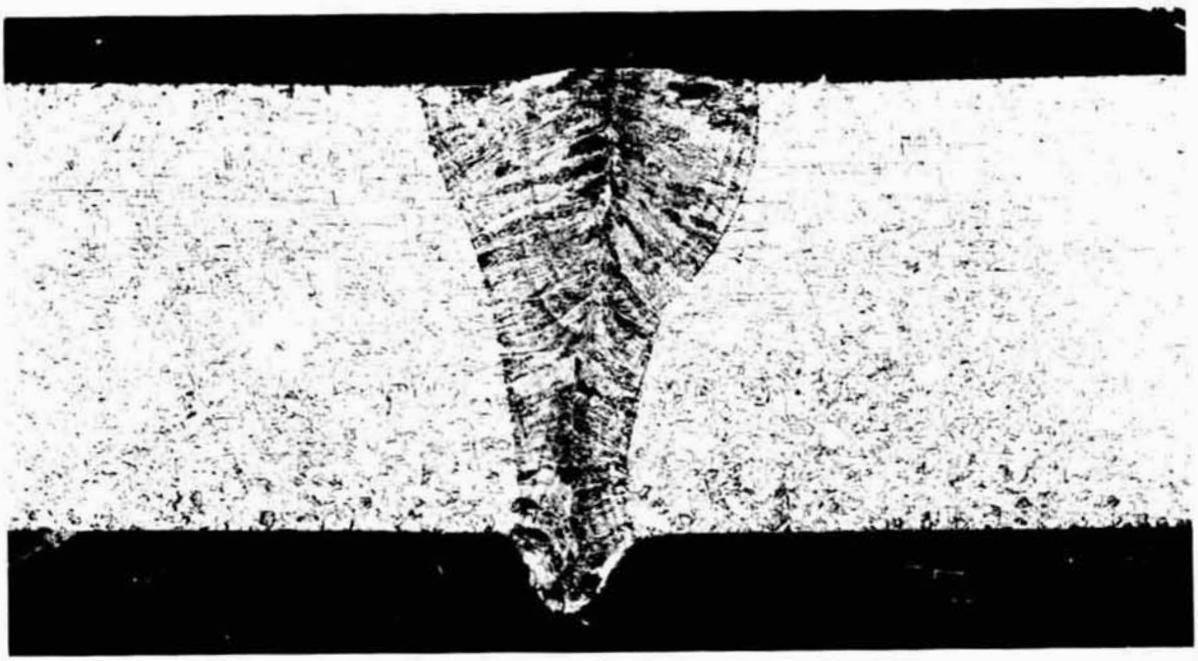

S/N-110 Ground

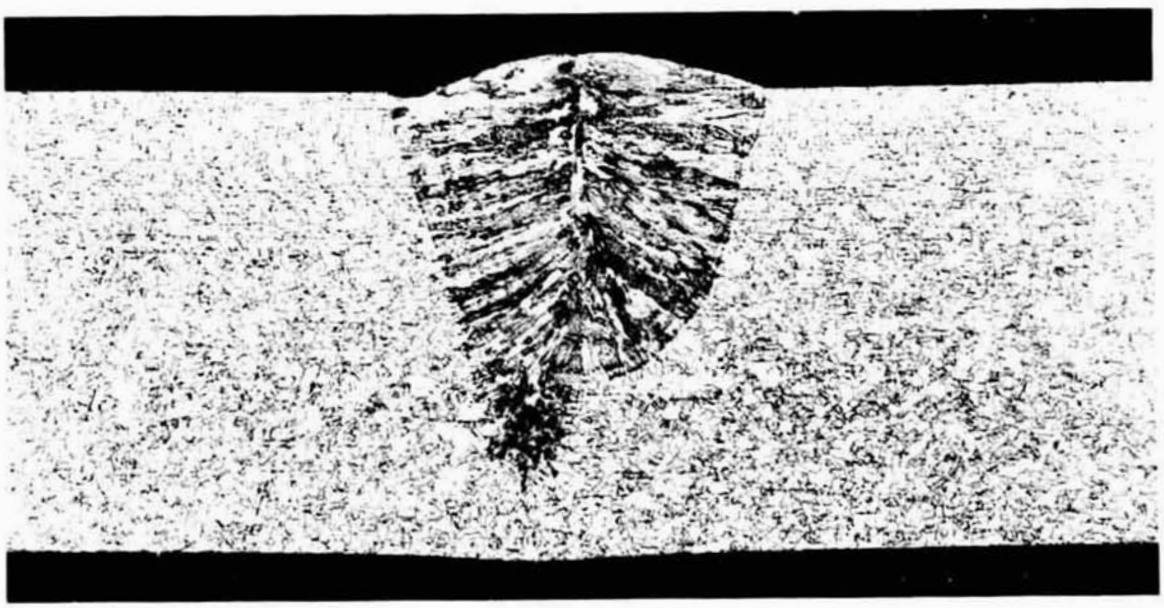

235° (+)

S/N 106 Skylab
Etched

9G257/253-20X

FIGURE B-24. CROSS SECTION THROUGH FULL PENETRATION REGIONS

Fusion Line

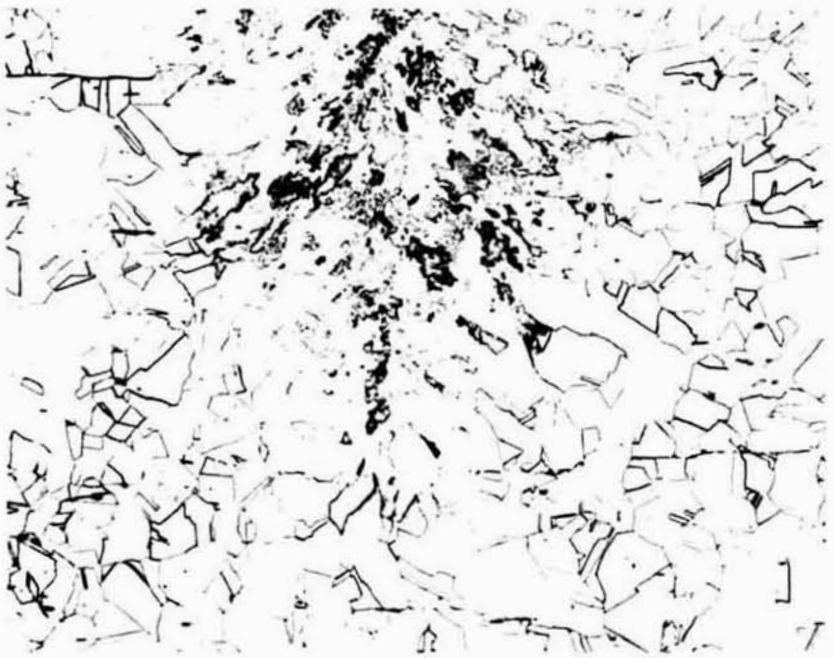

235° (+) Weld Root Etched 9G250/251-100X

FIGURE B-25. STRUCTURES IN FULL PENETRATION REGION - S/N 106 SKYLAB

S/N-106 Skylab

326° (+)

S/N-110 Ground

Etched

90252/256

FIGURE B-26. RADIAL SECTION OF DWELL REGIONS

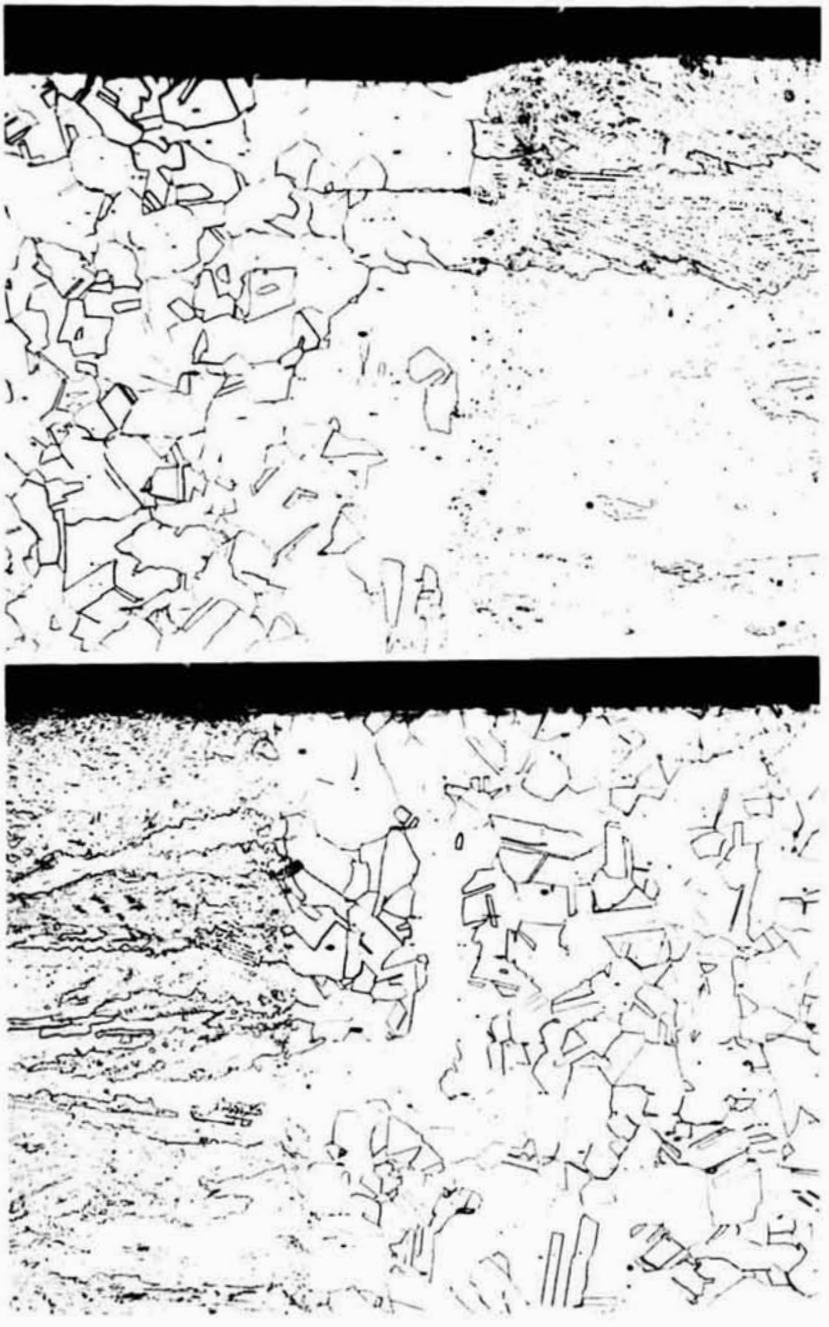

326° (+) Etched 9G247/246-100X

FIGURE B-27. CONTOUR OF TOP FUSION LINE AREAS IN DWELL REGION - S/N 106 SKYLAB

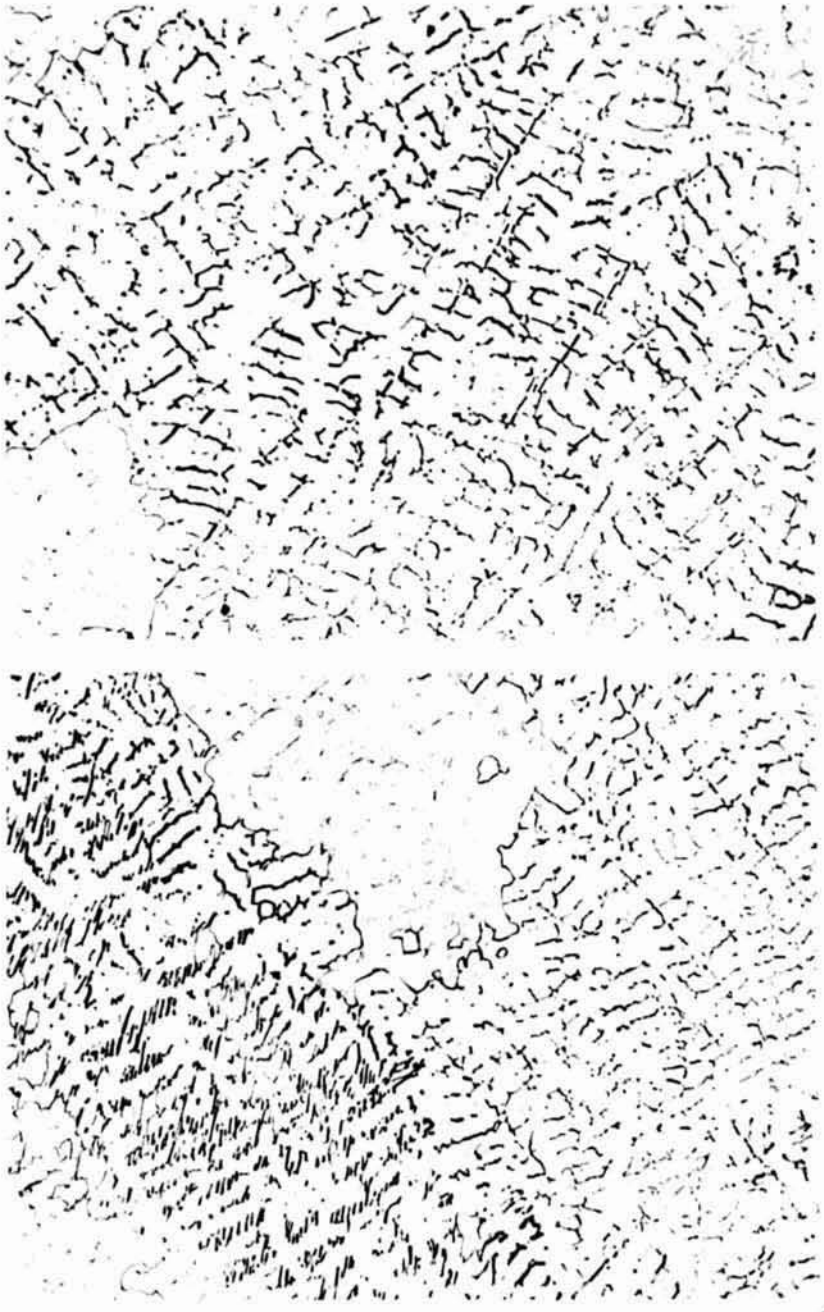

326° (+) Etched 9G248/249-250X

FIGURE B-28. INTERNAL MICROSTRUCTURES IN DWELL REGION - S/N 106 SKYLAB

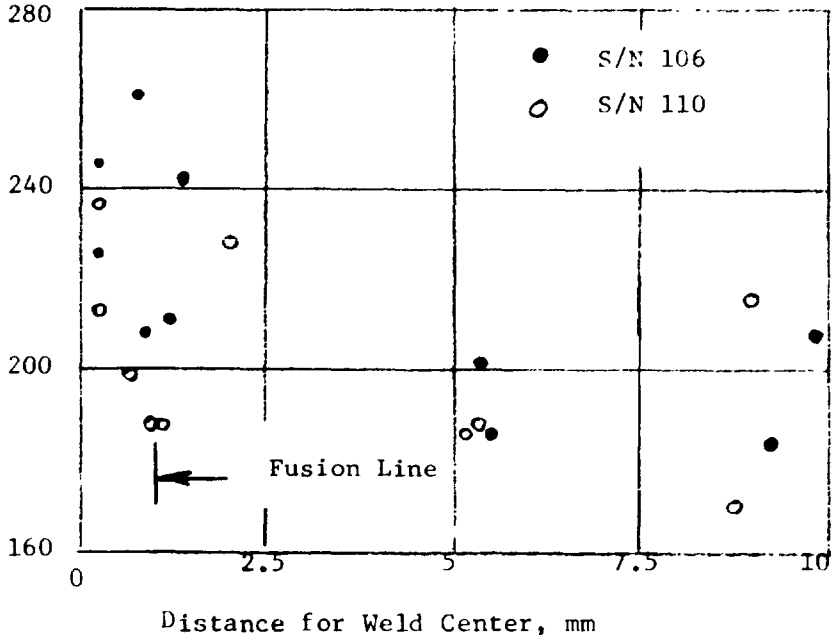

FIGURE B-29. HARDNESS SURVEY-STAINLESS STEEL FULL PENETRATION WELD

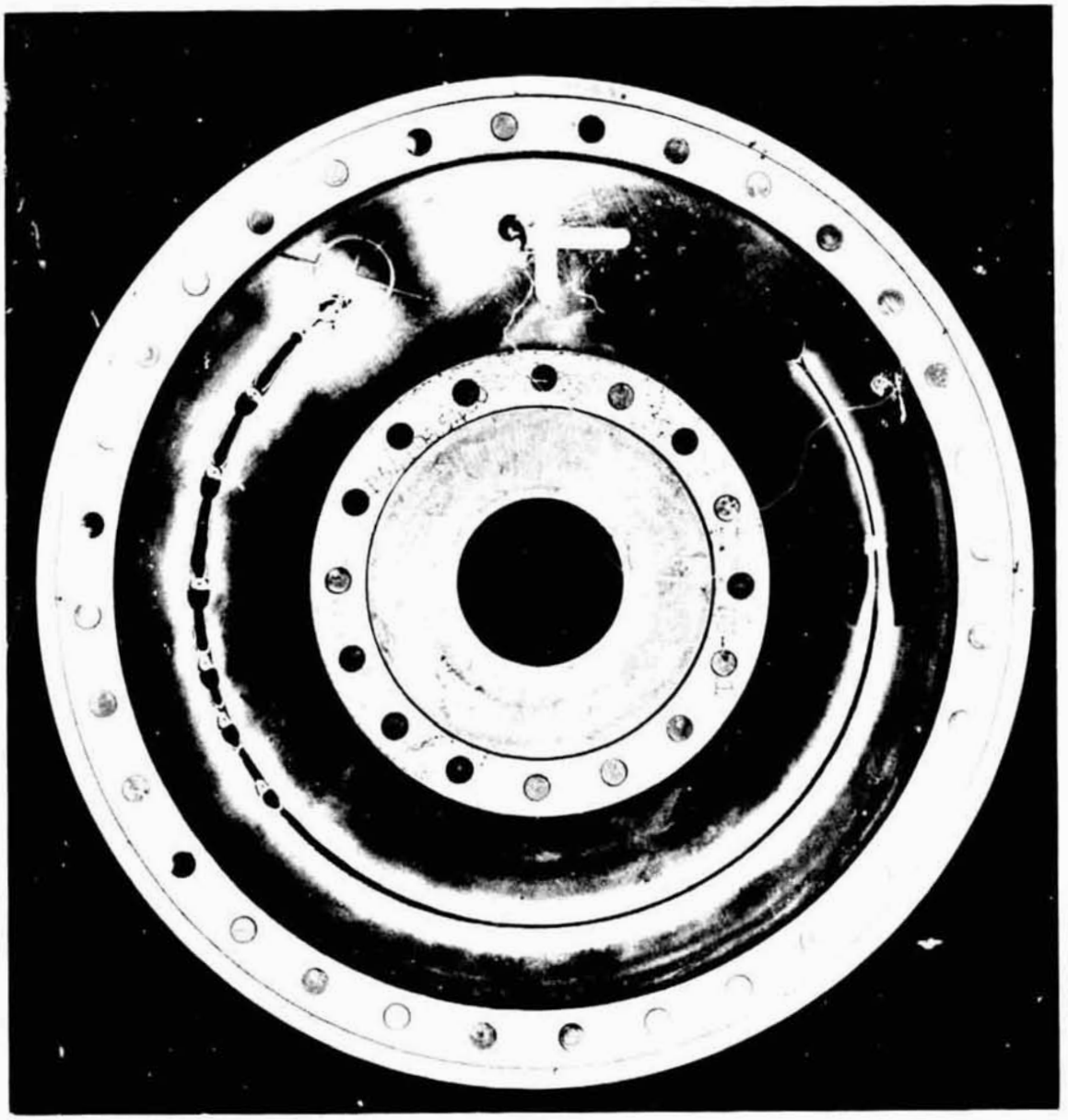

7G841-1X

FIGURE B-30. FRONT SURFACE S/N 145

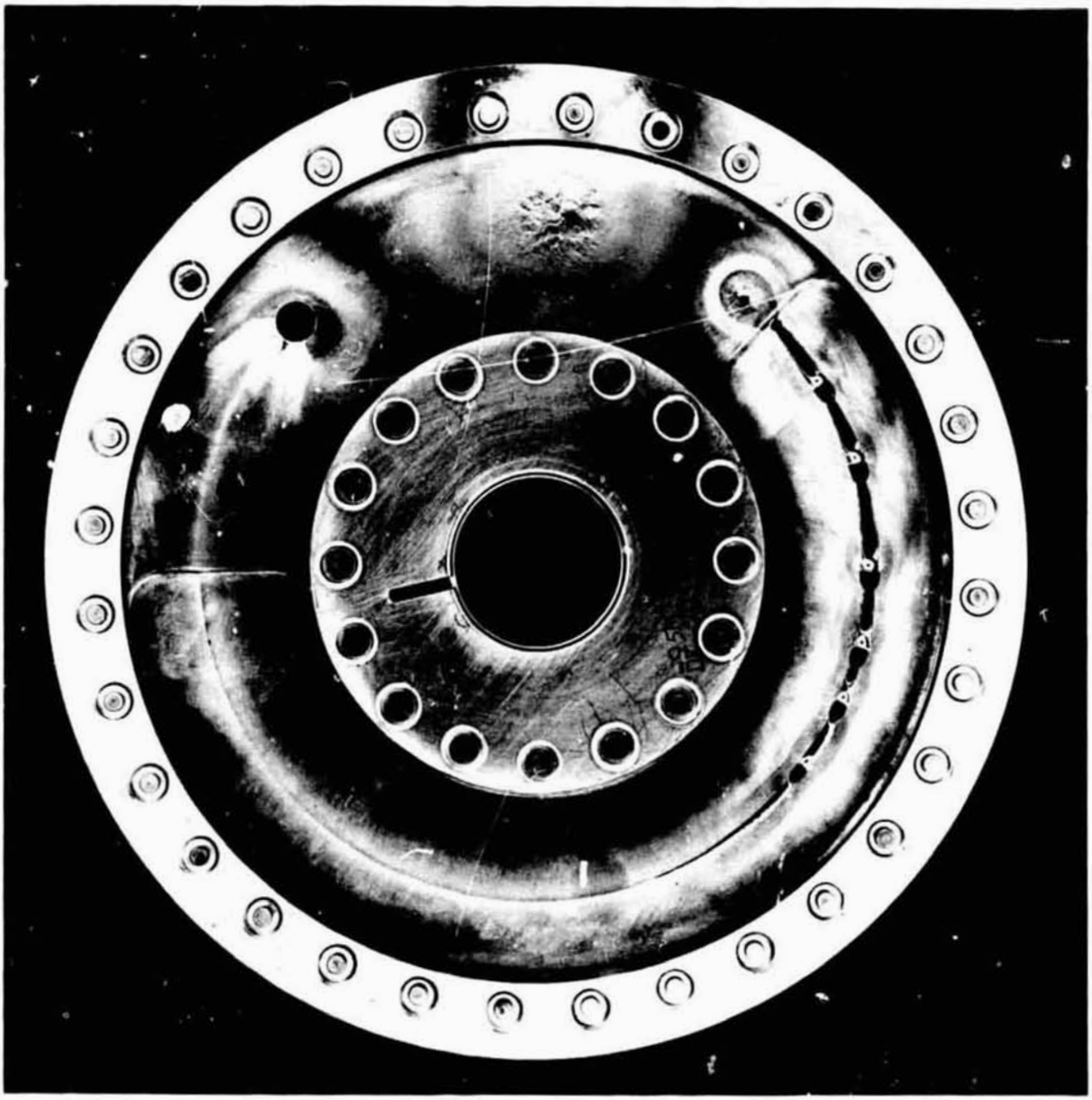

7G842-1X

FIGURE B-31. BACK SURFACE S/N 145

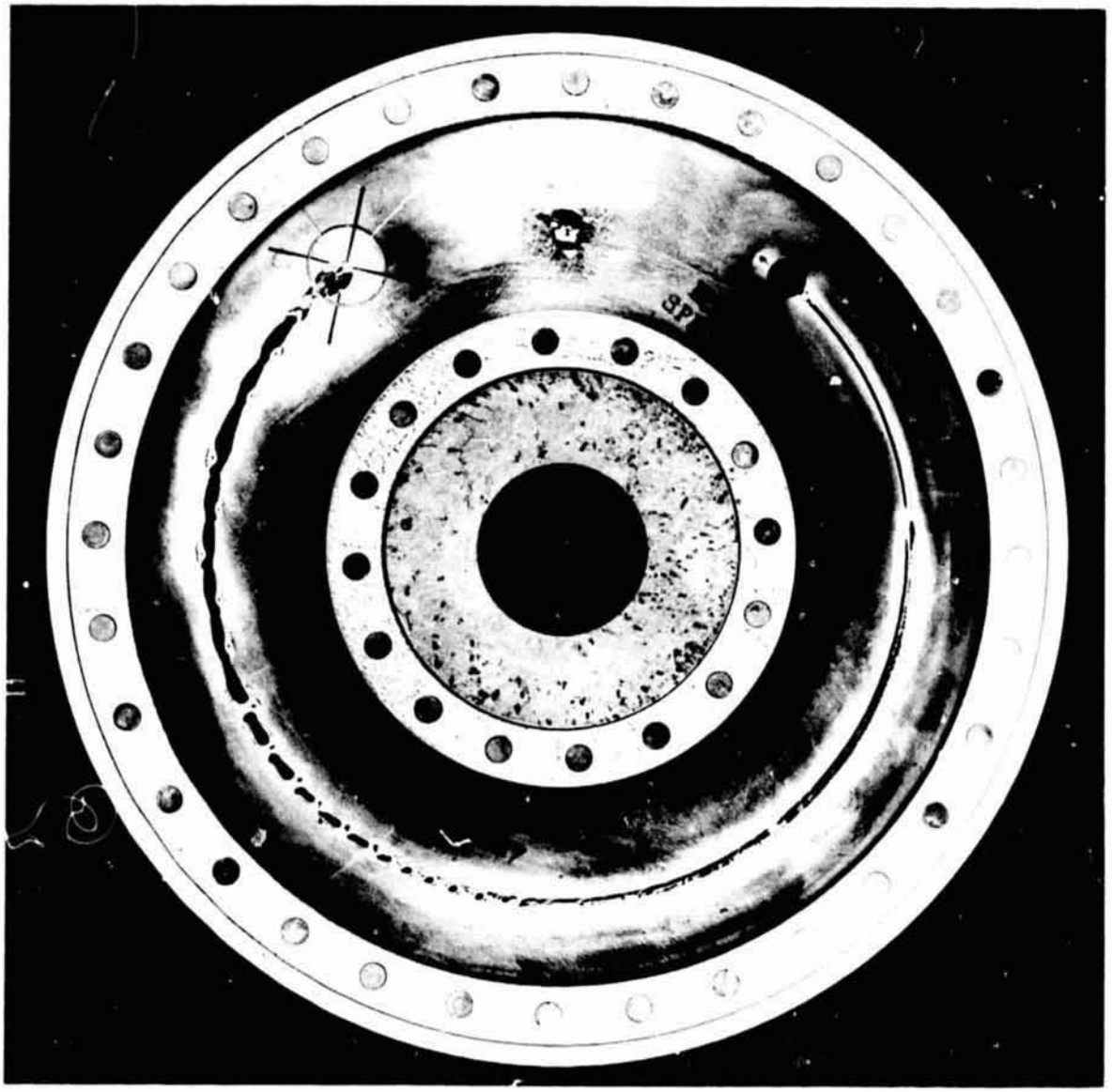

7G847-1X

FIGURE B-32. FRONT SURFACE S/N 147

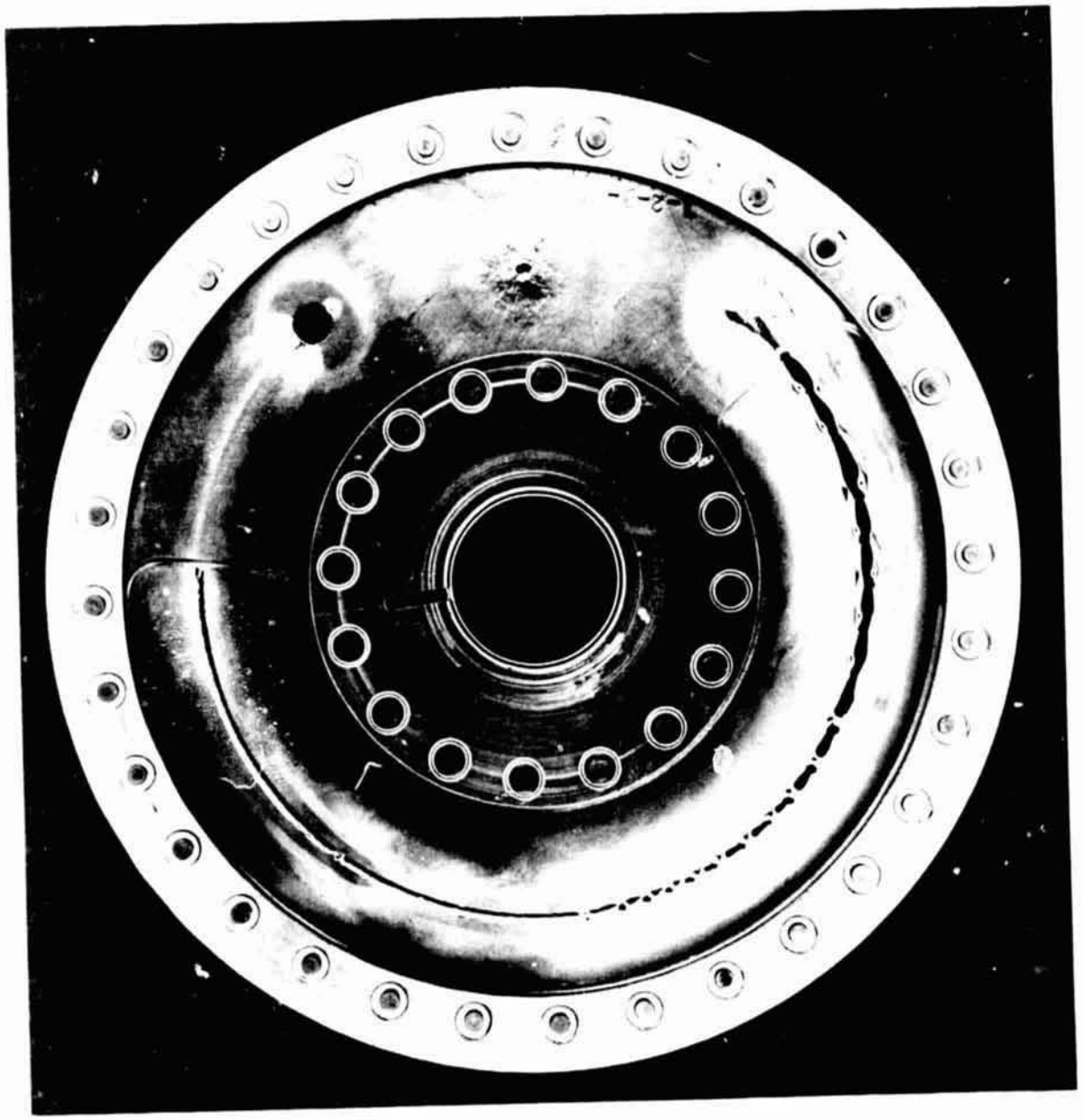

7C848-1X

FIGURE B-33. BACK SURFACE S/N 147

Front Surface S/N 145

The target is integral on this sample. The beam was initiated within the target area but a little beyond the zero point and slightly to the inside. The surfaces of the tantalum welds show both a ripple pattern where the beam was started and clear evidence of the grain structure on all of the surfaces. There is no evidence of any discoloration or oxidation. The cut region appears to start immediately at the thin section and is bridged periodically by a ball of molten tantalum. These balls show a ripple pattern on the side and clear grain structures elsewhere. There appears to be a cavity in the first ball evident on the top lower surface in the direction of increasing degrees. After each bridge, the gap tends to widen then narrow to a kerf which then tends to taper somewhat in width and also in the amount of molten metal that is piled up on each edge. This situation continues until the next bridge.

There is a total of 5 ball bridge regions. Each is quite similar in appearance to the first one described. Each bridge also appears to contain the cavity region described for the first ball. The bridges get progressively closer to one another along the length of the specimen. After the last bridge, there is a region that extends for about 9 millimeters with a hole at the end of this region. At this point, the weld itself starts. This weld is extremely uniform; one can see both the ripples and the surface grain structure quite readily. This weld continues on through to the termination point. At approximately 185 degrees, there is a single surface depression on the inside edge of the weld. In the region where the molybdenum tracer is placed on the disc, there is the appearance of undercut having started on both the inside and outside edges of the weld. Also within the tracer region, there is a change in the width of the weld bead with it becoming narrower at the point where the thickness of the disc increases. The slight undercut condition appears to continue on to the termination of the weld at the termination hole. There were no cracks or other defects aside from the single surface depression noted in examination of this weld.

Additional examination of the area where the slight depression was noted on the inside surface of the weld suggest that there may have been a defect in the plate material at that point. This appears to be a slight machining gouge.

Back Side of S/N 145

Starting in the weld target area on the reverse side of the target, there is evidence of complete penetration. In fact, there appear to be two separate spot areas which were melted through to the

back side and subsequently solidified. Surrounding the target area and still attached to the disc are a number of small spherical particles which are probably tantalum spatter that was ejected from the back side of the target area, bounced off the support plate, and then adhered to the tantalum. At least 8 of these small spheres can be seen in the field of view of the magnifying system. Moving away from the target once the beam-travel combination was initiated, penetration stopped until the thin section was reached at which point cutting action was initiated. The back side of the cut region does not appear to be significantly different from the front side with all of the same basic features being evident. The balls that constitute the bridges are raised above the bottom surface just as they were raised above the top surface on the front of the disc. Material present adjacent to the balls in the direction of increasing angle appears to have been pulled back into the bridge area. Appearance on the underside of the full penetration welds is quite similar to the appearance on the upper surface. The full penetration weld begins to taper after its initiation and there is no more penetration after about 135 degrees. Evidence of the presence of the weld continues as in the case of the stainless steel without full penetration being apparent. There is one short linear indication of full penetration at about 225 degrees. Some further evidence of welding is apparent on the reverse side even in the partial penetration region leading up to the termination hole. At the termination hole itself, there is evidence of penetration through the plate on the side where the weld was terminated. At the dwell region, there is no evidence of complete penetration although again, the grain structure and a surface roughening are quite evident.

Front Surface of Disc S/N 147

The electron beam was initiated almost exactly at the center of the target. A weld is started at this position and runs to the point where cutting begins. The cut is initially fairly wide (3 mm) and there are small molten balls collected on the edges along this initial region. The cut varies in width between 1 and 3 mm. The first two balls are on the inside of the cut; the next outside, then one inside, then one out, and two more inside. Following this region of the cut, there are bridges apparent; the first bridge existing at 75 degrees. There are a total of 10 bridges before welding starts. The bridges appear to get progressively smaller in size and closer together. Compared to the bridges on S/N 145, the bridges on S/N 147 do not appear to be as large or quite as spherical in shape. There is evidence of the same type of cavity on the top lower surface in the direction of increasing degrees as seen in S/N 145. The weld starts at approximately 130 degrees. The weld is uniform; about 2 mm wide, one can see both the ripples and the surface grain structure quite readily. This weld continues on through the termination point. A

surface perturbation occurs at about 180 degrees which is the point where a mass shift occurs. There is a slight depression in the weld as it enters the partial penetration region but this is quickly lost. The weld narrows slightly at this point to 1 mm, and is quite uniform in appearance on to completion. The weld goes on to the termination hole and also slightly beyond on the opposite side. The ripple pattern is not entirely uniform, being somewhat asymmetrical and displaced with its apex offset toward the inside of the disc.* The dwell region is located inside the intended target, but almost exactly on the center of the inside leg of the molybdenum tracer. The dwell is almost rectangular in shape with a center cavity and an apparent pore in the center region. There is no evidence of the ripple pattern on the dwell zone. Grain boundaries coming in from the base metal can be clearly seen to extend on to the surface of the molten zone. The dwell is 5 x 6 mm.

Backside of S/N 147

Starting at the target position, there is evidence of complete penetration through to the back surface of the disc. The cut begins at the transition to the thin section. The molten balls are evident on the rear of the plate and in addition, the same type of shrinkage cavity mentioned earlier on the bridges can be seen in these balls on the under surface. At the start of welding, both the ripple pattern and grain structure are quite evident. The ripple pattern on the underside is perfectly symmetrical with its apex along the weld centerline.** The weld appears quite uniform in appearance and in width. The same mass shift perturbation noted on the top surface is again noted on the under surface at 180 degrees. The weld continues throughout the intended full penetration region, but does not penetrate completely through the partial penetration region. There is a slight evidence of its existence in this region by virtue of a slightly discolored area.

Partial melting exists on both sides of the termination hole. In the cut region, there appears to be considerable evidence along either side of the weld of some type of vaporization and subsequent deposit. The same appearance is again evident at the position where the perturbation occurs. This vaporization material would appear to possibly come from the backing plate behind the tantalum. The dwell region is completely penetrated with the under side molten zone being

---

* See MSFC photographs 741072-3 or 741072-4.
** See MSFC photographs 741073-4 or 741073-5.

essentially a circular region about 3 millimeters in diameter. There is some evidence of surface roughening and grain structure apparent in the heat-affected zone. The under surface appears to be slightly depressed. There is no evidence of ripples being present in this region. Grain boundaries again extend in from base metal grain boundary regions to the molten zone.

Sectioring and Examination

Both tantalum discs were sectioned as shown in Figure B-34. An additional section was taken on these discs to include a bridge in the cut area. All sections were mounted and examined. Macro and microphotographs are shown in Figures B-35 through B-40.

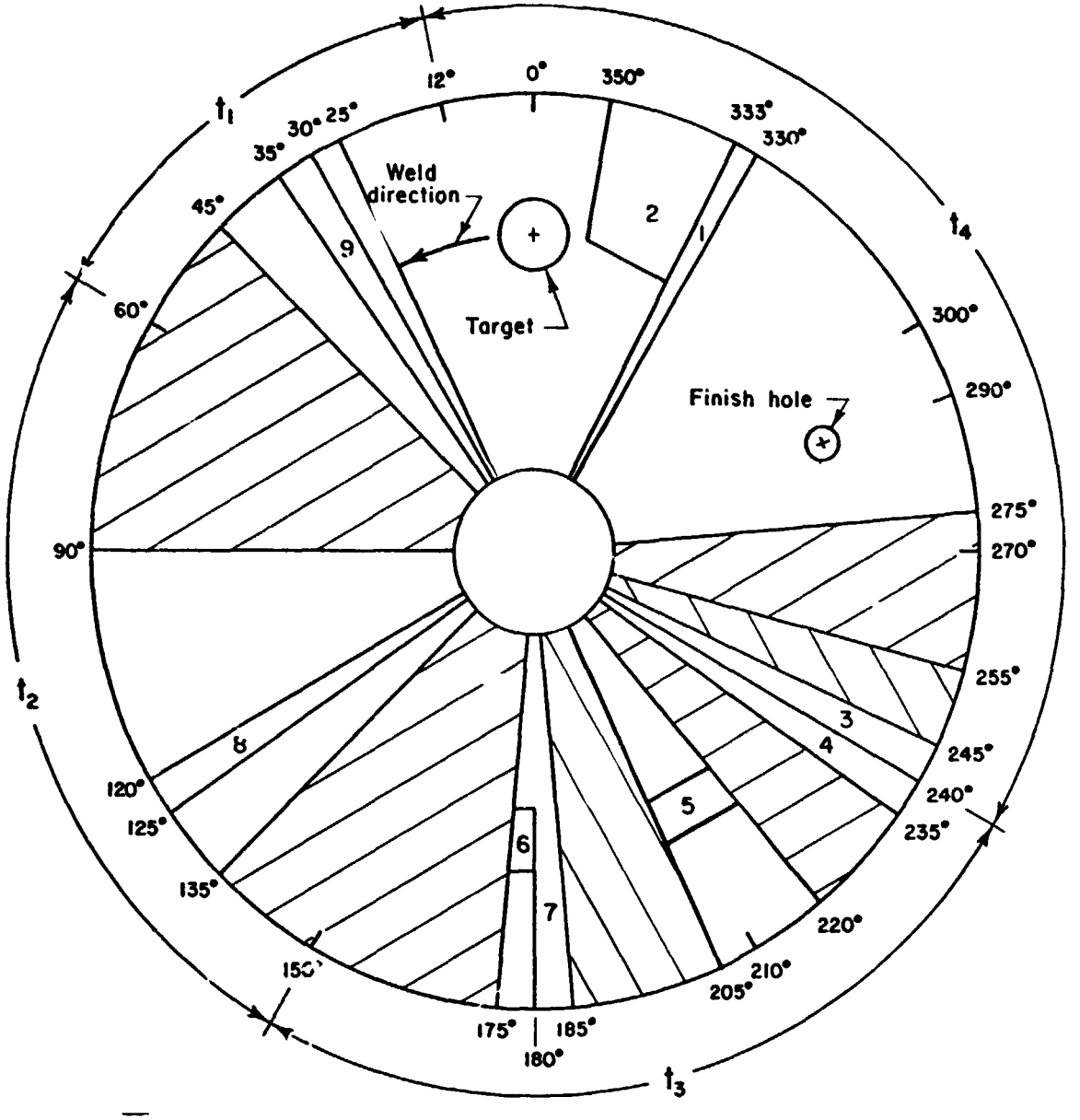

Numbered Sections - BCL

- MSFC
- UK

T_1 - Cut
T_2 - Ramp
T_3 - Full penetration
T_4 - Partial penetration/dwell

FIGURE B-34. SECTIONING PLAN S/N 145 & 147

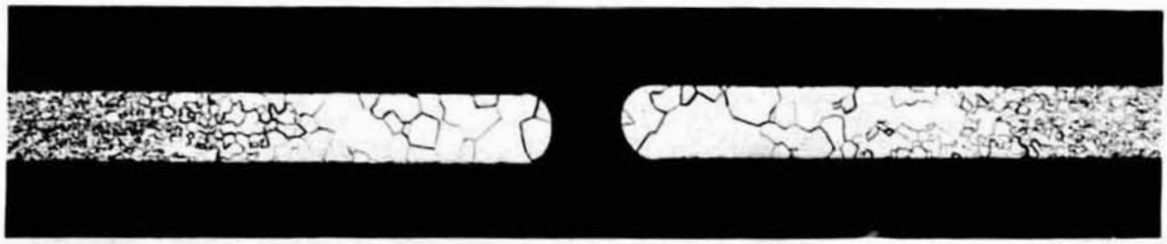

30° (+) Etched 9G307-20X

FIGURE B-35. SECTION THROUGH CUT REGION - S/N 145 SKYLAB

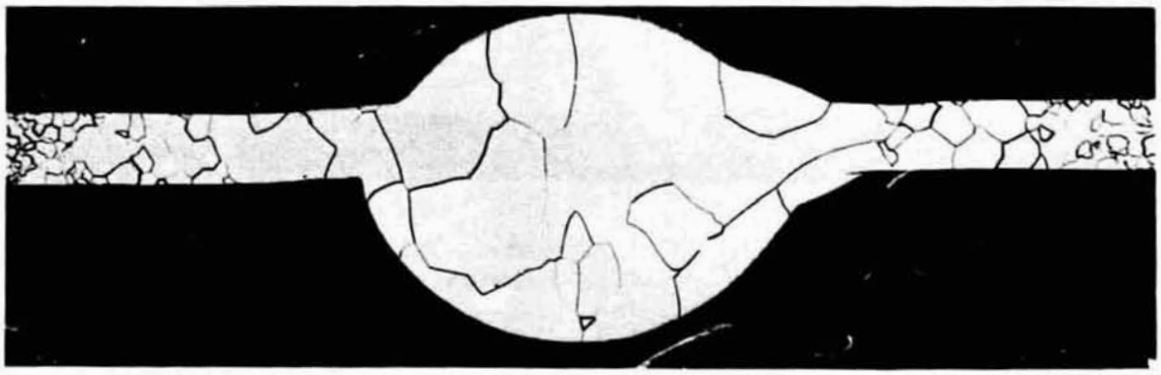

25° (+) Etched 9G308-20X

FIGURE B-36. SECTION THROUGH BRIDGE IN CUT REGION - S/N 145 SKYLAB

235° (+)

Etched
S/N 147 Ground

9C-311

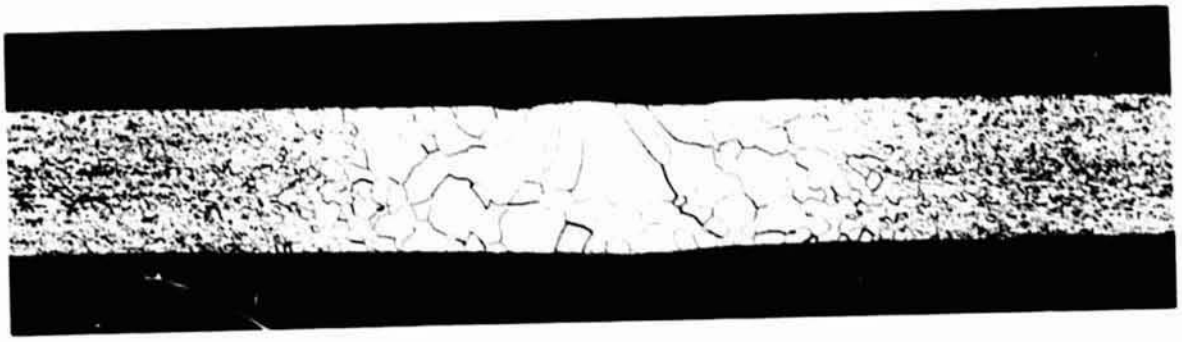

235° (+)

Etched
S/N 145 Skylab

9C-305

FIGURE B-37. WELD SECTIONS IN FULL PENETRATION REGION

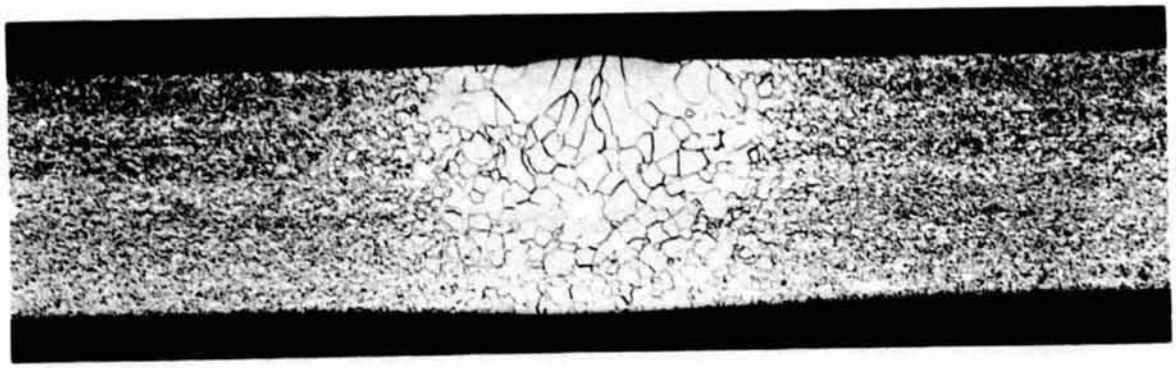

245° (-) Etched 9G304

FIGURE B-38. SECTION THROUGH PARTIAL PENETRATION REGION - S/N 145 SKYLAB

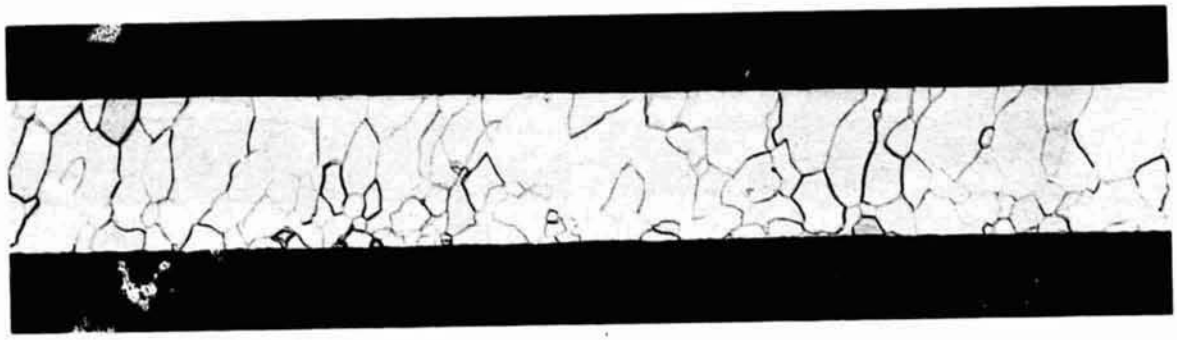

205-220° Etched 9G306-20X

FIGURE B-39. CHORD SECTION IN S/N 145 SKYLAB

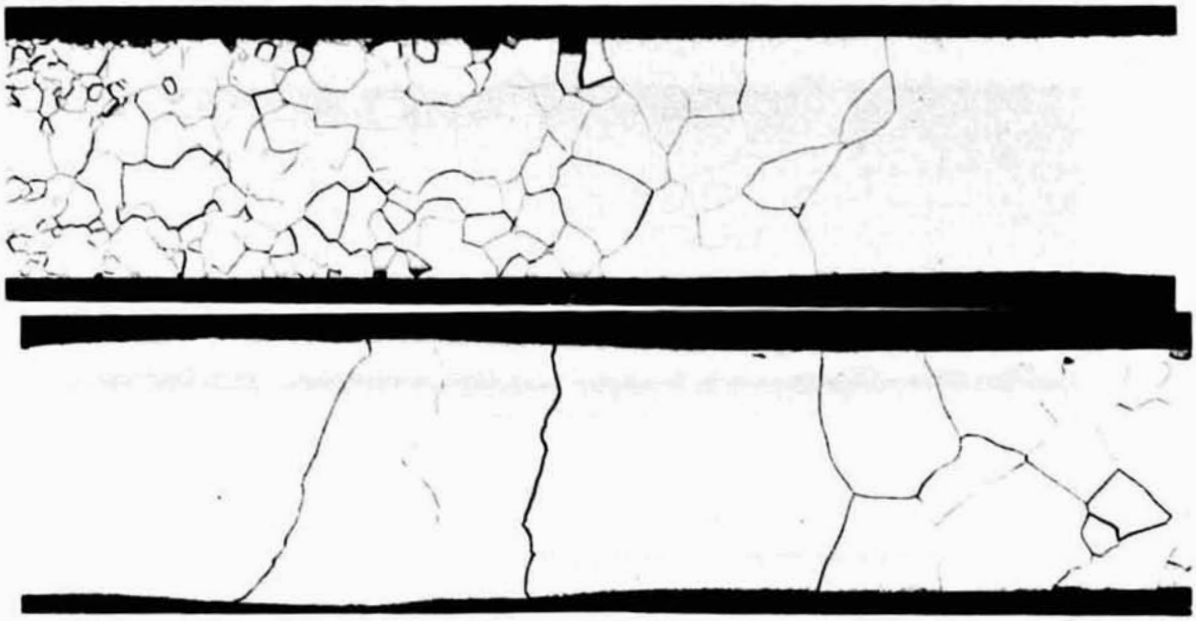

S/N 145 Skylab

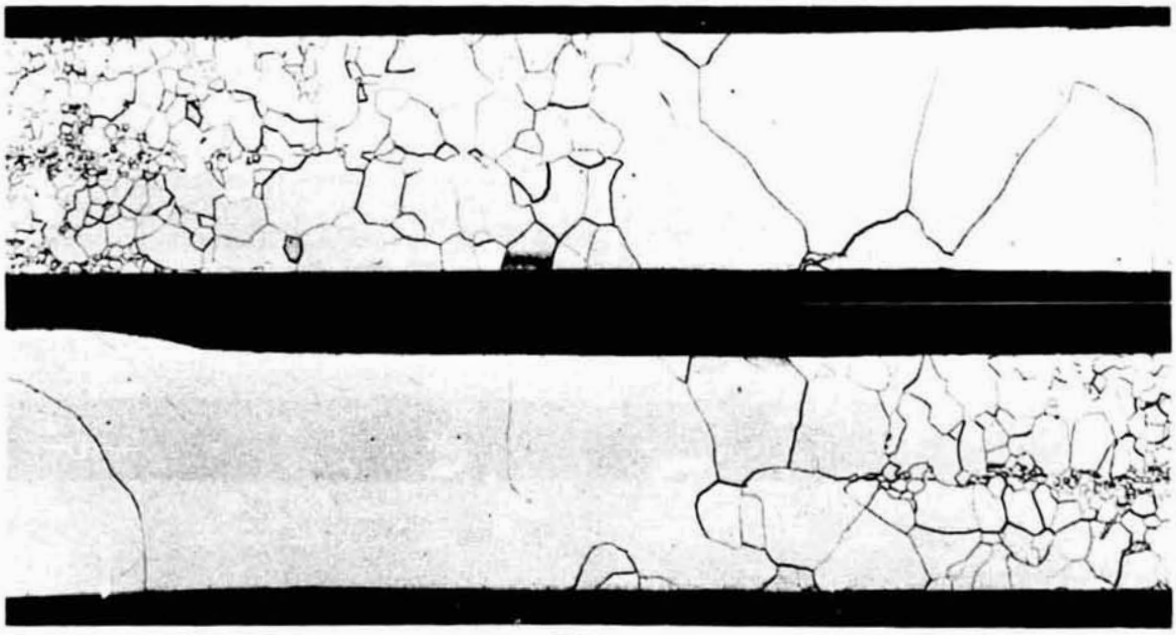

S/N 147 Ground Etched

333° (+)

9G302/303/309/310-20X

FIGURE B-40. SECTIONS THROUGH DWELL REGION
Right edge of top photo matches left edge of lower photo.

SECTION C. CONCLUSIONS

Results of the characterization studies conducted showed that the metals melting discs, both Skylab and ground, exhibited features and microstructures typical of electron beam melted metals. The applicability of electron beam welding and cutting operations in space were clearly demonstrated as applicable repair or manufacturing methods. Variations in the electron beam power density masked the possible subtle changes in microstructure that had been predicted in melts processed in space.

Significant findings from the aluminum discs were as follows:

(a) A significant difference in appearance is the change in the surface along the full penetration region. The Skylab sample (Figure B-3) exhibits a bright center region free of oxide. In contrast the ground characterization sample (Figure B-1) is covered with small oxide particles. These particles are believed to be transported from the back surface of the disc. Initially, both surfaces of the aluminum are covered with a thin film of aluminum oxide. The oxide on the front surface is removed from the weld center by impingement of the electron beam. Oxide on the back surface is not subject to the same conditions and is free to interact with the molten aluminum weld pool. It should also be noted that the surface of the partial penetration regions were always free of the small oxide particles, supporting the idea that the back surface oxide must be involved when the particles were present. Originally, it was suspected that a gravity induced convection effect was responsible for the observed surface oxide differences. Further review suggests that this is not a primary factor, although reliable data on the density of aluminum and aluminum oxide at temperatures of interest was not available. The difference can also be explained on the basis of lesser turbulence in the Skylab as suggested by Adams.

(b) Gravity effects on the final distribution of solidified metal are shown clearly in Figure B-13, showing sections through the dwell region. The molten metal in ground specimens flowed to the low points and formed a bulge above the original surface. This tendency was even more pronounced in other ground samples examined earlier.

(c) The contour at all intersections of base metal and weld metal tended to be flatter in the Skylab sections than in ground specimens. Again, this effect is more pronounced if the earlier ground samples are included in the comparison.

(d) Variations in the electron beam power density resulted in differences in cut and weld width, penetration, and shape that would overshadow some of the subtle changes in microstructure that might occur in zero gravity. All of the welds examined exhibited structures typical of electron beam welds in the 2219 aluminum alloy. Weld defects, porosity and cracks, were not as useful for examining possible zero gravity effects as we had originally hoped. Porosity was very infrequent, and then only occurred along the surface intersection regions of sections where the molten metal flowed back over the base metal. Cracks were restricted to predictable locations, at the weld start, in the dwell melt, and at the transition region from full to partial penetration. The length of weld start cracks is highly dependent on the initial size and shape of the melt zone. The significance of the greater length of weld start cracking in the Skylab specimen is difficult to assess.

(e) Efforts to use a molybdenum tracer to determine mixing and fluid flow in the weld and dwell regions were not successful. Electron probe scans of the sections expected to show these patterns only showed molybdenum present in identifiable amounts at locations on or very near the top surface. Sites of high molybdenum content could be observed as readily by optical metallography. The molybdenum layer was apparently sputtered from the surface by the impinging electron beam on these specimens.

For the stainless steel discs the following findings were made:

(a) The stainless steel welds exhibited the nail-head penetration shape commonly found in this material. However, the shape was asymmetrical in both welds (Figure B-24). Penetration was deeper on the ground sample than on the Skylab sample, but this probably reflects a slight difference in power density. The dwell regions (Figures B-17 and B-19) also indicated an effect of nonuniform power input. Normally, a circular melt zone would result from the spot heating in the dwell region. However, both discs exhibited an oblong melt zone about 18 x 10 mm in size. The melt shape indicates that the effective electron beam focal pattern was elongated.

(b) The dwell region sections (Figure B-26) dramatically show the effect of gravity on the melt zone. The thinning at the top, and bulge at the bottom of the ground specimen section are completely absent in the Skylab section. The ground section clearly shows an effect of orientation on melt zone shape, probably reflecting the flow pattern when liquid. In marked contrast, the Skylab section is very uniform in melt zone shape. This observation has practical significance for the future application of all our melting operations in space, since clearly the shape of the melt zone can be controlled precisely by controlling the heat input pattern and using calculated heat flow predictions based on idealized conditions.

(c) No significant differences in microstructure or hardness were evident between the Skylab and ground specimens.

Significant findings from the tantalum discs were:

(a) The weld ripple pattern of the ground based disc was asymmetrical; displaced with the apex offset toward the center (low side) of the disc. No clear explanation of this observation is apparent.

(b) The coarse equiaxed microstructures of the weld and heat-affected zone are typical of tantalum electron beam welds and do not display any effects of the gravity variation.

☆ U.S. GOVERMENT PRINTING OFFICE 1974 -- 640-447 / 119 REGION NO. 4